Protective role of Foxo3a in the regulatory T cells and dendritic cells of *IL-10*-deficient mice

Willem Brandt

Thesis submitted to the University of Ottawa
in partial fulfillment of the requirements for the
MSc degree in Microbiology and Immunology

Department of Biochemistry, Microbiology, and Immunology
Faculty of Medicine
University of Ottawa

Abstract

Inflammatory bowel disease (IBD) affects about 322,600 Canadians and is expected to rise to 470,000 Canadians by 2035. Crohn's disease (CrD) is a severe form of IBD, and in acute cases requires hospitalization and surgical intervention. CrD is mediated by complex gene-environment interactions where many genetic and environmental factors are associated with the disease. Current treatments manage the symptoms, but treatments that tackle the underlying cause are needed to improve patient outcomes. In this study, a novel mouse model for CrD was developed in which a susceptibility allele (*IL-10*) and a progression allele (*Foxo3a*) are deactivated. *Foxo3a*$^{-/-}$*IL-10*$^{-/-}$ mice spontaneously develop a Crohn's-like phenotype consistent with CrD in humans. Regulatory T cells (Tregs) play an important role in mediating immune homeostasis and peripheral self-tolerance, thus playing a key role in preventing chronic inflammation. DCs are important in regulating the response to the gut microbiota. This study demonstrates that Foxo3a plays a key role in maintaining the differentiation, stability, and suppressive capacity of Tregs in *IL-10*-deficient mice. This study demonstrates that Foxo3a plays a role in the *in vitro* differentiation of moDCs. Additionally, the results of this study indicate that excessive cytokine production by DCs can be inhibited through a variety of pathways. Foxo3a also regulates a key checkpoint in Treg differentiation and stability in *IL-10*-deficient mice. In sum, Foxo3a and IL-10 play antagonistic roles that maintain proper Treg and DC function and development. This study reveals novel pathways that can be targeted for therapeutic intervention in IBD.

Preface

Contribution of Collaborators

Willem Brandt planned and performed most of the experiments. Avni Bhan assisted with euthanasia and dissection of mice in most experiments and assisted with caring for the mouse colonies. Rayan El Hamra performed the RNAseq analysis. Dr. Julie Joseph and Dr. Stephanie Hajjar contributed to the conceptualization of the project and study design. Dr. Subash Sad conceptualized the study and assisted in experimental design and analysis.

Approvals

The experimental protocols (BMIe-3954 and BMIe-1638) were approved by the University of Ottawa Animal Care Committee.

Flow cytometry experiments were conducted at the Flow Cytometry and Virometry Core Facility at the University of Ottawa.

The work was funded by a grant from the Canadian Institutes of Health Research (CIHR).

Willem Brandt was supported by the Canadian Graduate Scholarship – Master's program from CIHR and the Ontario Graduate Scholarship from the Government of Ontario.

Acknowledgements

I would like to extend my greatest thanks to my supervisor Dr. Subash Sad. Since starting my honours project in 2022, he has supported me in my research and extracurricular endeavours. I am thankful for his encouragement to push through the roadblocks, which are inevitable in research. I will never forget the stories and anecdotes Dr. Sad told at lab meetings and lab dinners. I have endeavoured to try my best to be like Dr. Sad's son when he took him skiing — to always get back up no matter how hard the fall.

I would also like to thank Dr. Mireille Khacho and Dr. Seung-Hwan Lee for advising my project. Both have provided great ideas that have contributed to the success of my project. Thank you for challenging my knowledge and pushing me to learn more.

My time in the Sad lab has been some of the best years of my life. This comes in no small part because of the amazing members of the lab. Thank you, Avni Bhan, for always being there to help with the project and tolerating some late arrivals for experiments. Thank you, Rayan El Hamra, for helping me learn about 'Westerns' and being a great person to talk to on the long nights in the lab. Thank you, Sahil Yadav, for being a calming force in the lab and holding everything together. Thank you, Kate Hurley, for showing me what hard work looks like and helping me with flow no matter the time. Thank you, Adam Mahdi, for infecting me with your laugh whenever you are around. Thank you, Dr. Ardeshir Ariana, for all the great conversations and meaningful insight into experiments. Special thanks also goes out to Rachel Kaul, Dikcha Rijal, and Cameron Brown who were all amazing lab members and friends.

Thanks to all the members at ACVS for training me in animal care and helping take care of my colonies. Special thanks to Dr. Vera Tang for the countless hours of help with planning and troubleshooting the flow cytometry experiments.

Thank you to CIHR and OGS for funding my Master's research and giving me the opportunity to pursue my passion in science.

Finally, thank you to my family and friends who have been instrumental to my well-being throughout the process. I could not have completed my MSc without the support of my parents, Carey and James, and my sister, Alex. Thank you to my friends for providing a much-needed mental reset after long days and weeks in the lab.

Table of Contents

ABSTRACT ..... **II**

PREFACE ..... **III**

Contribution of Collaborators III
Approvals III

ACKNOWLEDGEMENTS ..... **IV**

LIST OF ABBREVIATIONS ..... **VIII**

LIST OF FIGURES AND TABLES ..... **XI**

1.0 INTRODUCTION **1**

1.1 Innate Immune System 1
1.1.1 Monocytes *2*
1.1.2 Dendritic Cells *3*
1.1.2.1 DC Subsets and Differentiation 3
1.1.2.2 DC Cytokine Production 4
1.2 Adaptive Immune System 4
1.2.1 T Cell Activation *5*
1.2.2 T Cell Development *6*
1.2.3 $CD8^+$ T cells *7*
1.2.4 $CD4^+$ T cells *8*
1.2.5 Regulatory T cells *9*
1.2.5.1 Treg subsets 9
1.2.5.2 Treg differentiation 10
1.2.5.3 Treg Suppression and Cytokine Production 11
1.2.5.4 Treg Stability 15
1.3 Immunometabolism 16
1.3.1 DC metabolism *17*
1.3.2 Treg metabolism *18*
1.4 Foxo3a 19
1.4.1 Foxo3a in DCs *20*
1.4.2 Foxo3a in Tregs *20*
1.5 Gut Immunity and Chronic Inflammatory Disease 21
1.5.1 Inflammatory Bowel Disease and Crohn's Disease *22*
1.5.1.1 DCs in Crohn's Disease 23
1.5.1.2 Treg in Crohn's Disease 23
1.5.1.3 Mouse models of CD 24
1.6 Rational 25
1.6.1 Hypothesis *26*
1.6.2 Objectives *26*

2.0 MATERIALS AND METHODS **27**

2.1 Mouse Strains 27
2.2 Monitoring Illness in *IL-10*$^{-/-}$ and *Foxo3a*$^{-/-}$*IL-10*$^{-/-}$ mice 27
2.3 Bone Marrow Cell Isolation 28
2.4 Monocyte Isolation 28
2.5 Flow Cytometry 30
2.6 Generation of Myeloid DCs from Monocytes 33
2.7 Generation of Myeloid DCs from BM 33
2.8 Splenocyte Isolation 33

2.9 Dendritic Cell Isolation 34
2.10 *In vitro* inhibition of DC cytokine production 34
2.11 Measurement of cytokines at the protein level 37
2.12 Isolation of $CD4^+$ T Cells 37
2.13 Isolation of $CD4^+CD25^+$ T Cells 39
2.14 Isolation of $CD8^+$ T Cells 39
2.15 Regulatory T cell Suppression Assay 39
2.16 *In Vitro* Differentiation of Regulatory T Cells 40
2.17 Live Measurement of Oxygen Consumption Rate 41
2.18 Characterization of iTreg Stability 43
2.19 Characterization of nTreg Stability 43
2.20 Intracellular Cytokine Analysis 43
2.21 Statistical Analysis 44

3.0 RESULTS 45

3.1 Foxo3a controls the differentiation of $CD11b^+$ DCs in *IL-10*-deficient mice. 45
3.2 Various inhibitors can control the excessive production of pro-inflammatory cytokines produced by *Foxo3a*$^{-/-}$*IL-10*$^{-/-}$ DCs. 48
3.3 Foxo3a modulates $CD4^+$ T cells in the spleen compartment of *IL-10*-deficient mice. 52
3.4 Foxo3a maintains Foxp3 expression in the nTregs of *IL-10*-deficient mice. 55
3.5 Foxo3a contributes to proper suppression by nTregs in *IL-10*-deficient mice. 58
3.6 Foxo3a contributes to proper suppression by iTregs in *IL-10*-deficient mice. 60
3.7 Foxo3a plays a non-redundant role in maintaining Treg differentiation *in vitro* in *IL-10*-deficient mice. 63
3.8 Foxo3a plays a critical role in maintaining proper proliferation of *IL-10*-deficient iTregs. 69
3.9 Foxo3a controls TCR signaling sensitivity in *IL-10*-deficient iTregs through development of a CrD-like phenotype. 72
3.10 Foxo3a modulates metabolic activity in *IL-10*-deficient iTregs. 75
3.11 Foxo3a is critical in maintaining Foxp3 expression in *IL-10*-deficient iTregs by preventing excessive DNA methylation. 77
3.12 Foxo3a maintains iTregs stability in *IL-10*-deficient mice by preventing over stimulation of the TCR at low thresholds of stimulation 83
3.13 In maintaining the stability of Foxp3, Foxo3a is critical in maintaining the proper balance of cytokine production in *IL-10*-deficient T cells. 85

4.0 DISCUSSION 87

4.1 Foxo3a control the differentiation and cytokine production in DCs of *IL-10*-deficient mice. 88
4.2 The development of a CrD-like phenotype compromises the differentiation of iTregs in *Foxo*3a-*IL-10*-deficient mice. 91
4.3 Foxo3a maintains Foxp3 expression in *IL-10*-deficient mice. 96

5.0 CONCLUSION 99

6.0 REFERENCES 101

7.0 CURRICULUM VITAE 115

8.0 SUPPLEMENTAL FIGURES 118

List of Abbreviations

ADP	adenosine diphosphate
AKT	protein kinase B
AMP	adenosine monophosphate
AMPK	AMP-activated kinase
ANOVA	analysis of variance
APC	antigen presenting cell
ATP	adenosine triphosphate
Bcl-6	B cell lymphoma 6
BCR	B cell receptor
BFA	Brefeldin A
BM	bone marrow
cAMP	cyclic AMP
CAR	chimeric antigen receptor
CCR	C-C chemokine receptor
CD	cluster of differentiation
cDC	conventional dendritic cell
CFSE	carboxyfluoresceine succinimidyl ester
CMP	common myeloid progenitor
CNS	conserved non-coding sequence
CrD	Crohn's Disease
CTLA-4	cytotoxic T-lymphocyte associated protein 4
DC	dendritic cell
DSS	dextran-sodium sulfate
Ebi3	Epstein-Barr virus induced gene 3
ELISA	enzyme-linked immunosorbent assay
ERK	extracellular signal regulated kinase
eTreg	effector regulatory T cell
EV	extracellular vesicle
FBS	fetal bovine serum
FLT3	FMS-like tyrosine kinase 3
Foxo	forkhead box class O
Foxp3	forkhead box class P3
GATA-3	GATA binding protein 3
GI	gastro-intestinal
GLUT1	glucose transporter 1

GM-CSF	granulocyte-macrophage colony-stimulating factor
GWAS	genome-wide association study
IBD	inflammatory bowel disease
ICER	inducible cAMP early receptor
IGFBP	insulin growth factor binding proteins 1 to 3
iNOS	inducible nitric oxide synthase
IFN-I	type I interferons
IL	interleukin
IL-2Rα	IL-2 receptor alpha chain
ILC	innate lymphoid cell
iTreg	induced regulatory T cell
JNK	c-JUN N-terminal kinase
Lag3	lymphocyte activation gene 3
LC	Langerhans cell
LMP	common lymphoid progenitor
LPS	lipopolysaccharides
M-CSF	macrophage colony-stimulating factor
MFI	median fluorescence intensity
miRNA	micro RNA
moDC	monocyte-derived dendritic cell
MHC	major histocompatibility complex
mTOR	mammalian target of rapamycin
NADPH	nicotinamide adenine dinucleotide phosphate
NFAT	nuclear factor of activated T cells
NF-κB	nuclear factor-κB
NK cell	natural killer cell
nTreg	natural regulatory T cell
OCR	oxygen consumption rate
PAMP	pathogen-associated molecular pattern
PBS	phosphate buffered saline
pDC	plasmacytoid dendritic cell
PPP	pentose phosphate pathway
PPARγ	peroxisome proliferator-activated receptor-γ
PRR	pattern recognition receptor
pTreg	peripheral regulatory T cell
RAR	retinoic acid receptor
RORγt	RAR-related orphan nuclear receptor γt
R8	RPMI-1640 supplemented with 8% FBS

SEM	standard error of the mean
Smad-3	mothers against decapentaplegic homolog 3
STAT	signal transducer and activator of transcription
$S1P_1$	sphingosine-1 phosphate receptor type 1
T-bet	t-box expressed in T cells
TCA	tricarboxylic acid
TCR	T cell receptor
TET	ten-eleven translocation
TGF-β	transforming growth factor β
TIGIT	T cell immunoreceptor with Ig and ITIM domains
TLR	toll-like receptor
TMB	3,3',5,5'-tetramethylbenzidine
TNF-α	tumor necrosis factor α
Treg	regulatory T cell
tTreg	thymic regulatory T cell
WT	wild type
XACT	X active specific transcript
XIAP	X-linked inhibitor of apoptosis protein
5hmC	5-hydroxymethylcytosine

List of Figures and Tables

Figure 1. Treg suppression pathways. 12
Figure 2. Isolation of BM monocytes and splenic DCs. 29
Figure 3. Gating strategy for identifying Tregs, their cell surface markers, and intracellular markers. 32
Figure 4. Purified $CD4^+CD25^+$ T cells from spleens serve as the best method for purifying nTregs from splenocytes....38
Figure 5. Protocol for the differentiation of iTregs from purified $CD4^+$ T cells....42
Figure 6. A greater number of *Foxo3a*$^{-/-}$*IL-10*$^{-/-}$ DCs differentiate from BM in response to GM-CSF. 47
Figure 7. *Foxo3a*$^{-/-}$*IL-10*$^{-/-}$ DCs' metabolic and immunologic pathways are heavily modulated. 50
Figure 8. Multiple pathways can be inhibited to reduce the production of TNF-α and IL-6 by *Foxo3a*$^{-/-}$*IL-10*$^{-/-}$ DCs stimulated by LPS.. 51
Figure 9. *Foxo3a*$^{-/-}$*IL-10*$^{-/-}$ mice have large spleens that increase in size as they develop a CrD-like phenotype. 53
Figure 10. *Foxo3a*$^{-/-}$*IL-10*$^{-/-}$ spleens have a reduced proportion of $CD4^+$ T cells and a similar overall number of Tregs.. 54
Figure 11. *Foxo3a*$^{-/-}$*IL-10*$^{-/-}$ nTregs have slightly reduced Foxp3 expression, which worsens upon development of a CrD-like phenotype. 56
Figure 12. *Foxo3a*$^{-/-}$*IL-10*$^{-/-}$ tTregs have slightly reduced Foxp3 expression which worsens upon development of a CrD-like phenotype. 57
Figure 13. The ability of *Foxo3a*$^{-/-}$*IL-10*$^{-/-}$ nTregs to suppress the proliferation of WT $CD4^+$ and $CD8^+$ T cells is compromised. 59
Figure 14. The ability of *Foxo3a*$^{-/-}$*IL-10*$^{-/-}$ iTregs to suppress the proliferation of WT $CD4^+$ T cells is compromised. 62
Figure 15. The development of a CrD-like phenotype in *Foxo3a*$^{-/-}$*IL-10*$^{-/-}$ mice compromises the *in vitro* differentiation of *Foxo3a*$^{-/-}$*IL-10*$^{-/-}$ iTregs. 65
Figure 16. *Foxo3a*$^{-/-}$*IL-10*$^{-/-}$ iTregs differentiated from *Foxo3a*$^{-/-}$*IL-10*$^{-/-}$ mice with a CrD-like phenotype have a lower expression of Foxp3. 66
Figure 17. No difference between genotypes in viability of iTregs during *in vitro* differentiation. 67
Figure 18. The ability of *Foxo3a*$^{-/-}$*IL-10*$^{-/-}$ iTregs to suppress the proliferation of WT $CD4^+$ is compromised irrespective of if differentiation is compromised. 68
Figure 19. *Foxo3a*$^{-/-}$*IL-10*$^{-/-}$ mice with a CrD-like phenotype demonstrate increased proliferation during iTreg differentiation. 70
Figure 20. *Foxo3a*$^{-/-}$*IL-10*$^{-/-}$ iTregs and $Foxp3^-CD4^+$ T cells undergo increased proliferation during iTreg differentiation. 71
Figure 21. The development of a CrD-like phenotype in *Foxo3a*$^{-/-}$*IL-10*$^{-/-}$ mice causes increased stimulation and proliferation by αCD3 antibodies. 73
Figure 22. The development of a CrD-like phenotype in *Foxo3a*$^{-/-}$*IL-10*$^{-/-}$ mice causes increased viability when stimulated with low concentrations of αCD3 antibodies. 74

Figure 23. *Foxo3a*$^{-/-}$*IL-10*$^{-/-}$ CD4^{+} T cells have increased lipids while *Foxo3a*$^{-/-}$*IL-10*$^{-/-}$ iTregs have similar levels of lipids and cholesterol to the control genotypes. 76
Figure 24. *Foxo3a*$^{-/-}$*IL-10*$^{-/-}$ and *Foxo3a*$^{-/-}$ iTregs have decreased stability in maintaining Foxp3 expression when co-cultured with WT CD4^{+} T cells. 79
Figure 25. *Foxo3a*$^{-/-}$*IL-10*$^{-/-}$ iTregs have reduced stability in maintaining Foxp3 expression when stimulated with αCD3 antibodies. 80
Figure 26. *Foxo3a*$^{-/-}$*IL-10*$^{-/-}$ iTregs have similar viability to the control genotypes when stimulated with αCD3 antibodies....81
Figure 27. *Foxo3a*$^{-/-}$*IL-10*$^{-/-}$ iTregs maintain CD25 expression for longer in the absence of αCD3 stimulation. 82
Figure 28. *Foxo3a*$^{-/-}$*IL-10*$^{-/-}$ iTregs have compromised stability which worsens as the concentration of αCD3 antibodies used to stimulate them increases. 84
Figure 29. *Foxo3a*$^{-/-}$*IL-10*$^{-/-}$ CD4^{+}Foxp3^{-} T cells produce significantly more IL-17a and IFN-γ upon stimulation with αCD3. 86
Figure 30. Visual representation of findings from this study. 100
Figure S31. The ability of *Foxo3a*$^{-/-}$*IL-10*$^{-/-}$ iTregs to suppress the proliferation of WT CD4^{+} T cells is restored with rapamycin treatment during co-culture.. 118
Figure S32. A DNA methyltransferase inhibitor does not rescue the compromised differentiation of *Foxo3a*$^{-/-}$*IL-10*$^{-/-}$ iTregs from mice with a CrD-like phenotype....119
Figure S33. *Foxo3a*$^{-/-}$*IL-10*$^{-/-}$ iTregs differentiated from mice with a CrD-like phenotype consume high levels of oxygen during differentiation. 120
Figure S34. *Foxo3a*$^{-/-}$*IL-10*$^{-/-}$ iTregs stability is partially rescued with a DNA methyltransferase inhibitor. 121
Figure S35. *Foxo3a*$^{-/-}$*IL-10*$^{-/-}$ nTregs have compromised stability when stimulated with αCD3 antibodies in the presence of growth factors. 122

Table 1. Antibodies used in flow cytometry. 31
Table 2. Inhibitors used in DC experiments. 35
Table 3. Pathways upregulated in *Foxo3a*$^{-/-}$*IL-10*$^{-/-}$ DCs and inhibitors used to target upregulated pathways....36

1.0 Introduction

1.1 Innate Immune System

The immune system is comprised of two branches: the adaptive immune system and innate immune system. Both branches are made of a complex network of organs, cells, and proteins that protect the body from endogenous and exogenous threats and maintain homeostasis. The innate immune system serves as the first line of defence against invading pathogens. Pathogens can be broken down into four categories: viruses, bacteria, parasites, and fungi. The first defences an invader encounters are chemical and physical barriers. For example, the skin physically separates the inside and outside of the body and has high acidity not conducive to pathogen survival. If a pathogen overcomes these barriers, they will encounter the complement system, antimicrobial peptides, and phagocytic immune cells. Macrophages and neutrophils are the phagocytic cells that play the most predominant role in innate immunity. Dendritic cells (DCs) also phagocytose pathogens but use the deconstructed pathogens to alert the immune system of the invader.

A long-established defining characteristic of the innate immune response is the speed at which the response is mounted[1]. To facilitate the quick response time, the innate immune system must recognize pathogens non-specifically. Innate immune cells recognize evolutionarily conserved structures on pathogens, called pathogen-associated molecular patterns (PAMPs) through pattern recognition receptors (PRRs)[2]. Lipopolysaccharides (LPS), flagellin, and peptidoglycans are present on many pathogens and activate the innate immune system through recognition by PRRs[3-5]. Recognition of PAMPs by PRRs trigger signaling pathways, which activate transcription factors such as the nuclear factor-κB (NF-κB)[6]. Nuclear transcription factors such as NF-κB regulate the transcription of genes leading to the production of pro-inflammatory cytokines, chemokines, defence receptors, and immune cell

recruitment. All these factors lead to inflammation, which helps kill the invading pathogen, at the infection site.

1.1.1 Monocytes

Monocytes differentiate from progenitors in the bone marrow (BM) and circulate throughout the body[7]. Once they have migrated into peripheral tissues, monocytes can differentiate into macrophages and DCs[8, 9]. Murine monocytes are separated into two classes that differ in Ly-6C expression: inflammatory monocytes (Ly-6C^{hi}), and patrolling monocytes (Ly-6C^{low})[10]. Inflammatory monocytes tend to differentiate into macrophages, while patrolling monocytes differentiate into DCs[10]. Thus, the primary role of monocytes is to replenish macrophages and DCs in peripheral tissue.

During infection, monocytes are recruited to the sites of infection via C-C chemokine receptor (CCR2)-mediated recruitment[11]. Once in the peripheral tissues, a suite of PAMPs, inflammatory signals, and growth factors are balanced to induce monocyte differentiation into DCs[12, 13]. Granulocyte-macrophage colony-stimulating factor (GM-CSF) has been shown to have a great impact on DC generation from monocytes *in vivo* as mice deficient for the GM-CSF receptor have a reduction in DC subsets, but conversely, seems to not be necessary for the differentiation of inflammatory DCs[14]. In contrast, *in vitro* differentiation of DCs from monocytes is much simpler. BM cells cultured with GM-CSF induce differentiation, while other studies report the necessity of GM-CSF and interleukin-4 (IL-4) for the *in vitro* differentiation of monocyte-derived DCs[15, 16]. Interestingly, some studies have also shown that monocytes and/or monocyte-derived DCs promote T cell responses in draining lymph nodes[17, 18]. Macrophage differentiation from monocytes is much simpler; both *in vitro* and *in vivo* models suggest that macrophage colony-stimulating factor (M-CSF) is responsible for differentiation of macrophages from monocytes[19].

1.1.2 Dendritic Cells

DCs are professional antigen presenting cells (APCs). DCs are responsible for phagocytosing and breaking down pathogens, then presenting antigens to lymphocytes[20]. This process is indispensable in beginning the activation of the innate immune response. Upon antigen capture and recognition of PAMPs or stimulation by pro-inflammatory cytokines, DC maturation is induced. Upon maturation, major histocompatibility complex II (MHCII) bound to antigens are trafficked to the cell membrane via endosomal compartments[21]. DCs also up-regulate the expression of the co-stimulatory molecules cluster of differentiation 80 (CD80) and CD86, MHC I, T cell adhesion molecules, and chemokine receptors[22]. Upregulation of CCR7 allows DCs to migrate to secondary lymphoid organs, like the draining lymph nodes, where they present antigens to T cells[23]. DCs also play other important roles in the initial immune response. DCs produce cytokines and recognize pathogens early, activating the surrounding innate immune cells (e.g., innate lymphoid cells (ILCs) and/or natural killer (NK) cells)[24, 25].

1.1.2.1 DC Subsets and Differentiation

DCs originate from both a myeloid and lymphoid origin. DCs are classified into unique subsets: conventional DCs (cDC), which are further classified as cDC1 and cDC2; plasmacytoid DCs (pDCs); monocyte-derived DCs (moDCs); and Langerhans cells (LCs). cDCs undertake the conventional role of antigen presentation and activation of T cells. pDCs are poor antigen presenters and are specialized at producing type I interferons (IFN-I)[26]. moDCs differentiate in the presence of inflammation in mucosal tissues and promote Th1 and Th17 differentiation[27]. LCs are also antigen presenting cells that reside in the stratified squamous epithelium[28]. cDC1s and cDC2s both differentiate from common myeloid progenitors (CMP) and common lymphoid progenitors (LMP)[29, 30]. Some studies, however, suggest that cDCs originate only from a myeloid origin[31]. The majority of pDCs originate from

myeloid CDPs, while a minority of pDCs seem to be of lymphoid origin[32, 33]. moDCs differentiate from monocytes as described above. Overall, DCs have diverse origins and specialized functions, and their relative proportions are modulated based on need.

1.1.2.2 DC Cytokine Production

DCs produce pro-inflammatory cytokines to aid with the innate and adaptive immune response. pDCs and moDCs primarily play the role of cytokine producers. Upon activation and maturation, via stimulation with PAMPs and pro-inflammatory cytokines, DCs produce cytokines of their own. Under pro-inflammatory conditions, DCs will produce pro-inflammatory cytokines, primarily IL-12p70, IL-6, and tumor necrosis factor α (TNF-α). Stimulation with LPS leads to low level production of IL-6 and TNF-α, but live bacteria *in vitro* are needed for the production of IL-12p70[34]. Increased production of these pro-inflammatory cytokines is often linked with diseased states. IL-6 causes differentiation of plasma cells, proliferation of cytotoxic T cells, differentiation of Th17 cells, and the production of IL-2, the latter of which contributes to T cell proliferation[35-37]. IL-12 is essential for proliferation and differentiation of Th1 cells[38, 39]. TNF-α is strongly linked with the pathogenesis of many autoimmune diseases, and αTNF-α antibodies have proven to successfully treat these autoimmune diseases[40, 41].

1.2 Adaptive Immune System

The adaptive immune system differs from the innate immune system in that it responds much slower, but it develops a specific, targeted response to the invading pathogen. The adaptive immune system also retains memory of past infections so that it can fight them off more effectively in the future. The adaptive immune system is effective in killing its targets; thus, it is imperative that it does not attack the host. One of the most important aspects of the innate immune system is its ability to distinguish what is self and what is foreign. Failures of

this system result in autoimmune diseases. The adaptive immune system also works in tight conjunction with the innate immune system. To avoid unnecessary reactions, the adaptive immune system is only activated when innate immune cells recognize PAMPs, which identify dangerous pathogens. Problems with this interaction result in allergies.

The adaptive immune response is mediated by B and T cells. B cells are primarily responsible for antibody production, while T cells play a variety of roles depending on their distinct subset and are necessary for mounting a robust immune response[42, 43]. What allows B and T cells to mount a specific response to pathogens is the B cell receptor (BCR) and T cell receptor (TCR). The BCR and TCR have incredible diversity in their ability to bind antigens through random recombination of Variable (V), Diversity (D), and Joining (J) regions of the receptors[44-46]. The diversity of BCRs and TCRs on B cells and T cells, respectively, is what allows the adaptive immune system to mount a specific response to a pathogen. Another subset of lymphoid cells are NK cells. The primary role of NK cells is to destroy infected and tumor cells through cell-to-cell interactions[47-49]. Recently, ILCs have been discovered that do not express the TCR and mount both innate and adaptive responses to pathogens[50].

1.2.1 T Cell Activation

T cell activation requires three signals. Signal one is the recognition of an antigen on an MHCII of an APC by the T cell's TCR[51]. Signal two is the co-stimulatory signal provided by CD80 and CD86 on an APC, both of which are ligands to CD28 on T cells. Signal three is provided by cytokines secreted by APCs and other immune cells. Signal 3 also determines the lineage of the T cell. Upon TCR engagement with an antigen, many pathways are activated, such as extracellular signal regulated kinase (ERK), c-JUN N-terminal kinase (JNK), NF-κB, and nuclear factor of activated T cells (NFAT), all of which contribute to the induction of effector functions[52-54]. Co-stimulation through CD28 leads to an increase in

production of IL-2, an increase in T cell proliferation, and T cell viability[55]. IL-2 promotes T cell survival by activating the protein kinase B (AKT) pathway[56]. Without CD28 co-stimulation, the threshold for T cell activation is much higher[57]. Full activation of $CD8^+$ and $CD4^+$ T cells requires IL-12 and IFN-I and IL-1, respectively, to develop full effector functions[58, 59].

Upon activation, $CD4^+$ T cells express the surface marker CD25 and differentiate into various helper T cell subsets while $CD8^+$ T cells differentiate into different cytotoxic T cell subsets, all of which express various identifying markers. Activation allows $CD4^+$ and $CD8^+$ T cells to carry out their respective functions related to host defense. In general, activated $CD4^+$ T cells help activate innate immune cells, B cells, $CD8^+$ T cells, and nonimmune cells, and prevent an excessive immune reaction. In contrast, activated $CD8^+$ T cells (cytotoxic) kill infected or malignant cells through effector cytokines, cytotoxic granules, and death receptor-dependant cytotoxicity[60-62].

1.2.2 T Cell Development

T cell development starts in the BM. T cell precursors migrate from the BM to the thymus in early stages of life. The thymus secretes thymosin, thymotaxin, thymopoietin, and other thymic factors, all of which collectively draw the T cell precursors to the thymus. In the thymus, T cell precursors begin expressing TCRs, CD8, and CD4 (double-positive T cell). Thymic epithelial cells expressing MHCI and MHCII then bind CD8 and CD4, respectively; this binding process is called positive selection[63-66]. If this recognition event does not happen, the double positive T cell undergoes apoptosis through FAS signaling[67]. After positive selection, the double-positive T cell then interacts with thymic epithelial cells presenting self-antigens on MHCI and MHCII. If the TCR on the double-positive T cell recognizes the self-antigen, it undergoes apoptosis through FAS signaling; this latter process is called negative selection[68, 69]. Lastly, the double-positive T cell arbitrarily interacts with either an $MHCI^+$ or

MHCII$^+$ thymic epithelial cell. If it interacts with an MHCI$^+$ thymic epithelial cell, it down-regulates CD4 and upregulates CD8, creating a CD8$^+$ T cell. The opposite happens when the double-positive T cell interacts with an MHCII$^+$ thymic epithelial cell, creating a CD4$^+$ T cell[70]. These T cells then migrate into the secondary lymphoid organs to await antigen presentation, activation, and maturation.

1.2.3 CD8$^+$ T cells

CD8$^+$ T cells are responsible for killing (i.e. lysing) infected or malignant cells. Upon recognition of an antigen on an MHCI of a DC, CD8$^+$ T cells become activated and expand in number. Most of this expanded population will be effector CD8$^+$ T cells tasked with killing the infected cells, while a minority of the population become memory CD8$^+$ T cells[71]. Activated CD8$^+$ T cells will make the metabolic switch from oxidative phosphorylation to aerobic glycolysis to meet the demands of making new cells[72]. IL-2 and IL-12 both play critical roles in the development of effector functions in activated CD8$^+$ T cells[73, 74]. When effector CD8$^+$ T cells bind an antigen on the surface of a cell, they release granules containing perforin and granzymes. Perforin creates pores in the membrane of the target cell, contributing to cell death[75, 76]. Granzymes induce apoptosis in the target cell through a number of pathways including the activation of caspases[77]. Memory CD8$^+$ T cells are responsible for maintaining molecular memory of defense against the pathogen. This information is conserved in their TCR, so that if the pathogen returns, the immune system can fight it off more efficiently[78]. When a pathogen has been cleared, the majority of effector CD8$^+$ T cells undergo apoptosis, while memory T cells persist in the blood, secondary lymphoid organs, and non-lymphoid tissues[79].

1.2.4 CD4⁺ T cells

CD4⁺ T cells facilitate the activation of other immune cells and regulate the immune response. CD4⁺ T cells are separated into several subsets: Th1, Th2, Th17, follicular helper T cell (Tfh), and regulatory T cells (Tregs). Th1 cells express the transcription factor t-box expressed in T cells (T-bet) and signal transducer and activator of transcription 1 (STAT1). They are involved in the type I T cell response, producing IFN-γ[80, 81]. Th1 cells are primarily responsible for activating macrophages and cytotoxic T cells and mediating the immune response against intracellular pathogens[82]. Upon activation, CD4⁺ T cells will differentiate into Th1 cells if signal 3 is provided by IL-12 or IFN-γ[38, 39, 83]. Th2 cells express the transcription factor GATA binding protein 3 (GATA-3) and STAT6[84]. They are involved in the type II T cell response, producing IL-4, IL-5, IL-9 and IL-13[80]. Th2 cells are responsible for mediating the B cell immune response and defence against parasites[85, 86]. Upon activation, CD4⁺ T cells will differentiate into Th2 cells if signal 3 is provided by IL-4[87]. Th17 express RAR-related orphan nuclear receptor γt (RORγt) and STAT3 and are involved in the type III T cell response, producing IL17 and IL-22[36, 88, 89]. This response is important for the immune response to extracellular bacteria and fungal invasion[90, 91]. Th17 cell differentiation from activated CD4⁺ T cells is associated with IL-6 and transforming growth factor β (TGF-β) *in vitro*[92]. Tfh express B cell lymphoma 6 (Bcl-6) and are involved in forming germinal centres. Tfh differentiation is governed through IL-6 and interaction with B cells in the follicles of secondary lymphoid organs[93]. Tregs express forkhead box class P3 (Foxp3) and are involved in maintaining self-tolerance and in regulating the immune response. A subset of activated CD4⁺ T cells also become memory CD4⁺ T cells. The memory CD4⁺ T cells persist after infection so that when a pathogen returns, CD4⁺ T cells with a TCR that recognizes the pathogen are able to mount a quick response and fight off the pathogen[94].

1.2.5 Regulatory T cells

Tregs were first identified as being $CD4^+CD25^+$ T cells that were able to protect against autoimmunity caused by neonatal thymectomy[95]. This was followed by great controversy as to the actual existence of Tregs. The seminal finding that led to their acceptance was the discovery of the transcription factor Foxp3 and its mostly unique expression in Tregs[96]. Foxp3 serves as a global regulatory transcription factor of Treg function[97]. A decrease in the expression of Foxp3 leads to a decrease in their ability to suppress the proliferation of T cells[97]. Foxp3 is the only reliable marker for Treg identification discovered to date. The primary roles of Tregs are to prevent autoimmune disease by maintaining self-tolerance, suppressing immune responses to non-threatening antigens (e.g., allergy, fetus, weak antigen simuli, etc.), and protecting commensal bacteria from immune responses[95, 98-101].

1.2.5.1 Treg subsets

Treg populations *in vivo* are heterogenous and are broken down into well-established general subsets, and less well-established specific subsets. Tregs that have committed to their lineage and/or differentiated in the host are termed natural Tregs (nTregs). nTregs are further divided into thymic Tregs (tTregs) and peripheral Tregs (pTregs). tTregs originate from the thymus, whereas pTregs differentiate from naïve $CD4^+$ T cells in the periphery. tTregs are separated from pTregs based on their expression of Helios, where tTregs are $Helios^+$ and pTregs are $Helios^-$ [102]. *In vitro* generated Tregs from naïve $CD4^+$ T cells are called induced Tregs (iTregs). iTregs are also $Helios^-$. tTregs are able to trigger the generation of pTregs *in vivo* and iTregs *in vitro* from $Foxp3^-CD4^+$ T cells[103]. Thus, it is possible that tTregs play an important role in the development of pTregs.

Tregs are needed to suppress diverse immune responses and, therefore, need to acquire specialized function in the periphery, becoming effector Tregs (eTregs). The determining factor for their specialization is their TCR affinity[104]. Low-affinity TCR eTregs upregulate TCR-independent suppressive pathways including Epstein-Barr virus induced gene 3 (Ebi3) and amphiregulin. Ebi3 is responsible for IL-35-mediated suppression and amphiregulin is a growth factor involved in tissue regeneration[105, 106]. High-affinity TCR eTregs upregulate TCR-dependant suppressive pathways, including cytotoxic T-lymphocyte associated protein 4 (CTLA-4), T cell immunoreceptor with Ig and ITIM domains (TIGIT), lymphocyte activation gene 3 (Lag3), and IL-10[107]. eTregs also develop specialized functions unique to the tissue, such as RORγt$^+$ eTregs in the lamina propria of the intestine that have enhanced suppressive capacity unique to that tissue[108]. It is hypothesized that these specializations arise from the unique inflammatory environment of the tissue in health or disease[109]. Characterizing eTreg specializations in other tissues has yet to be fully elucidated.

1.2.5.2 Treg differentiation

Tregs differentiate through two different pathways *in vivo*. Firstly, tTregs differentiate in the thymus. When exposed to self-antigens in the canonical negative selection step of T cell maturation, CD4$^+$ T cells with higher affinity to the self antigen than conventional T cells, but lower than conventional T cells which undergo apoptosis, become Foxp3 expressing Tregs[110]. Many pathways downstream of TCR signaling such as NF-κB, DNA methyltransferase activity, mammalian target of rapamycin (mTOR), sphingosine-1 phosphate receptor type 1 ($S1P_1$), NFAT, forkhead box class O1 (Foxo1), and Foxo3 have been shown to play important roles in tTreg development[111-116]. IL-2, and to a lesser degree, IL-7 and IL-15, also play an important role in tTreg differentiation[117, 118]. Evidence suggests that this is potentiated through STAT5 signaling[119]. It seems that tTreg generation is

independent of TGF-β signaling or that TGF-β signaling is redundant in tTreg development[120, 121].

pTregs differentiate from naïve $CD4^+$ T cells in the periphery. pTreg development seems to be distinct from tTreg development in that TCR engagement does not happen with self-antigens, rather it occurs with allergens or commensal bacteria[122-124]. The TCR repertoire of pTregs seems to be specific to the antigens encountered in the tissues in which they reside[124]. High affinity TCR recognition along with insufficient co-stimulation favour Foxp3 induction in $CD4^+$ T cells[125]. In contrast to tTregs, pTreg differentiation requires TGF-β induced signaling in the periphery[126]. IL-2 is also necessary for the differentiation of pTregs by preventing the differentiation of $CD4^+$ T cells into Th17 cells, likely through STAT5-mediated activation of Foxp3 expression[127]. TGF-β and TCR signaling both prevent the recruitment of DNA methyltransferases to the Foxp3 locus, preventing methylation and promoting expression of Foxp3[123].

1.2.5.3 Treg Suppression and Cytokine Production

Tregs play a role in suppressing the functions of a variety of immune cells, but the primary immune cells they express are T cells. Tregs suppress T cells through the following mechanisms: production of anti-inflammatory cytokines, cell-to-cell interactions, IL-2 consumption, adenosine production, cAMP production, and extracellular vesicles (EVs) (**Figure 1**). If one of the suppressive mechanisms is compromised, Tregs are still able to suppress T cells through the remaining mechanisms. Tregs are also plastic in nature, being able to acquire the expression of other helper T cell subset specific transcription factors. This acquirement seems to allow them to inhibit their T helper counterparts more effectively[128-131].

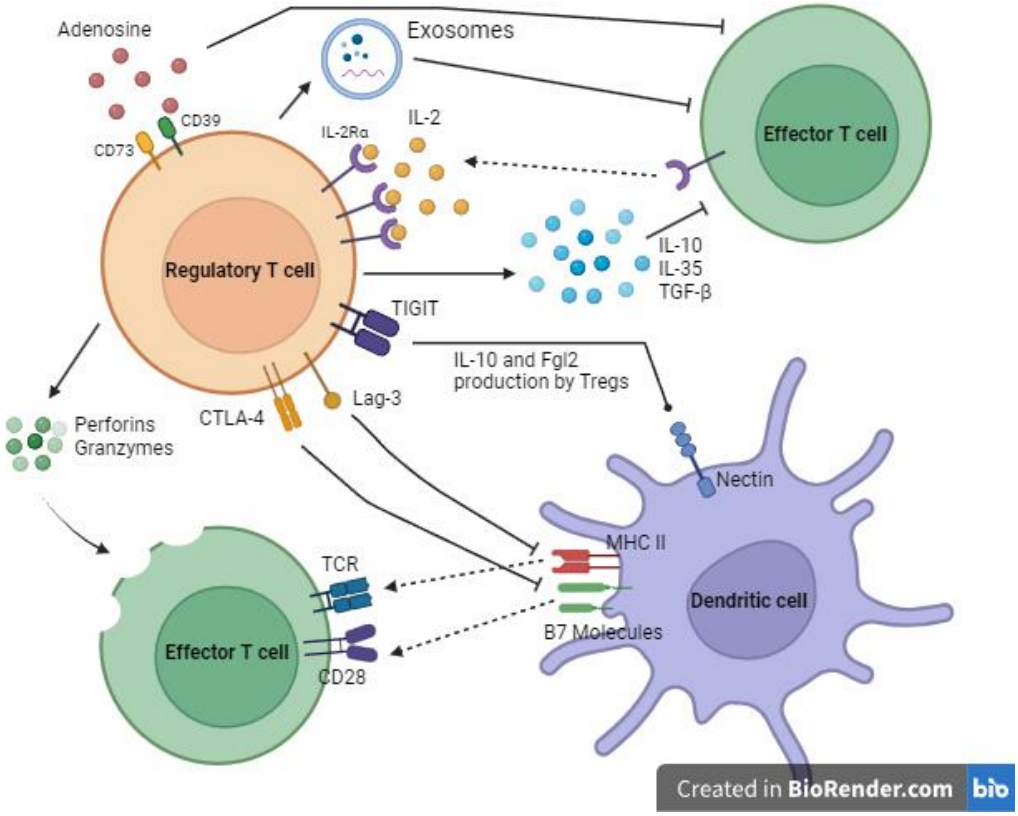

Figure 1. Treg suppression pathways. Created in BioRender.

Tregs produce TGF-β, IL-10, and IL-35, all of which are potent anti-inflammatory cytokines. Tregs produce high amounts of TGF-β, and blocking their production reduces their suppressive capacity *in vitro*[132]. TGF-β production by Tregs has been shown to be necessary to prevent colitis in mouse models[133, 134]. TGF-β production also induces the differentiation of pTregs as outlined above, increasing the number of pTregs and contributing to suppression. IL-10 has been shown to have anti-inflammatory effects on multiple cell types[135]. IL-10 is an important mediator of intestinal inflammation, and its absence prevents Tregs from preventing colitis[136]. IL-10 is needed to suppress Type I and Type 3 T cell responses but seems to be needed only in suppressing inflammation at environmental interfaces[137-139]. IL-35 production in Tregs inhibits T cell proliferation in murine models but is not constitutively expressed in human Tregs[105, 140].

Tregs express high levels of CD25, the IL-2 receptor alpha chain (IL-2Rα). IL-2 promotes the survival and proliferation of T cells. IL-2Rα has a higher affinity to IL-2 than IL-2R, therefore increased expression of CD25 on Tregs causes consumption of the IL-2 needed for T cell proliferation and survival. Addition of exogenous IL-2 is able to prevent the suppression of T cell proliferation by Tregs *in vitro*[141]. Other studies show that blocking CD25 on human Tregs does not result in a decrease in suppression[142]. This may occur because of compensatory mechanisms. Overall, it remains unclear as to the necessity of IL-2 consumption to the suppressive capacity of Tregs. It appears that the requirement of IL-2 consumption may be dependant on the specific environment in which the Tregs are acting.

Tregs suppress other immune cells through direct cell-to-cell interactions using a variety of cell surface receptors. CTLA-4 is expressed on the cell surface of activated T regs[143, 144]. CTLA-4 competes with CD80 and CD86 for binding to CD28, preventing co-stimulation and Signal 2 for the activation of T cells[145]. Mice with Tregs lacking CTLA-4

develop fatal autoimmune disease, demonstrating the importance of CTLA-4 to Treg function[146]. Tregs also express Lag-3, which binds to MHCII molecules, and thus inhibits the ability of APCs to activate T cells[147]. Tregs can express TIGIT, which binds to CD155 on DCs and prevents IL-12 production and which is also involved in suppressing T cell activation and proliferation[148, 149]. Through these interactions, Tregs inhibit the contacts between T cells and DCs necessary for T cell activation[150]. Tregs also express granzyme A and granzyme B, both of which have been shown to contribute to the contact-dependant suppression of T cells by Tregs[151, 152].

Tregs express the molecules CD39 and CD73 on their surface[153, 154]. Both CD39 and CD73 convert extracellular adenosine triphosphate (ATP) to adenosine diphosphate (ADP) or adenosine monophosphate (AMP). AMP inhibits DC and T cell function through the A2A adenosine receptor by elevating cyclic AMP (cAMP) levels[155]. Tregs that lack expression of CD39 have compromised suppressive activity *in vitro* and *in vivo*[156]. Tregs also produce high amounts of cAMP[157]. cAMP induces expression of the inducible cAMP early receptor (ICER), which acts as a repressor at the loci for IL-2 and IL-4, key proteins for T cell proliferation, and survival[158].

EVs are secreted by many different cell types and maintain many of the properties unique to the cell type of origin. Treg EVs mediate suppression of immune cells in a contact-independent manner. Similar to Tregs, Treg EVs express high levels of CD25, low-levels of CTLA-4, CD73, and CD39[159]. These proteins perform the same functions on Treg EVs as they do on Tregs. Treg EVs also express surface-bound IL-35[160]. Treg EVs contain micro RNAs (miRNA). miRNAs bind to specific DNA sequences, negatively regulating their expression. Some of these Treg EVs inhibit specific immune responses. For example, Treg EVs contain miR-155, let-7b, and let-7d to Th1 cells, all of which inhibit their proliferation and

production of IFN-γ[161]. Treg EVs also contain miRNA that inhibit DC function such as miR-150-5p and miR-142-3p, both of which induce DCs to be polarized into a tolerogenic phenotype[162]. Treg EVs transfer miR-503 along with inducible nitric oxide synthase (iNOS) enzyme, both of which induce apoptosis in the target cell[163]. Other miRNA in Treg EVs inhibit the differentiation of naïve $CD4^+$ T cell into pro-inflammatory subsets[164].

1.2.5.4 Treg Stability

Under homeostatic conditions, the expression of Foxp3 in Tregs is stable[165]. In an autoimmune environment, a subpopulation of Tregs lose Foxp3 expression, contributing to inflammation[166]. The basal promotor for Foxp3 is weak at inducing transcription of Foxp3[167]. This means that the induction of Foxp3 requires other enhancers and promotors to facilitate and maintain its expression. The conserved non-coding sequence 1 (CNS1) is critical for TGF-β mediated differentiation of Tregs. CNS1 contains binding sites for NFAT, retinoic acid receptor (RAR), and TGF-β-activated mothers against decapentaplegic homolog 3 (Smad-3)[168]. CNS3 seems to be the earliest mediator of initiation of Foxp3 expression, as CNS3 accessibility is linked with the probability of Foxp3 expression among $CD4^+$ T cell precursors[121]. CNS3 is also responsible for setting the threshold of TCR stimulation needed for Foxp3 expression[169].

iTregs have unstable Foxp3 expression, stemming from the heavily methylated CNS2 region[170]. Other studies have shown that demethylation at the Foxp3 promotor and CNS2 are needed for stable Foxp3 expression[171, 172]. An inhibitor of DNA methylation, azacytidine, and iTregs stimulated with IL-2-anti-IL-2 antibody complex both demethylated CNS2 and promoted Foxp3 stability[173, 174]. DNA demethylation is regulated by 5-hydroxymethylcytosine (5hmC) and the ten-eleven translocation (TET) family of enzymes[175-177]. Interestingly, vitamin

C has been shown to activate TET enzymes, leading to demethylation of CNS2[176]. Foxp3/Runx1/CBFβ protein complexes, CREB/ATF, NF-κB, and Ets-1 all bind to CNS2 and facilitate stable expression of Foxp3[121, 178]. Thus, CNS2 is responsible for Foxp3 stability in response to TCR stimulation[171].

1.3 Immunometabolism

There are six main metabolic pathways that cells use: glycolysis, the tricarboxylic acid (TCA) cycle, the pentose phosphate pathway (PPP), fatty acid synthesis, fatty acid oxidation, and amino acid metabolism. Activated immune cells use large amounts of glucose to power their activated states[179, 180]. Activated cells use glycolysis because they can quickly upregulate the enzymes needed to increase the rate of glycolysis. Glycolysis also provides many key intermediates that support cell growth[181]. The PPP produces large amounts of nicotinamide adenine dinucleotide phosphate (NADPH), which is important to both the production of reactive oxygen species and antioxidants via NADPH oxidase used for clearing infections by neutrophils and macrophages[182]. The PPP is also required to produce nucleotides needed for cellular proliferation. The TCA cycle is used by most T cell subsets, although as mentioned previously, effector T cells shift towards the use of glycolysis instead of the TCA[181]. Rapidly proliferating activated immune cells rely on aerobic glycolysis, whereas immune cell subsets with longer lifespans, such as Tregs and memory T cells, rely on fatty acid oxidation[181, 183]. Fatty acid oxidation is linked with the development of anti-inflammatory immune cells, whereas fatty acid synthesis is linked with pro-inflammatory immune cells. For example, increased fatty acid oxidation has been linked to decreased production of pro-inflammatory cytokines in tolerogenic macrophages, whereas LPS-stimulated macrophages have increased fatty acid synthesis[184, 185]. The mTOR pathway senses levels of amino acids and

uses this information to regulate cellular growth and proliferation. Thus, amino acid metabolism plays an important role in immune cell function. Glutamine is needed in macrophages to produce nitric oxide, contributing to their anti-pathogenic functions[186]. In T cells, glutamine consumption increases upon activation and is needed to respond to TCR stimulation[187]. Tryptophan and arginine have been shown to play important roles in immune cell function[188, 189].

1.3.1 DC metabolism

Metabolic changes occur upon cellular differentiation. During moDCs differentiation via GM-CSF and IL-4, the peroxisome proliferator-activated receptor-γ (PPARγ) is upregulated[190]. PPARγ upregulation leads to mitochondrial biogenesis and an increase in the production of acetyl-CoA[191]. Acetyl-CoA is necessary for fatty acid synthesis, and preventing the latter has been shown to block the differentiation of DCs in the periphery[192]. Therefore, fatty acid synthesis plays a key role in the differentiation of DCs from monocytes.

mTOR plays a key role in the regulation of cellular metabolism[193]. mTOR also plays in role in DC differentiation through FMS-like tyrosine kinase 3 (FLT3) and inhibition of mTOR with rapamycin prevents DC differentiation from BM *in vitro* and it reduces DC numbers *in vivo*[194, 195]. Conversely, increasing mTOR signaling leads to an increase in the number of DCs across subsets *in vivo*[196]. Similar results have been reported from stimulation of BM with GM-CSF[197].

Quiescent DCs require less energy and, as such, mostly rely on fatty acid oxidation to fuel oxidate phosphorylation[198]. This is consistent with the general rule that anti-inflammatory immune cells rely on fatty acid oxidation. Quiescent DCs consume glucose, but the use of the glucose for ATP production via oxidative phosphorylation or for other metabolic pathways remains unclear.

Upon activation, DCs exhibit increased glycolysis and glucose consumption consistent across myeloid and lymphoid lineages[198]. Blocking glycolysis upon activation of DCs with toll-like receptor (TLR) agonists results in inhibited activation. The increase in glycolysis results in production of acetyl-CoA needed to fuel the TCA cycle and produce ATP. This supports the diverse functions that activated DCs are required to perform to mediate the immune response[199]. Activated DCs also increase the use of fatty acid metabolism to promote the growth of the endoplasmic reticulum and golgi bodies[200]. The growth of the ER is needed to support the increase in protein output of activated DCs. The increase in fatty acid synthesis results in an increase in lipid droplets to store the fatty acids[201]. Sustained activation of DCs leads to a metabolic switch to Warburg metabolism[198]. In Warburg metabolism, the cell uses aerobic glycolysis and lactic acid fermentation to generate ATP[202]. This conserves metabolic resources for cellular proliferation and activated pathways, rather than allowing the metabolites to be fully catabolized in ATP production through the TCA cycle.

1.3.2 Treg metabolism

Upon receiving Signal 1 and Signal 2, the now activated T cells switch from oxidative phosphorylation to glycolysis to allow for cell growth, proliferation, and protein production[203]. Effector T cells maintain glycolysis and activate glutaminolysis to generate the ATP they need for effector functions[203]. Subsequently, after the initial activation and proliferation phase post-activation, Tregs switch to the use of oxidative phosphorylation and fatty acid oxidation for their metabolic needs[204]. Increasing oxidative phosphorylation in Tregs increases their suppressive capacity[205]. During proliferation, Tregs upregulate glucose transporter 1 (GLUT1) and mTOR. This following change is correlated with decreased suppressive capacity[206]. Increasing expression of GLUT1 leads to increased proliferation but decreased suppressive capacity. Conversely, starving Tregs of glucose prevents effector Th cell differentiation and favours Treg differentiation[207]. Foxp3 expression restrains GLUT1 expression, maintaining

proper differentiation and suppressive function[206]. Foxp3 also regulates Treg metabolism by supressing glycolysis and enhancing oxidative phosphorylation[204]. Discarding the need for glucose is important for Treg function in inflammatory environments, which lack high levels of glucose.

Tregs use fatty acid oxidation as a primary metabolic pathway. Treg fatty acid oxidation is regulated by AMP-activated kinase (AMPK), which inhibits fatty acid synthesis[208]. Activating AMPK leads to an increase in the proportion and number of Tregs *in vivo*[205]. Reduction in lipid droplets leads to an increase in Treg differentiation. This is most likely caused by an initial decrease in fatty acid synthesis[209]. Inhibition of fatty acid oxidation leads to decreased differentiation of Tregs, but not effector Th cells[205]. Tregs express higher levels of the genes required for fatty acid oxidation than effector Th cell subsets[210].

As outlined previously, mTOR is crucial in regulating transcription, cell growth, translation, and metabolism in response to exogenous factors. mTOR inhibition in Tregs is associated with an increase in suppressive function, while active mTOR is needed only for effector Th cells[112, 181]. mTOR inhibition leads to an increase in oxidative phosphorylation and reduction in glycolysis. mTOR activation in Tregs leads to decreased stability and lower Foxp3 expression through metabolic changes[211].

1.4 Foxo3a

Forkhead box O (Foxo) transcription factors are a family consisting of Foxo1, Foxo3, Foxo4, and Foxo6[212]. Foxo transcription factors mostly function as transcriptional activators. Foxo1 plays the most prominent role of these transcription factors, with Foxo3 playing a largely supportive or redundant role[116, 213-215]. Foxo3b is a pseudogene, as such, Foxo3a is synonymous with Foxo3. Foxo3a is prominently regulated through phosphorylation, which leads to retention in the cytosol[216, 217]. Therefore, active Foxo3a must be dephosphorylated to

act on the DNA in the nucleus. Foxo3a has been primarily studied as a longevity and tumor suppressor gene[218-220]. Interestingly, Foxo3a is the only gene associated consistently with the populations of “blue zones”, which are the human populations with the highest life expectancies[221]. Foxo3a has been identified as restraining NF-κB signaling and promoting activation induced-cell death in T cells[222-225]. Foxo3a has also been identified to play a largely anti-inflammatory role in different tissues[226, 227]. Unfortunately, conflicting evidence exists in both the two previous cases[228, 229]. Thus, the overarching role of Foxo3a in the immune system remains unclear.

1.4.1 Foxo3a in DCs

Foxo3a has been studied in DCs primarily in relation to cytokine production and its role in DC development and function outside of cytokine production has not been characterized. Decreased expression of *Foxo3a* in DCs leads to an increase in the expression of IL-6, IL-12, IL-15, TNF-α, and IFN-β[230, 231]. Foxo3a also restrains the capacity of DCs to activate T cells and maintain T cell viability by limiting the production of IL-6[230]. Tolerogenic DCs also produce IL-10 to mediate the immune response. In macrophages infected with mycobacterium, Foxo3a has been shown to restrain the production of IL-10. Loss of *Foxo3a* in mycobacteria-infected macrophages leads to an increase in the production of IL-10, suggesting a compensatory mechanism for the loss of suppressive function in the case of *Foxo3a* deficiency[232].

1.4.2 Foxo3a in Tregs

Foxo transcription factors have been found to be integral in Treg development and function through the control of Foxp3 expression[214, 233, 234]. Foxo1 and Foxo3a seem to play a redundant role and the deficiency in both is required for proper expression of Foxp3[116]. Foxo transcription factors must also be important in Treg function, as they bind to 662 genes in

Tregs[214]. Tregs deficient in *Cbl-b*, which is an activator of *Foxo3a*, have been shown to have compromised differentiation. Of note, Cbl-b also activated Foxo1; thus, loss of Cbl-b leads to a decrease in Foxo1 and Foxo3 expression, causing similar defects as in *Foxo1*$^{-/-}$*Foxo3*$^{-/-}$ mice[234]. The effects of Foxo3 on Treg development and function have not been studied in Tregs outside of models with inactive Foxo1 and Foxo3.

1.5 Gut Immunity and Chronic Inflammatory Disease

The gastro-intestinal (GI) tract's immune defenses are composed of three layers: the intestinal microbiota, the intestinal epithelial layer, and the mucosal immune system. The intestinal microbiota are composed of many different microorganisms (bacteria, fungi, and viruses) that have a symbiotic relationship with the host[235]. The composition of the microbiota in the GI tract is governed by many factors including genetics, diet, gender, age, environmental factors, socio-economic factors, and stress[236]. Commensal or "healthy" microbiota outcompete harmful bacteria for resources, maintaining homeostasis in the GI tract[237].

The intestinal epithelial layer physically separates the microbiota from the interior of the host. The mucus layer of the epithelial layer is the first defense that prevents direct interactions between epithelial cells and the microbiota[238]. Tight-junction complexes form barriers between intestinal epithelial cells, but toxins released by certain bacteria disrupt these complexes[239]. Changes in microbiota composition leads to a disruption in mucus production and local inflammation[240].

Most of the immune cells in the GI tract reside in the lamina propria. The GI tract represents a major secondary lymphoid organ and is the location where the immune system interacts with the largest amount of antigens because of the GI tract's massive surface area and the mucosal surface. Antigens enter the GI tract via DCs, macrophages, or by crossing

the epithelium[241, 242]. Gut immunity is governed by complex interactions between the immune system and microbiota, and dysregulation of the immune response, microbiota composition, or both leads to chronic inflammation.

1.5.1 Inflammatory Bowel Disease and Crohn's Disease

Canada has the highest incidence of inflammatory bowel disease (IBD) worldwide[243]. The progression and severity of IBD is governed by complex gene-environment interactions[243]. This means the cause of the disease can vary from person-to-person, complicating treatment. Currently, IBD affects about 322,600 Canadians and is expected to rise to 470,000 Canadians by 2035[244]. Unlike ulcerative colitis, the mild form of IBD, Crohn's Disease (CrD) affects the whole digestive tract, is discontinuous, and affects the entire thickness of the bowel wall[243]. Treatment of IBD progresses from simple drug treatment to surgery in severe cases, leading to poor quality of life and poor patient outcomes for patients suffering with the disease. The chronic nature of the disease is worsened by the fact that current treatments are limited to managing symptoms, rather than dealing with the underlying cause. As the underlying mechanisms are poorly understood and vary from person-to-person, there is a great need for personalized treatment options that address the underlying cause.

Recently, genome-wide association studies (GWASs) have identified about 200 loci that are associated with the development of IBD, most of them being associated with CrD as well[245]. The most closely associated genes being X-linked inhibitor of apoptosis protein (*XIAP*) and *IL-10*. However, these loci are not associated with progression of the disease to the severe form. New GWASs studies have been able to identify 4 loci associated with the progression of IBD. The 4 loci that have been identified to be associated with a poor prognosis of CrD are human *Foxo3a*, X active specific transcript (*XACT*), *MHC*, and insulin growth factor binding proteins 1 to 3 (*IGFBP*)[246]. This led to the hypothesis that "the genetic contribution to

prognosis in CrD is largely independent from the contribution to disease susceptibility," which possibly narrows the focus of research from 200 loci to 4 in regard to severe IBD.

1.5.1.1 DCs in Crohn's Disease

DCs are very important in regulating the response to the gut microbiota. DCs appear to play a critical role in the maintenance of chronic inflammation in CrD[247, 248]. Activated DCs tend to accumulate at the sites of inflammation in CrD patients, activating T cells and increasing inflammation[249, 250]. This contributes to the aberrant activation of T cells common in CrD patients. IL-10 plays an important role in inhibiting APC function, and the pro-inflammatory environment in CrD skews DCs to increased activation of T cells[135]. DCs play a central role in activating the adaptive immune response, but their overall role in the pathogenesis of CrD remains to be fully elucidated.

1.5.1.2 Treg in Crohn's Disease

Tregs play an essential role in mediating the immune response to bacteria in the gut. Several studies have suggested that Tregs may be critical in preventing the development of spontaneous intestinal inflammation in IBD[251, 252]. Patients with CrD have reduced numbers of pTregs in the lamina propria[253]. It seems that IL-10 plays a prominent role in this rescue[251]. Other studies demonstrate the importance of balance between Tregs and effector Th cells in the management of CrD[254, 255]. A cutting-edge study in a mouse model showed that a single transfer of functional Tregs was able to rescue a colitic phenotype[256]. As a suppressive cytokine, IL-10 plays a key role in suppression of T cells by Tregs. Mice with *IL-10*-deficient Tregs develop severe immune-mediated colitis[138]. Studies using chimeric antigen receptor (CAR)-Tregs directed against inflammatory ligands have been shown to be effective at

suppressing colitis in mice, and a new study shows promising results in humans[257-259]. These studies outline the importance of suppression by Tregs in the management of CrD[255].

1.5.1.3 Mouse models of CD

Current mouse models for CrD fall into 3 groups: bacteria-infected, gene-manipulated, or spontaneous models. Bacteria-infected models are problematic as infection is not included in the natural progression of CrD in humans. Most gene manipulated models show inconsistent development of CrD or require perforation of the gut barrier using artificial means, such as dextran-sodium sulfate (DSS). Spontaneous models in mice are limited to the SAMP1/YitFc mouse strain, and as CrD is caused by diverse factors, more representative models are needed to study the pathogenesis of CrD[260].

GWASs have shown that inactivation of a susceptibility allele and progression allele are needed for the development of severe CrD. We have created a novel mouse model for CrD in which a susceptibility allele, *IL-10*, and a progression allele, *Foxo3a*, have been deactivated. *Foxo3a*$^{-/-}$*IL-10*$^{-/-}$ mice spontaneously develop a CrD-like phenotype and spontaneously lose weight after day 36 post birth[261]. The phenotype includes many CrD-associated symptoms: diarrhea, weight loss, rectal bleeding, focal erosion of submucosa, loss of epithelial integrity, and patchy inflammation. The CrD-like phenotype of *Foxo3a*$^{-/-}$*IL-10*$^{-/-}$ mice is reminiscent of CrD in humans (focal erosion, apoptotic crypt abscess, crypt dropout, crypt distortion, expansion of lamina propria, and inflammatory changes)[261]. We have previously reported that *Foxo3a*$^{-/-}$*IL-10*$^{-/-}$ T cells experience excessive glutaminolysis, where Foxo3a mediates a critical checkpoint that prevents the development of colitis in *IL-10*-deficient mice[261]. Preliminary data suggests Treg function in *Foxo3a*$^{-/-}$*IL-10*$^{-/-}$ mice is also compromised, which we hypothesize skews them towards a pro-inflammatory state. Unpublished data also show that *Foxo3a*$^{-/-}$*IL-10*$^{-/-}$ DCs activate CD4^{+} T cells to a greater

extent, leading to the production of greater amounts of pro-inflammatory cytokines. Overall, Foxo3a seems to play a protective role in the interactions between $CD4^+$ T cells, DCs, and Tregs that maintains inflammatory homeostasis.

1.6 Rational

The lamina propria of *Foxo3a*$^{-/-}$*IL-10*$^{-/-}$ mice contains a higher proportion of DCs than the control genotypes (WT, *Foxo3a*$^{-/-}$, and *IL-10*$^{-/-}$), which is reflected among all DC subsets[261]. The greatest difference comes from $CD11b^+$ DCs ($CD11b^+$; $CD11c^+MHCII^+$). The lamina propria of *Foxo3a*$^{-/-}$*IL-10*$^{-/-}$ mice also contains a higher proportion of monocytes[261]. *Foxo3a*$^{-/-}$ *IL-10*$^{-/-}$ DCs produce significantly more IL-12p70, TNFα, and IL-6[262]. In addition, *Foxo3a*$^{-/-}$*IL-10*$^{-/-}$ and *Foxo3a*$^{-/-}$ DCs contribute to increased $CD4^+$ T cell proliferation and survival[262]. Therefore, an aim of this study was to determine the source of the increased number of dysregulated *Foxo3a*$^{-/-}$*IL-10*$^{-/-}$ DCs that contribute to CrD-like phenotype.

The development of intestinal inflammation leading to the CrD-like phenotype in *Foxo3a*$^{-/-}$*IL-10*$^{-/-}$ mice is highly dependant on the microbiota. Because *Foxo3a*$^{-/-}$*IL-10*$^{-/-}$ mice are kept in a pathogen free facility, the limited bacteria to which they are exposed can change greatly from month to month. As such, there has recently been changes in the development of intestinal inflammation in the *Foxo3a*$^{-/-}$*IL-10*$^{-/-}$ mice. This has allowed the study of differences between sick and healthy *Foxo3a*$^{-/-}$*IL-10*$^{-/-}$ mice. nTregs from the lamina propria of *Foxo3a*$^{-/-}$ *IL-10*$^{-/-}$ mice have lower expression of Foxp3, indicating compromised function[262]. In addition, using αCD4 and αCD8 antibodies to deplete $CD4^+$ and $CD8^+$ T cells rescues the CrD-like phenotype in *Foxo3a*$^{-/-}$*IL-10*$^{-/-}$ mice[261]. In addition, Foxo3a restrains mTORC1 signaling by repressing the transcription of GLS/GLS2 in activated T cells[261]. Therefore, the function of *Foxo3a*$^{-/-}$*IL-10*$^{-/-}$ Tregs was investigated given the role they have been shown to play in the development of CrD.

1.6.1 Hypothesis

The inflammatory milieu in *Foxo3a*$^{-/-}$*IL-10*$^{-/-}$ mice drives the plasticity of Tregs towards a pro-inflammatory phenotype and increases the ability of DCs to activate T cells.

1.6.2 Objectives

Develop an understanding of the mechanisms behind progression alleles of IBD to determine novel pathways that can be targeted for therapeutic intervention.

Aim 1: Determine the causes of increased stimulation of CD4^{+} T cells by *Foxo3a*$^{-/-}$*IL-10*$^{-/-}$ DCs.

Aim 2: Determine the underlying mechanisms causing decreased suppression by *Foxo3a*$^{-/-}$ *IL-10*$^{-/-}$ Tregs on effector T cells.

Aim 3: Characterize the differentiation of *Foxo3a*$^{-/-}$*IL-10*$^{-/-}$ iTregs.

Aim 4: Characterize the stability of *Foxo3a*$^{-/-}$*IL-10*$^{-/-}$ iTregs under varying conditions.

2.0 Materials and Methods

2.1 Mouse Strains

Mice were housed in the University of Ottawa animal care facility. Care for the mice was in accordance with the Canadian Council on Animal Care guidelines. Wild-type (WT) CD45.2^{+} (C57BL/6J), WT CD45.1^{+} (B6.SJL2), and *IL-10*$^{-/-}$ mice were obtained from Jackson Laboratories (Bar Harbor, Maine, USA). The aforementioned colonies were maintained by breeding homozygous females with homozygous males. *Foxo3a*$^{-/-}$ mice were generated using a gene-trap targeting strategy, which deactivates the *Foxo3a* allele. The *Foxo3a*$^{-/-}$ colony was maintained by breeding *Foxo3a*$^{+/-}$ females with *Foxo3a*$^{-/-}$ males. *Foxo3a*$^{-/-}$*IL-10*$^{-/-}$ mice were generated by breeding *Foxo3a*$^{+/-}$*IL-10*$^{-/-}$ males and females. *Foxo3a*$^{-/-}$ female mice are unable to reproduce, and as such, *Foxo3*$^{+/-}$ female mice were used for all breeding. *Foxo3a* and *Foxo3a-IL-10* pups were genotyped using genomic polymerase chain reaction (PCR) on ear samples. Mice were bred and maintained on protocols and procedures (BMIe-3954 and BMIe-1638) approved by the University of Ottawa Animal Care Committee and Ethics Board.

2.2 Monitoring Illness in *IL-10*$^{-/-}$ and *Foxo3a*$^{-/-}$*IL-10*$^{-/-}$ mice

The development of spontaneous intestinal inflammation was monitored in *IL-10*$^{-/-}$ and *Foxo3a*$^{-/-}$*IL-10*$^{-/-}$ male and female mice twice weekly. Both sexes were equally distributed between groups. Age-matched and sex-matched mice were used in all experiments. Mice were euthanized upon reaching humane endpoint as defined by >15% weight loss, rectal bleeding, rectal prolapse, soft stool, poor movement, M1-M2 hunching, and M1-M2 piloerection. Experiments that used a *Foxo3a*$^{-/-}$*IL-10*$^{-/-}$ mouse that had not developed a Crohn's-like phenotype are denoted as healthy, while experiments that used a *Foxo3a*$^{-/-}$*IL-10*$^{-/-}$ mouse that had developed a Crohn's-like phenotype are denoted as sick.

2.3 Bone Marrow Cell Isolation

Mouse tibia, femur, and hip bones were extracted from the hind limbs. Ends of the bones were cut using dissection scissors, then flushed from the bones with RPMI-1640 (Gibco™ #31800-089) supplemented with 8% fetal bovine serum (FBS) (Gibco™ #12483-020), 55 µM 2-marcaptoethanol (Gibco™ #21985023), and 50 ng/mL gentamycin (Gibco™ #15750060) (R8). BM was flushed through a 70 µM (Fisherbrand™ #22-363-548) filter using 27.5-gauge needle (Terumo #SS-01T2713)) into a 50 mL falcon tube over ice. BM cells were centrifuged at 500g for 5 mins and re-suspended in R8. Cells were then stained using 3% acetic acid with methylene blue (StemCell Technologies™ #07060) and then counted manually using a hemocytometer. Methylene blue does not stain red blood cells, thus only immune cells were counted.

2.4 Monocyte Isolation

BM cells were harvested as described in the section **Bone Marrow Cell Isolation**. The EasySep™ Mouse Monocyte Isolation Kit (StemCell Technologies™ #19861) was used to isolate monocytes. The manufacturer's protocol was followed except BM cells were resuspended at 200 million cells/mL in EasySep™ Buffer (StemCell Technologies™ #20144) before beginning isolation. The purity of monocytes was confirmed by flow cytometry ($CD11b^{+}Ly\text{-}6C^{+}Ly\text{-}6G^{-}$ and $CD49b^{-}CD45R^{-}CD3^{-}CD170^{-}CD117^{-}$) (**Figure 2 a**).

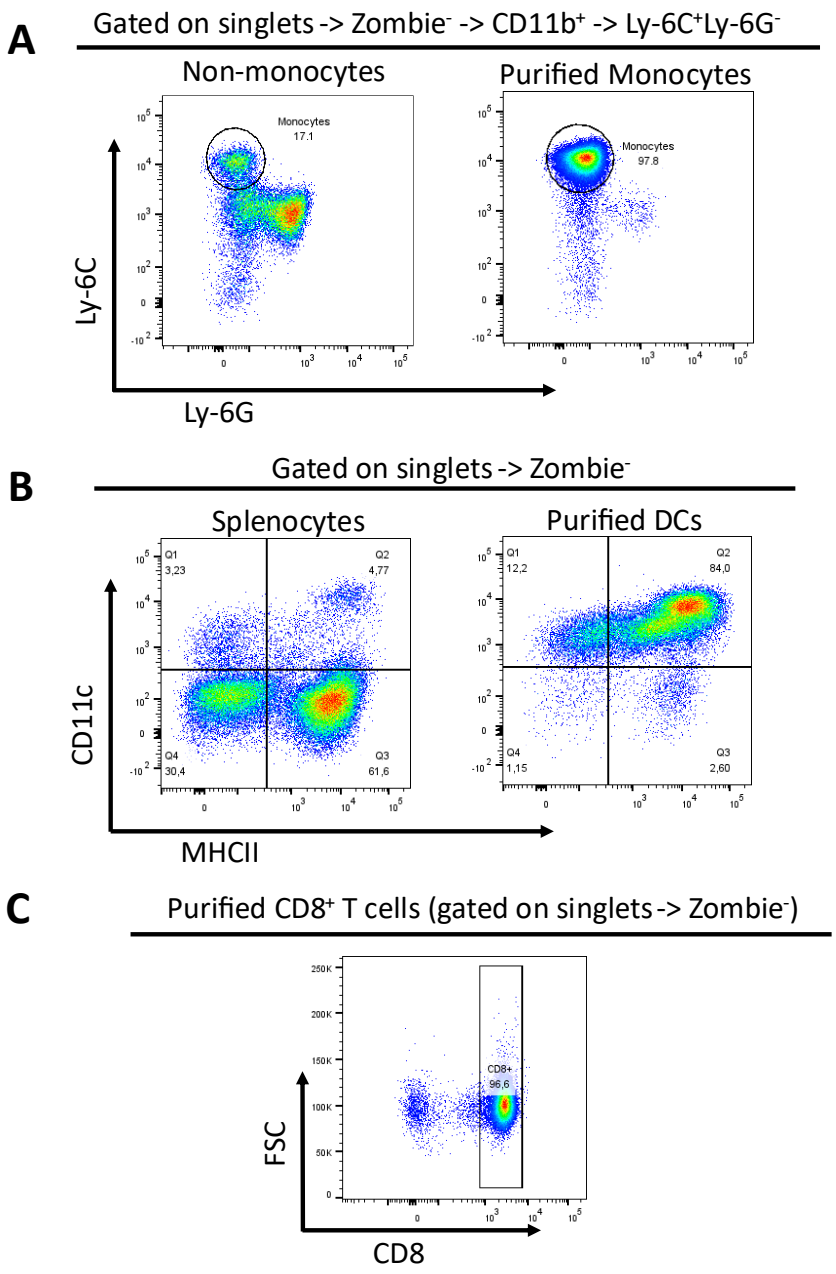

Figure 2. Isolation of BM monocytes and splenic DCs. (A) Representative FACS plots of purified monocytes ($CD11b^+Ly\text{-}6C^+Ly\text{-}6G^-$) from the BM of a WT mouse using the Stemcell™ EasySep™ Mouse Monocyte Isolation Kit (#19861). Monocytes were CD49b, CD45R, CD3, CD170, and CD117 negative. **(B)** Representative FACS plots of purified DCs from the spleen of a WT mouse using the Stemcell™ EasySep™ Mouse CD11c Positive Selection Kit II (#18780). **(C)** Representative FACS plots of purified $CD8^+$ T cells from the spleen of a WT mouse using the Stemcell™ EasySep™ Mouse $CD8^+$ Isolation Kit (#19853). Cells were stained with fluorescent antibodies, acquired on a BD LSRFortessa™, and analyzed using FlowJo™ software.

2.5 Flow Cytometry

Flow cytometry was used to identify different cell types and metabolic and cytokine profiles. A BD LSRFortessa™ or Cytek® Aurora was used for recording all samples. Between $3*10^5$ and $3*10^6$ cells were added to FACS tubes. Cells were washed twice with 1x phosphate buffered saline (PBS). If used in the experiment, 2 µM Bodipy 493/503 (Invitrogen™ #D3922) was added to the cells and they were incubated at 37°C for 20 minutes then washed once with 1X PBS. Zombie Yellow™ (Biolegend® #423103) was then added to each sample at 1:100 dilution and incubated for 10 minutes at room temperature to assess cell viability. Subsequently, cells were incubated with Fc block (BD Pharminogen™ #553142) for 5 mins at 4°C to prevent non-specific binding of antibodies. Fluorochrome-conjugated antibodies were added according to the experiment (**Table 1**). Cells were incubated for 30 minutes at 4°C. Cells were protected from light during all incubation steps. Cells were then washed twice with 1x PBS to remove unbound fluorochrome-conjugated antibodies and resuspended in 1x PBS. For intracellular staining, the eBioscience™ Foxp3/Transcription Factor Staining Buffer Set (eBioscience™ #00-5523-00) was used according to the manufacturer's protocol. For all washing steps, half the amount of buffer was used. Data were analyzed using FlowJo™ V10 (BD Life Science). If used in the experiment, 0.05 mg/mL Filipin III (Sigma-Aldrich #SAE0089) was added to the cells and they were subsequently incubated 37°C for 30 minutes followed by a wash with fixation buffer. The gating strategy for identifying Tregs is shown in **Figure 3**.

Table 1. Antibodies used in flow cytometry.

Antibody	Conjugated Fluorophore	Manufacturer	Catalog/Reference Number
Foxp3	APC	Invitrogen™	17-5773-82
CD25	PE	Biolegend®	102007
	BV421	Biolegend®	102033
CD4	FITC	Biolegend®	100406
	PE	Biolegend®	100511
ST2	PerCP-efluor™710	Invitrogen™	46-9335-80
CTLA-4	PE-Cyanine7	Invitrogen™	25-1522-80
TIGIT	BV421	Biolegend®	124111
TNF-α	PE-Cyanine7	Invitrogen™	25-7321-81
IFN-γ	PE-Cyanine7	Biolegend®	505825
IL-17a	PE-Cyanine7	Biolegend®	506921
Brefeldin A	N/A	Invitrogen™	00-4506-51
MHCII	APC	Biolegend®	107613
	APC	Invitrogen™	17-5321-81
CD11c	FITC	Biolegend®	117305
	efluor™450	Invitrogen™	48-0114-81
CD11b	PE-Cyanine7	Biolegend®	101216
Lag3	APC-Cyanine7	Biolegend®	152225
CD45.2	APC-Cyanine7	Biolegend®	109825
CD45.1	PE	Invitrogen™	12-0453-82
CD8α	APC	Biolegend®	100711
Ly-6C	PE	Biolegend®	128008
Ly-6G	efluor™450	Invitrogen™	48-9668-82
CD3	APC	Biolegend®	100236
CD117	APC	StemCell Technologies™	60034A2.1
CD170	APC	Biolegend®	155507
CD45R	APC	eBiosciences™	17-0453-81
CD49b	APC	eBiosciences™	17-5971-81

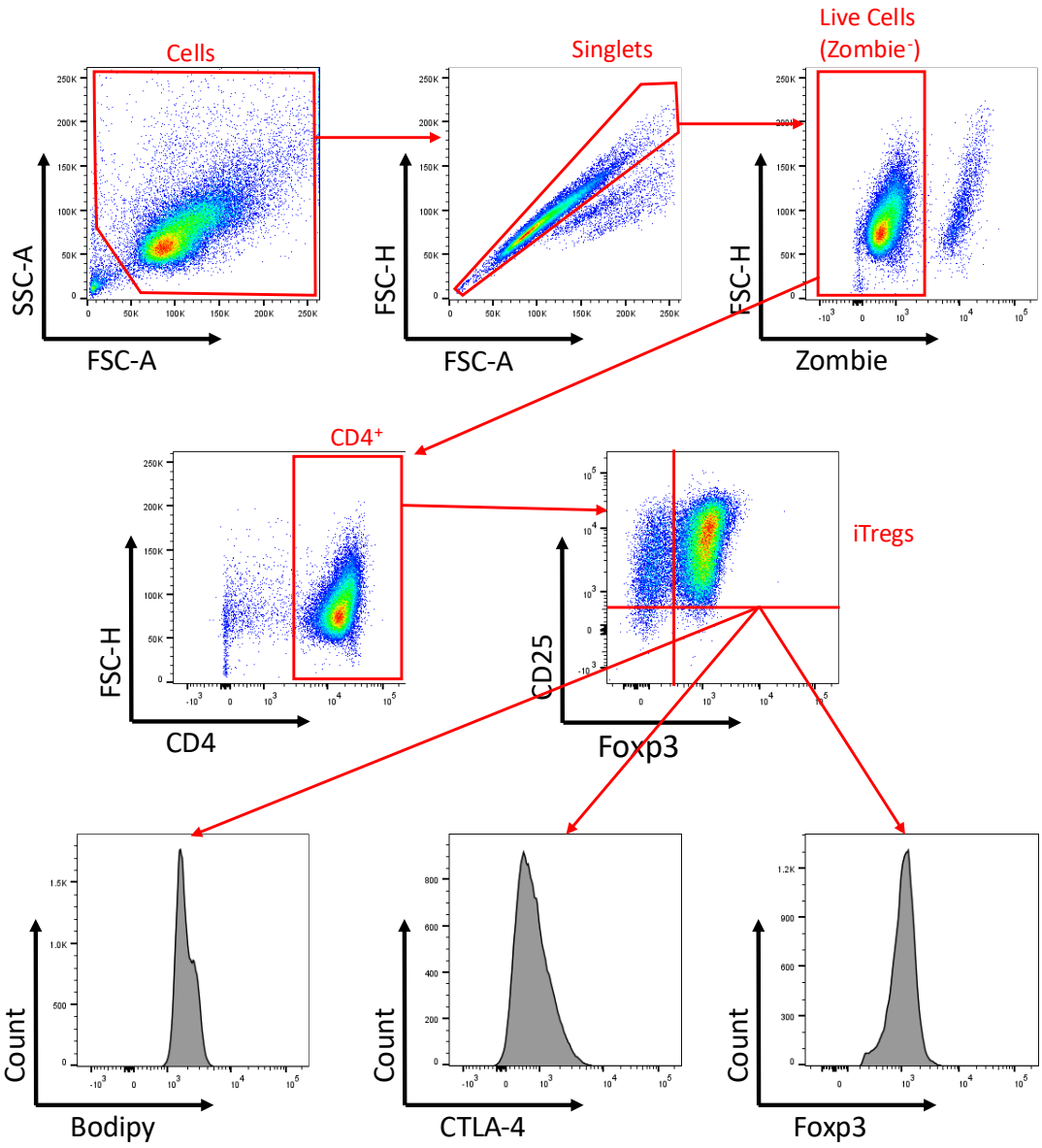

Figure 3. Gating strategy for identifying Tregs, their cell surface markers, and intracellular markers. Representative FACS plots depicting the gating strategy used to identify Tregs. Gating strategy is as follows: cells -> singlets -> Zombie$^-$ -> CD4$^+$ -> CD25$^+$Foxp3$^+$ -> other markers. Cells were obtained through *in vitro* differentiation of iTregs from purified splenic CD4$^+$ T cells and then stained with fluorescent antibodies, acquired on a BD LSRFortessa™, and analyzed using FlowJo™ software.

2.6 Generation of Myeloid DCs from Monocytes

Monocytes were isolated as described **Monocyte Isolation**. $1*10^5$ monocytes were seeded per well in a 96-well plate in R8 media supplemented with 10 ng/mL GM-CSF (StemCell Technologies™ #78017.1). After incubating for 48 hours at 37°C, cells were harvested and stained for flow cytometry. moDC purity was confirmed by flow cytometry ($CD11b^+CD11c^+MHCII^+$).

2.7 Generation of Myeloid DCs from BM

BM cells were isolated as described in **Bone Marrow Isolation**. $1*10^5$ BM cells were seeded per well in a 96-well plate in R8 media supplemented with 10 ng/mL GM-CSF (StemCell Technologies™ #78017.1). After incubating for 72 hours at 37°C, cells were harvested, manually counted, and stained for flow cytometry. moDC purity was confirmed by flow cytometry ($CD11b^+CD11c^+MHCII^+$).

2.8 Splenocyte Isolation

Spleens were harvested from mice and placed in R8 media in a petri dish over ice. Spleen weight and length were measured if required to determine differences between genotypes. The spleens were mashed between two double-frosted slides (VWR™ # 16004-418) and passed through a 70 µM filter into an empty 50 mL falcon tube over ice. The splenocytes were centrifuged at 500g for 5 mins and resuspended in R8 media. The cells were then manually counted.

2.9 Dendritic Cell Isolation

Splenocytes were isolated as described in **Splenocyte Isolation**. The EasySep™ Mouse CD11c Positive Selection Kit II (StemCell Technologies™ #18780) was used to isolate DCs according to the manufacturer's protocol. After adding the selection cocktail, fluorochrome-conjugated αCD11c antibody was added at 0.4 µg/mL to stain $CD11c^+$ cells that would otherwise be occupied with the selection cocktail. Addition of CD11c antibody allows the purity of DCs to be confirmed by flow cytometry ($CD11b^+CD11c^+MHCII^+$) (**Figure 2 b**).

2.10 *In vitro* inhibition of DC cytokine production

DCs were purified as outlined in **Dendritic Cell Isolation**. DCs were resuspend in R8 media and 10^5 DCs were seeded per well in a 96-well plate. To ensure both proper adherence and that cells were not stressed, they were incubated for 1 hour at 37°C. Various inhibitors were added (**Table 2** and **Table 3**), and cells were incubated again for 1 hour at 37°C to allow inhibitors to inhibit their respective signaling pathways before stimulation. A solution of 100 ng/mL LPS was then added to stimulate the DCs. Supernatants were collected at 6 and 12 hours post-stimulation at 37°C for cytokine analysis.

Table 2. Inhibitors used in DC experiments.

Inhibitor	Manufacturer	Catalog/Reference Number
Rapamycin	LC Laboratories	R-5000
Paquinomod	Millipore Sigma	SML-2833-5MG
Cerulenin	Tocris Biosciences	6702
C75	MedChem Express	HY-12364
Denifanstat	Selleckchem	S9714
STATTIC	Selleckchem	S7024
mCAN10	Cantargia	Gift (N/A for sale)
MK2 Inhibitor	Selleckchem	S6930

Table 3. Pathways upregulated in *Foxo3a*$^{-/-}$*IL-10*$^{-/-}$ DCs and inhibitors used to target upregulated pathways.

Inhibitor	Pathway	Method of Inhibition
STATIC	STAT3 signaling	Binds to SH2 domain of STAT3 and prevents activation and dimerization
Paquinimod	S100A8/A9 signaling through TLR4	Binds to TLR4 and prevents S110A8/A9 binding
CAN10	IL-1 family of cytokines signaling	IL-1RAP antibody
Denifanstat	Fatty acid synthesis	Targets the β-ketoacyl synthase domain of fatty acid synthase
C75	Fatty acid synthesis	Targets the β-ketoacyl synthase domain of fatty acid synthase
Cerulenin	Fatty acid synthesis	Targets the β-ketoacyl synthase domain of fatty acid synthase
MK2 Inhibitor	TNF-α production	Inhibits MK2, which prevents degradation of TNF-α
Rapamycin	mTOR signaling	Forms complex with FKBP12, which binds and inhibits mTORC1

2.11 Measurement of cytokines at the protein level

Sandwich enzyme-linked immunosorbent assays (ELISA) were used to measure cytokine concentrations in the supernatants collected from various experiments. The following kits were used to analyze cytokine concentration: BD OptEIA™ Mouse IL-6 ELISA Set (BD Biosciences #555240), BD OptEIA™ Mouse TNF (Mono/Mono) ELISA Set (BD Biosciences #555268), ELISA MAX™ Mouse IL-17a (Biolegend® #432501), and ELISA MAX™ Mouse IFN-γ (Biolegend® #430801). Extra-high binding 96-well plates (Thermo Scientific™ #439454) were used for the assays and 3,3',5,5'-tetramethylbenzidine (TMB) (Invitrogen™ #002023) was used as the chromogenic substrate for visualization. The reaction was stopped with 2 N sulphuric acid diluted in water. Absorbance was detected at 450-570 nm on a FilterMax F5 multimode microplate reader (Molecular Devices). Data were analyzed using SoftMax Pro software (Molecular Devices).

2.12 Isolation of $CD4^+$ T Cells

Splenocytes were isolated as described in **Splenocyte Isolation**. The EasySep™ Mouse $CD4^+$ T cell Isolation Kit (StemCell Technologies™ #19852) was used to isolate $CD4^+$ T cells. The manufacturer's protocol was followed except splenocytes were resuspended at 200 million cells/mL in EasySep™ Buffer (StemCell Technologies™ #20144) before beginning isolation. The purity of $CD4^+$ T cells was confirmed by flow cytometry ($CD4^+$) (**Figure 4 c**).

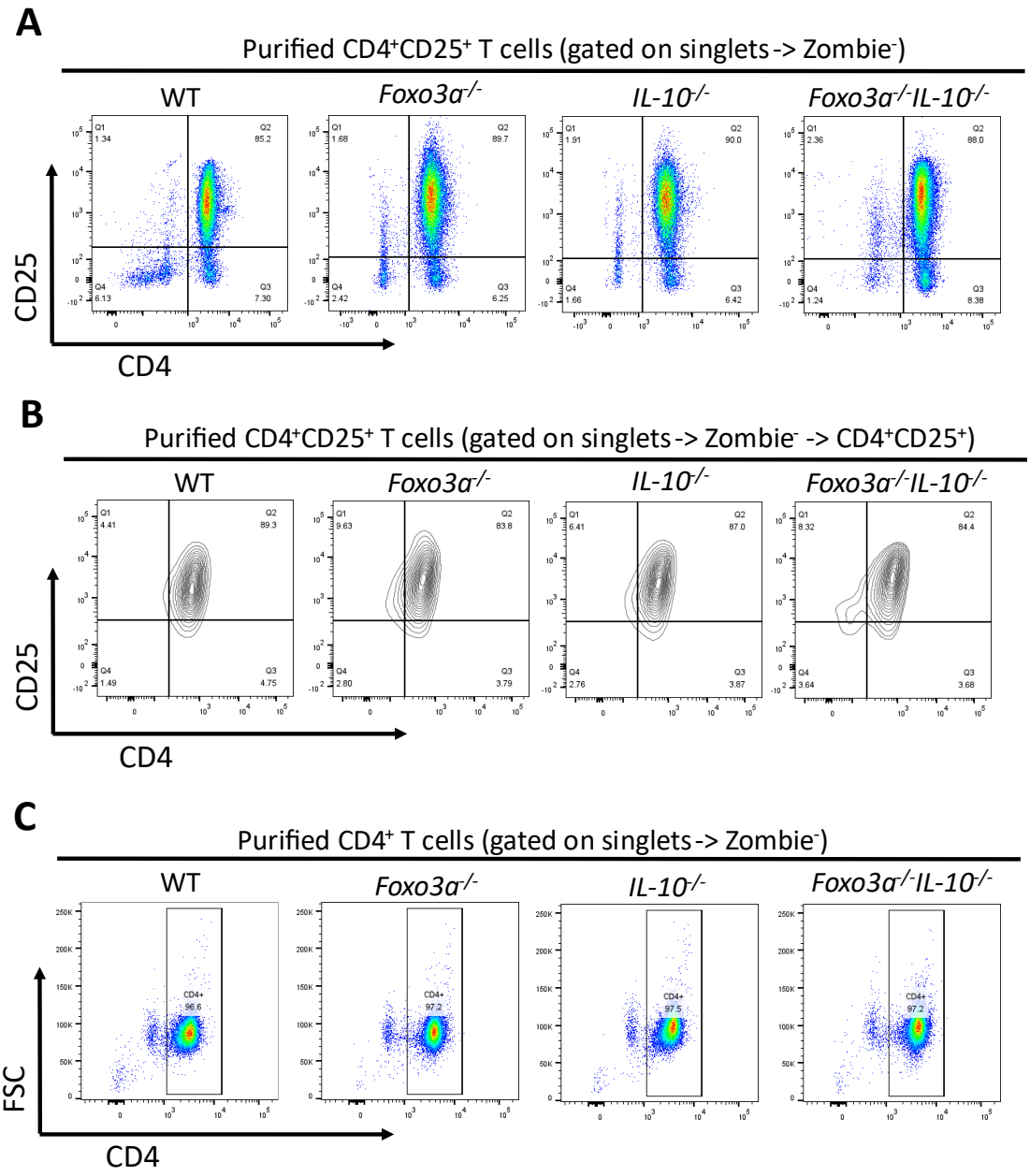

Figure 4. Purified CD4⁺CD25⁺ T cells from spleens serve as the best method for purifying nTregs from splenocytes. (A) Representative FACS plots of purified CD4⁺CD25⁺ T cells from the spleens of all four genotypes using the Stemcell™ EasySep™ Mouse CD4⁺CD25⁺ Regulatory T Cell Isolation Kit II (#18783). **(B)** Representative FACS plots of CD4⁺CD25⁺Foxp3⁺ T cells from purified CD4⁺CD25⁺ T cells from the spleens of all four genotypes. **(C)** Representative FACS plots of purified CD4⁺ T cells from the spleens of all four genotypes using the Stemcell™ EasySep™ Mouse CD4⁺ T Cell Isolation Kit (#19852). Cells were stained with fluorescent antibodies, acquired on a BD LSRFortessa™, and analyzed using FlowJo™ software.

2.13 Isolation of $CD4^+CD25^+$ T Cells

$CD4^+CD25^+$ T cells serve as the best alternative for isolating nTregs from mice without a Foxp3-GFP reporter. In each experiment, WT, *Foxo3a*$^{-/-}$, *IL-10*$^{-/-}$, and *Foxo3a-IL-10*$^{-/-}$ mice are used, which makes FACS sorting unrealistic. Splenocytes were isolated as described in **Splenocyte Isolation.** The EasySep™ Mouse $CD4^+CD25^+$ Regulatory T cell Isolation Kit II (StemCell Technologies™ #18783) was used to isolate $CD4^+$ T cells according to the manufacturer's protocol. The purity of $CD4^+CD25^+$ T cells and $CD4^+CD25^+Foxp3^+$ T cells (Tregs) were confirmed by flow cytometry ($CD4^+CD25^+$ and $CD4^+CD25^+Foxp3^+$) (**Figure 4 a, b**). A limitation of purifying $CD4^+CD25^+$ T cells is that it results in a low number of $CD4^+CD25^+$ T cells to use for experiments. To overcome this limitation, a protocol was optimized to differentiate iTregs from purified $CD4^+$ T cells, resulting in much higher cell numbers to be used for experiments (**Figure 5**).

2.14 Isolation of $CD8^+$ T Cells

Splenocytes were isolated as described in **Splenocyte Isolation**. The EasySep™ Mouse $CD8^+$ T cell Isolation Kit (StemCell Technologies™ #19853) was used to isolate $CD8^+$ T cells. The manufacturer's protocol was followed except splenocytes were resuspend at 200 million cells/mL in EasySep™ Buffer (StemCell Technologies™ #20144) before beginning isolation. The purity of $CD8^+$ T cells was confirmed by flow cytometry ($CD8^+$) (**Figure 2 c**).

2.15 Regulatory T cell Suppression Assay

To distinguish between Tregs and T cells using flow cytometry, $CD45.1^+$ WT mice were used so isolate $CD4^+$ T cells. $CD45.1^+$ WT splenocytes and $CD45.2^+$ splenocytes from the four

genotypes were isolated as described in **Splenocyte Isolation**. CD45.1$^+$ WT splenocytes were resuspended at 1*10^7 cells/mL in 0.125 µM carboxyfluoresceine succinimidyl ester (CFSE) (Sigma-Aldrich #21888) in 1x PBS for 10 minutes at 37°C. Excess CFSE was quenched with an equal volume of R8 media and placed on ice for 5 minutes. Cells were then washed twice with 1x PBS and resuspended in R8 media. R8 media contained rapamycin (LC Laboratories #R-5000) if used in the experiment. CFSE stains proteins with a finite amount of a fluorescent label, so when they divide, this signal from the fluorescent label reduces. This allows tracking of cell division through time. WT CD45.1$^+$CD4$^+$ (or CD8$^+$) T cells and CD4$^+$CD25$^+$ T cells (or iTregs) from the four genotypes were isolated as described in **Isolation of CD4$^+$ T cells**, **CD8$^+$ T cells**, and **CD4$^+$CD25$^+$ T cells**. 5*10^4 WT CD45.1$^+$CD4$^+$ (or CD8$^+$) T cells and CD4$^+$CD25$^+$ T cells (or iTregs) from the four genotypes were added per well in a 96-well plate coated for 3 hours at 37°C with 20µg/mL αCD3 antibodies (BioXCell #BE0001-1) in 1x PBS. At this point, inhibitors were added if needed in the experiment. After 72 hours co-culture at 37°C, the cells and supernatants were harvested. Cells were stained for flow cytometry and supernatants were frozen at -80°C until cytokine analysis.

It is important to note that because CD8$^+$ T cells proliferate at a greater rate than CD4$^+$ T cells, an earlier time point should have been used. It was later found that the reason for decreased suppression by *Foxo3a$^{-/-}$IL-10$^{-/-}$* Tregs was independent of cell type, so the Treg suppression assay with WT CD8$^+$ T cells was not further optimized.

2.16 *In Vitro* Differentiation of Regulatory T Cells

CD4$^+$ T cells were isolated as described in **CD4$^+$ T Cell Isolation**. If iTreg proliferation was tracked during differentiation, splenocytes were stained with CFSE as described in **Treg Suppression Assay**. before purification of CD4$^+$ T cells. The latter cells were washed in 1x PBS and resuspended in X-Vivo™ 15 serum-free Hematopoietic Cell Medium (Lonza

Bioscience # 02-053Q) supplemented with 20 ng/mL IL-2 (Biolegend® #575404), 10 ng/mL TGF-β (Biolegend® #763104), 10 µg/mL αIL-4 antibody (BioXCell #BE0045), and 10 µg/mL αIFN-γ antibody (BioXCell #BE0054) at 1 million cells/mL. In certain experiments, 50 nM or 100 nM decitabine (MedChemExpress® #HY-A0004) was added to the culture media. One million cells were added per well in a 24-well plate coated for 3 hours at 37°C with 20µg/mL αCD3 antibodies in 1x PBS. After 96 hours incubation at 37°C, iTregs were harvested and counted, then used for downstream experiments. The purity and viability of iTregs was confirmed by flow cytometry ($CD4^+CD25^+Foxp3^+$) (**Figure 5**). From this point forward, if iTregs are mentioned, it indicates that this protocol has been followed and iTregs were harvested and washed to be used for downstream experiments. iTregs also serve as an approximation of pTregs that were differentiated in the periphery via TGF-β.

2.17 Live Measurement of Oxygen Consumption Rate

iTregs differentiation was modified from **In Vitro Differentiation of Regulatory T Cells**. All steps were the same except that $1.5*10^5$ $CD4^+$ T cells were plated in a 96-well plate rather than a 24-well plate. Oxygen consumption rate (OCR) was then measured over the 96 hours of differentiation using the Lucid Scientific Recipher. Data were analyzed using the Lucid Scientific Lucid Lab software. When possible, cells were counted per well and OCR was normalized to the number of cells per well.

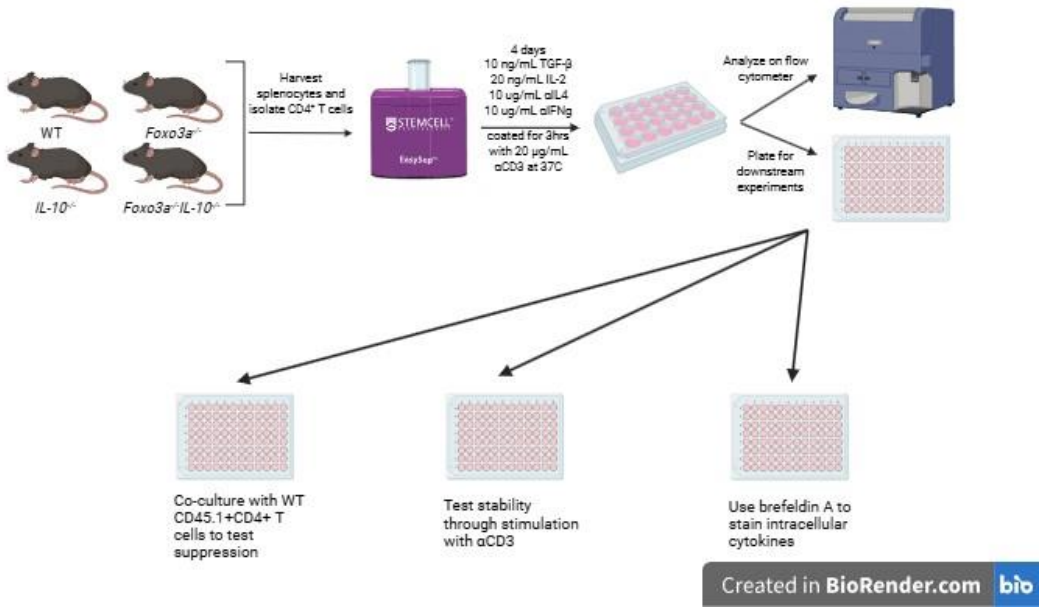

Figure 5. Protocol for the differentiation of iTregs from purified CD4⁺ T cells. Flow chart depicts isolation of CD4⁺ T cells using a Stemcell™ EasySep™ Mouse CD4⁺ T Cell Isolation Kit (#19852) from the spleens of all 4 genotypes, followed by differentiation into iTregs after 96 hours in a 24-well plate coated for 3 hours at 37° with 20 µg/mL αCD3 C in the presence of TGF-β (10ng/mL), IL-2 (20ng/mL), αIL-4, and αIFN-γ (10 µg/mL). The illustration depicts how iTregs are harvested, then used for downstream experiments or are stained with fluorescent antibodies and acquired on a flow cytometer. Flowchart created in BioRender.

2.18 Characterization of iTreg Stability

iTregs were differentiated as described **In Vitro Differentiation of Regulatory T Cells**. iTregs were washed once with R8 media and resuspended at 1 million cells/mL in R8 media with or without 2.5 ng/mL IL-2. iTregs were seeded at $1*10^5$ cells per well in a 96-well plate in wells with or without a coating of 20µg/mL αCD3 antibodies for 3 hours at 37°C. In certain experiments, 50 nM or 100 nM decitabine was added to the culture media. After the 96-well plate was incubated for 24 hours at 37°C, cells were harvested and stained for flow cytometry.

2.19 Characterization of nTreg Stability

$CD4^+CD25^+$ T cells were isolated as described in **$CD4^+CD25^+$ T cell Isolation**. iTregs were washed once with R8 media and resuspended at 1 million cells/mL in R8 media with 2.5 ng/mL IL-2 and 2.5 ng/mL TGF-β. iTregs were seeded at $1*10^5$ cells per well in a 96-well plate coated for 24 hours at 4°C with 1µg/mL αCD3 antibodies in 1x PBS. After the 96-well plate was incubated for 24 hours at 37°C, cells were harvested and stained for flow cytometry.

2.20 Intracellular Cytokine Analysis

iTregs were induced as described in **In Vitro Differentiation of Regulatory T Cells**. iTregs were washed once with R8 media and resuspended at 1 million cells/mL in R8 media. iTregs were seeded at $1*10^5$ cells per well in a 96-well plate coated for 3 hours at 37°C with of 20µg/mL αCD3 antibodies in 1x PBS. After 10 hours incubation at 37°C, Brefeldin A (BFA) (Invitrogen™ #00-4506-51) was added according to manufacturer guidelines. After another 14 hours incubation at 37°C, cells were harvested and stained for flow cytometry.

2.21 Statistical Analysis

Error bars represent the standard error of the mean (SEM). Unpaired parametric T-test and 1-way analysis of variance (ANOVA) were used as mentioned in the text. Pairwise comparisons were made using Tukey's pairwise comparisons test and a significance level of $\alpha = 0.05$. Statistical analyses were performed using the Graphpad Prism version 10 software. In all figures, "*n*" refers to biological replicates.

3.0 Results

Aim 1 - Determine the causes of increased stimulation of CD4⁺ T cells by Foxo3a$^{-/-}$IL-10$^{-/-}$ DCs.

3.1 Foxo3a controls the differentiation of CD11b⁺ DCs in *IL-10*-deficient mice.

To determine the cause of the increased number of DCs in the lamina propria of *Foxo3a$^{-/-}$IL-10$^{-/-}$* mice, an assessment was completed to determine if monocytes differentiate into DCs. Purified WT monocytes differentiated completely into CD11b^{+} DCs (CD11c^{+}MHCII^{+}) after 48 hours with GM-CSF (**Figure 6 a**). Only a small proportion of non-monocytes differentiate into CD11b^{+} DCs after 48 hours with GM-CSF (**Figure 6 a**).

To determine if DCs differentiate from monocytes at a greater rate in *Foxo3a$^{-/-}$IL-10$^{-/-}$* mice, BM cells from all four genotypes were cultured with GM-CSF for 72 hours. In optimization experiments, DC differentiation occurs slower from BM than from purified monocytes; therefore, a time point of 72 hours was used (data not shown). Culturing BM cells instead of purified monocytes better replicates the internal environment of the mouse. There is an insignificant increase in the total cell number of *Foxo3a$^{-/-}$IL-10$^{-/-}$* cells after 72 hours of differentiation with GM-CSF compared to each of the control genotypes (e.g., WT vs *Foxo3a$^{-/-}$IL-10$^{-/-}$*, $P = 0.9162$; **Figure 6 b**). The lowest number of cells after differentiation is from the *IL-10$^{-/-}$* mice, which is insignificant compared to *Foxo3a$^{-/-}$IL-10$^{-/-}$* ($P = 0.2094$). *Foxo3a$^{-/-}$* and WT have similar numbers of cells after 72 hours of differentiation with GM-CSF ($P = 0.9862$). Additionally, there is an increase in the proportion of CD11b^{+} DCs from *Foxo3a$^{-/-}$IL-10$^{-/-}$* BM as compared to the other genotypes after 72 hours of differentiation in the presence of GM-CSF (**Figure 6 c**). The proportion of CD11b^{+} DCs is similar between the control genotypes.

When the proportion of CD11b$^+$ DCs is combined with the cell numbers post-differentiation, there is a significant increase in the number of *Foxo3a*$^{-/-}$*IL-10*$^{-/-}$ CD11b$^+$ DCs that differentiate from BM in the presence of GM-CSF compared to the control genotypes (e.g., WT vs *Foxo3a*$^{-/-}$*IL-10*$^{-/-}$, $P = 0.0353$; **Figure 6 d**). The control genotypes have similar numbers (e.g., WT vs *Foxo3a*$^{-/-}$, $P = 0.8388$), with the number of WT CD11b$^+$ DCs being the closest to the number of *Foxo3a*$^{-/-}$*IL-10*$^{-/-}$ CD11b$^+$ DCs.

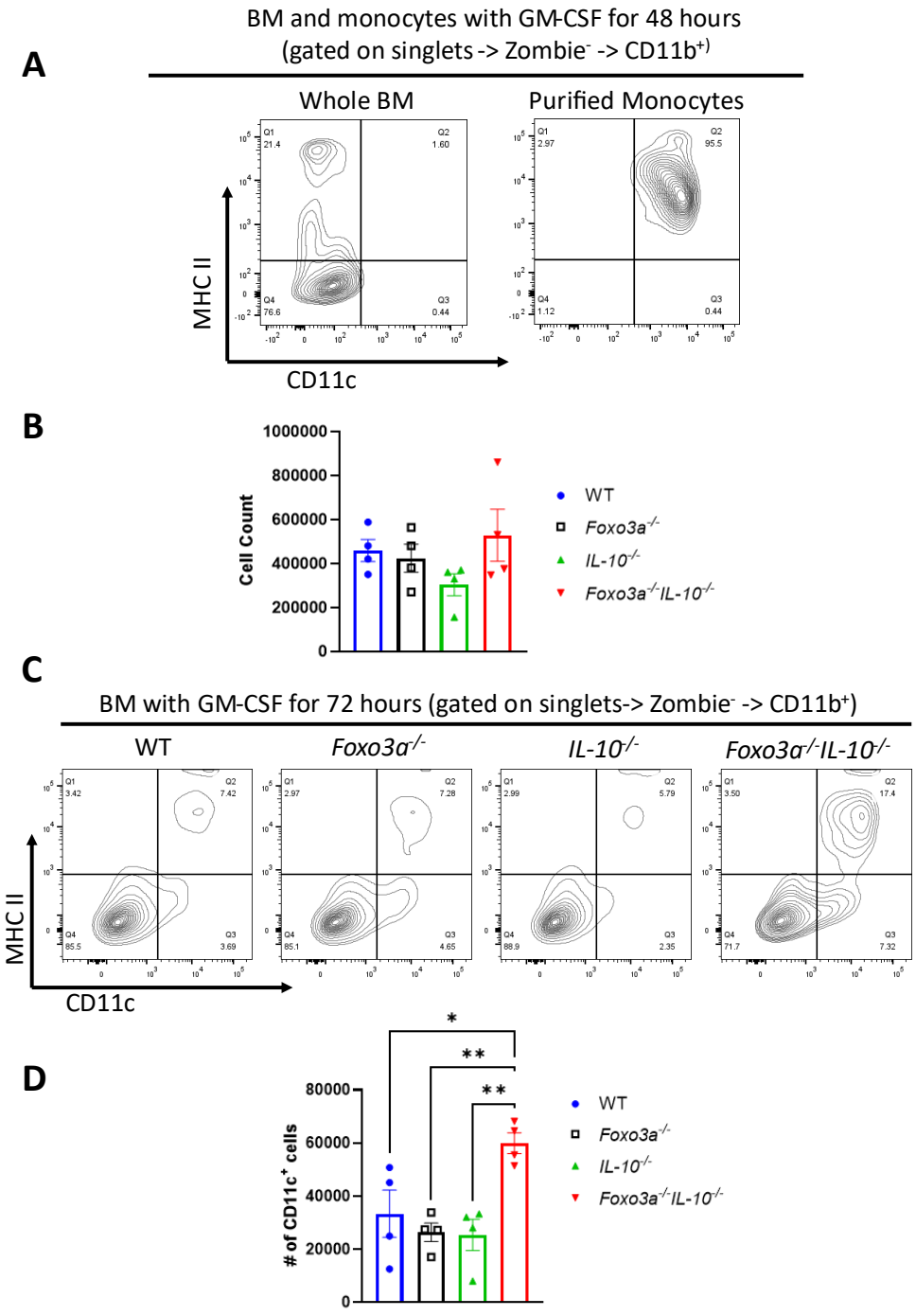

Figure 6. A greater number of *Foxo3a*$^{-/-}$*IL-10*$^{-/-}$ DCs differentiate from BM in response to GM-CSF. (A) Representative FACS plots of CD11b^{+}CD11c^{+}MHCII^{+} DCs differentiated from WT whole BM and purified neutrophils that were incubated for 48 hours with 10 ng/mL GM-CSF (*n*=1). **(B)** Bar graph of the number of cells harvested (*n*=4). **(C)** Representative FACS plots of CD11b^{+}CD11c^{+}MHCII^{+} DCs (*n*=4). **(D)** Bar graph depicting the number of CD11b^{+}CD11c^{+}MHCII^{+} DCs (*n*=4). **B-D** shows cells from 8 wells of a 96-well plate that were initially seeded with 10^5 BM cells per well, then differentiated with 10 ng/mL GM-CSF for 72 hours. Experiments conducted on 8-week-old to 12-week-old mice. Cells were stained with fluorescent antibodies, acquired on a BD LSRFortessa™, and analyzed using FlowJo™ software. Individual bars depict the respective mean ± SEM. Statistical significance determined using a 1-way ANOVA and reported for each comparison by "*" (*P<0.05, **P<0.01, ***P<0.001, ****P<0.0001).

3.2 Various inhibitors can control the excessive production of pro-inflammatory cytokines produced by *Foxo3a*$^{-/-}$*IL-10*$^{-/-}$ DCs.

In a RNAseq performed on purified DCs from the 4 genotypes many metabolic and immune pathways are modulated in *Foxo3a*$^{-/-}$*IL-10*$^{-/-}$ DCs (**Figure 7**). The most prominent of these gene sets being those involved in adipogenesis, defence to bacterium, the innate immune response, G2 M cell cycle, and myeloid leukocyte activation. Loss of *Foxo3a* and/or *IL-10* leads to an increase in the IFN-α and IFN-γ response and TNF signaling via NF-κB in DCs. The gene expression from general immune pathways is increased in *Foxo3a*$^{-/-}$ *and Foxo3a*$^{-/-}$*IL-10*$^{-/-}$ DCs, such as cytokine production, the innate immune response, the inflammatory response, and myeloid cell migration. In addition, genes related to hematopoiesis also have increased expression in *Foxo3a*$^{-/-}$ *and Foxo3a*$^{-/-}$*IL-10*$^{-/-}$ DCs. These pathways include myeloid cell development and leukemic signaling, extramedullary hematopoiesis, GATA1 targets, abnormal erythrocyte physiology, leukemic stem cells, hemolytic anemia, and CML stem cells. Additionally, genes related to metabolism have increased expression in *Foxo3a*$^{-/-}$ *and Foxo3a*$^{-/-}$*IL-10*$^{-/-}$ DCs. These pathways include adipogenesis, and heme metabolism. In *IL-10*$^{-/-}$ DCs, the genes from the general immune pathways, hematopoiesis, and metabolism are down regulated.

To reduce the excessive production of inflammatory cytokines by *Foxo3a*$^{-/-}$*IL-10*$^{-/-}$ DCs, a selection of the pathways that are upregulated in the RNAseq can be inhibited (**Table 3**). Denifanstat, C75, MK2 inhibitor, stattic, CAN10, and rapamycin significantly reduce the production TNF-α and IL-6 from purified DCs stimulated with LPS compared to no inhibitors (e.g., for TNF-α; $P < 0.0001$, $P < 0.0001$, $P < 0.0001$, $P = 0.0003$, $P = 0.0016$, $P = 0.0192$, respectively; **Figure 8 a, b**). Stattic, denifanstat, and MK2 inhibitor can reduce TNF-α production to levels similar to DCs that are not stimulated with LPS ($P > 0.9999$, $P = 0.9936$, $P > 0.9999$, respectively). Additionally, stattic, C75, and MK2 inhibitor can reduce IL-6

production to levels similar to DCs that are not stimulated with LPS ($P > 0.9999$, $P = 0.0193$, $P = 0.0904$, respectively). Cerulenin makes the smallest difference (IL-6: $P < 0.0001$, TNF-α: $P = 0.2715$) of the fatty acid synthase inhibitors and paquinimod does not significantly reduce the production of IL-6 or TNF-α ($P = 0.9631$, $P = 0.0699$, respectively). Of the inhibitors that significantly reduce IL-6 and TNF-α production, rapamycin makes the smallest difference (IL-6: $P = 0.0251$, TNF-α: $P = 0.0192$) as rapamycin does not directly inhibit their production, but rather, slows the metabolism of the cell.

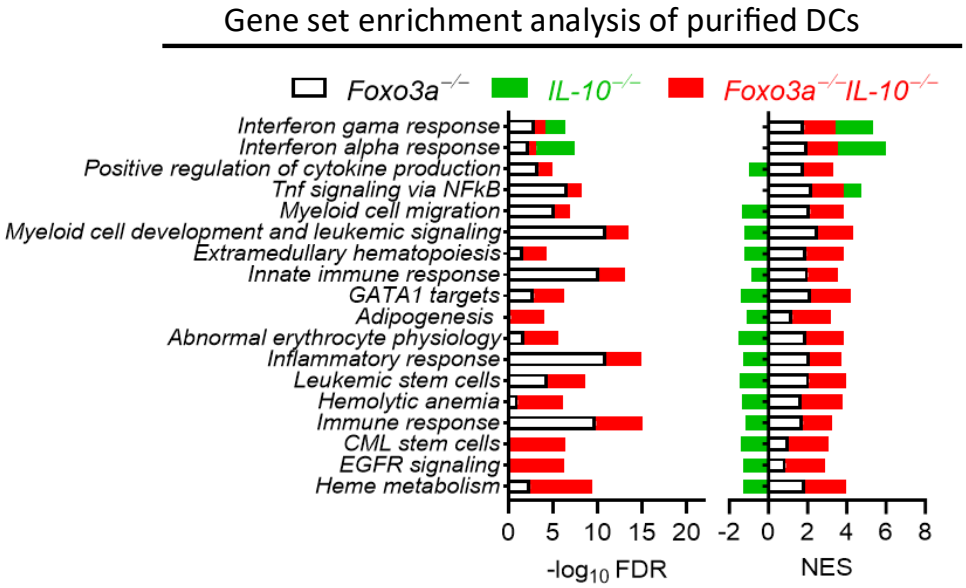

Figure 7. *Foxo3a*$^{-/-}$*IL-10*$^{-/-}$ DCs' metabolic and immunologic pathways are heavily modulated. Bioinformatics plots of RNAseq data from purified DCs comparing normalized enrichment score of gene sets in *Foxo3a*$^{-/-}$, *IL-10*$^{-/-}$, and *Foxo3a*$^{-/-}$*IL-10*$^{-/-}$ DCs compared to WT DCs. The graph on the left depicts adjusted *P*-values and the graph on the rights depicts normalized enrichment scores.

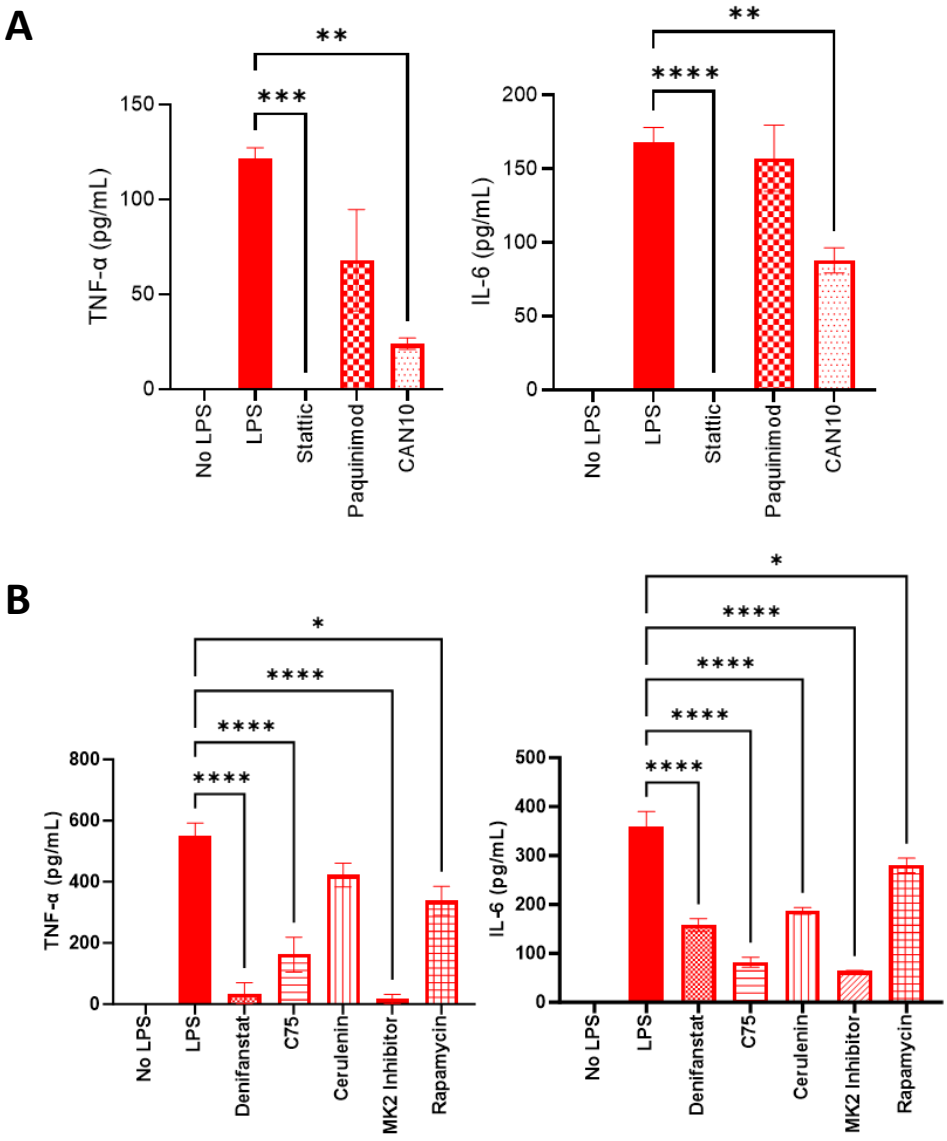

Figure 8. Multiple pathways can be inhibited to reduce the production of TNF-α and IL-6 by *Foxo3a*$^{-/-}$*IL-10*$^{-/-}$ DCs stimulated by LPS. (A) Bar graphs depicting cytokine production by *Foxo3a*$^{-/-}$*IL-10*$^{-/-}$ DCs cultured with Stattic (4 μM), paquinimod (1 μM), and CAN10 (1 μg/mL) (*n*=3). **(B)** Bar graphs depicting cytokine production by *Foxo3a*$^{-/-}$*IL-10*$^{-/-}$ DCs cultured with denifanstat (50 μM), C75 (10 μM), cerulenin (25 μM), MK2 Inhibitor (2.5 μM), and rapamycin (1 μM) (*n*=3). In **A-B**, *Foxo3a*$^{-/-}$*IL-10*$^{-/-}$ DCs were purified from spleens and seeded 10^5 cells per well, then stimulated with 100 ng/mL LPS. Supernatants were collected at 6- and 24-hours post-stimulation and analyzed for TNF-α (left) and IL-6 (right), respectively. Concentrations of TNF-α and IL-6 were determined using sandwich ELISA. Experiments conducted on 8-week-old to 12-week-old mice. Individual bars depict the respective mean ± SEM. Statistical significance determined using a 1-way ANOVA and reported for each comparison by "*" (*P<0.05, **P<0.01, ***P<0.001, ****P<0.0001).

Aim 2 - Determine the underlying mechanisms causing decreased suppression by Foxo3a$^{-/-}$IL-10$^{-/-}$ Tregs.

3.3 Foxo3a modulates CD4^{+} T cells in the spleen compartment of *IL-10*-deficient mice.

The spleens of *Foxo3a$^{-/-}$IL-10$^{-/-}$* mice were investigated first to characterize nTregs and CD4^{+} T cells. Sick and healthy *Foxo3a$^{-/-}$IL-10$^{-/-}$* mice have significantly larger spleens than the control genotypes both in size and in mass (e.g., WT vs *Foxo3a$^{-/-}$IL-10$^{-/-}$*, $P < 0.0001$; **Figure 9 a, b**). Spleens from *Foxo3a$^{-/-}$* mice are slightly larger in mass and size than spleens from *IL-10$^{-/-}$* mice ($P = 0.2265$). The difference in size of *Foxo3a$^{-/-}$IL-10$^{-/-}$* spleens is reflected in the splenocyte count with the exception that spleens from healthy *Foxo3a$^{-/-}$IL-10$^{-/-}$* mice do not have significantly more cells than spleens from *Foxo3a$^{-/-}$* mice ($P = 0.0708$; **Figure 9 c**). Spleens from *Foxo3a$^{-/-}$* mice have insignificantly more cells than spleens from *IL-10$^{-/-}$* mice ($P = 0.1978$). The spleen mass and splenocyte count from healthy and sick *Foxo3a$^{-/-}$IL-10$^{-/-}$* mice are not significantly different ($P = 0.1303$, $P = 0.1484$, respectively; **Figure 9 d**). There is a higher proportion of CD4^{+} T cells in the lamina propria of *Foxo3a$^{-/-}$IL-10$^{-/-}$* mice[262]. Thus, the proportion of CD4^{+} T cells in the spleens was also investigated. The spleens of *Foxo3a$^{-/-}$IL-10$^{-/-}$* mice have a significantly lower proportion of CD4^{+} T cells than the control genotypes, and no significant differences in the overall number of nTregs T cells (e.g., WT vs *Foxo3a$^{-/-}$IL-10$^{-/-}$*, $P = 0.0083$, $P = 0.1068$, respectively; **Figure 10 a-c**). The spleens of *Foxo3a$^{-/-}$IL-10$^{-/-}$* mice have significantly more CD4^{+} T cells than *IL-10$^{-/-}$* mice ($P = 0.0365$; **Figure 10 d**). The control genotypes are similar in proportion of CD4^{+} T cells, overall number of CD4^{+} T cells, and overall number of nTregs (e.g., WT vs *Foxo3a$^{-/--}$*, $P = 0.9937$, $P = 0.1030$, $P = 0.8592$, respectively).

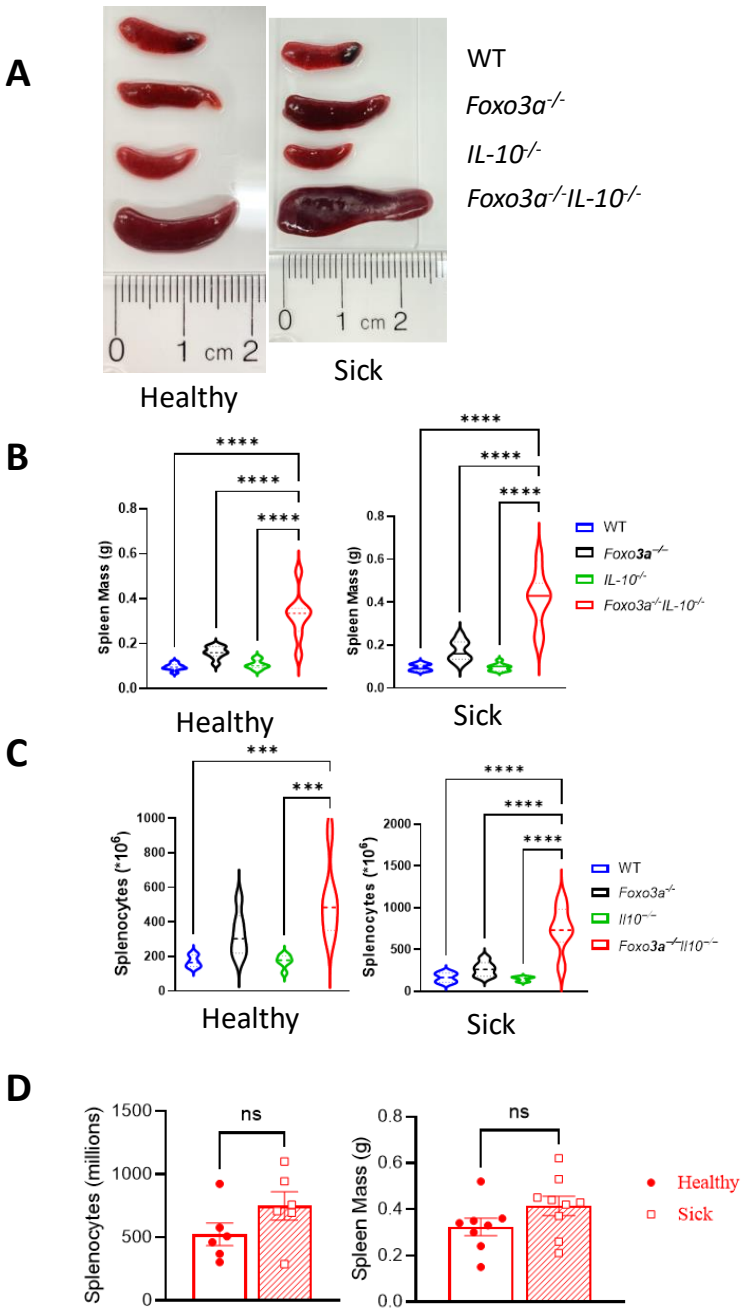

Figure 9. *Foxo3a*$^{-/-}$*IL-10*$^{-/-}$ mice have large spleens that increase in size as they develop a CrD-like phenotype. (A) Representative photographs of the spleens of healthy (left) or sick (right) *Foxo3a*$^{-/-}$*IL-10*$^{-/-}$ mice and control genotypes. **(B)** Violin plots depicting the mass of spleens of healthy (left) or sick (right) *Foxo3a*$^{-/-}$*IL-10*$^{-/-}$ mice and control genotypes. **(C)** Violin plots depicting the splenocyte count of healthy or sick *Foxo3a*$^{-/-}$*IL-10*$^{-/-}$ mice and control genotypes. Splenocytes were counted manually using methylene blue and a hemocytometer. Statistical significance determined using a 1-way ANOVA. **(D)** Bar graphs depicting the splenocyte counts (left) and spleen mass (right) comparing healthy and sick *Foxo3a*$^{-/-}$*IL-10*$^{-/-}$ mice. Experiments conducted on 8-week-old to 12-week-old mice. Individual bars depict the respective mean ± SEM. Statistical significance determined using unpaired t-tests (**P*<0.05, ***P*<0.01, ****P*<0.001, *****P*<0.0001) (min. *n*=6).

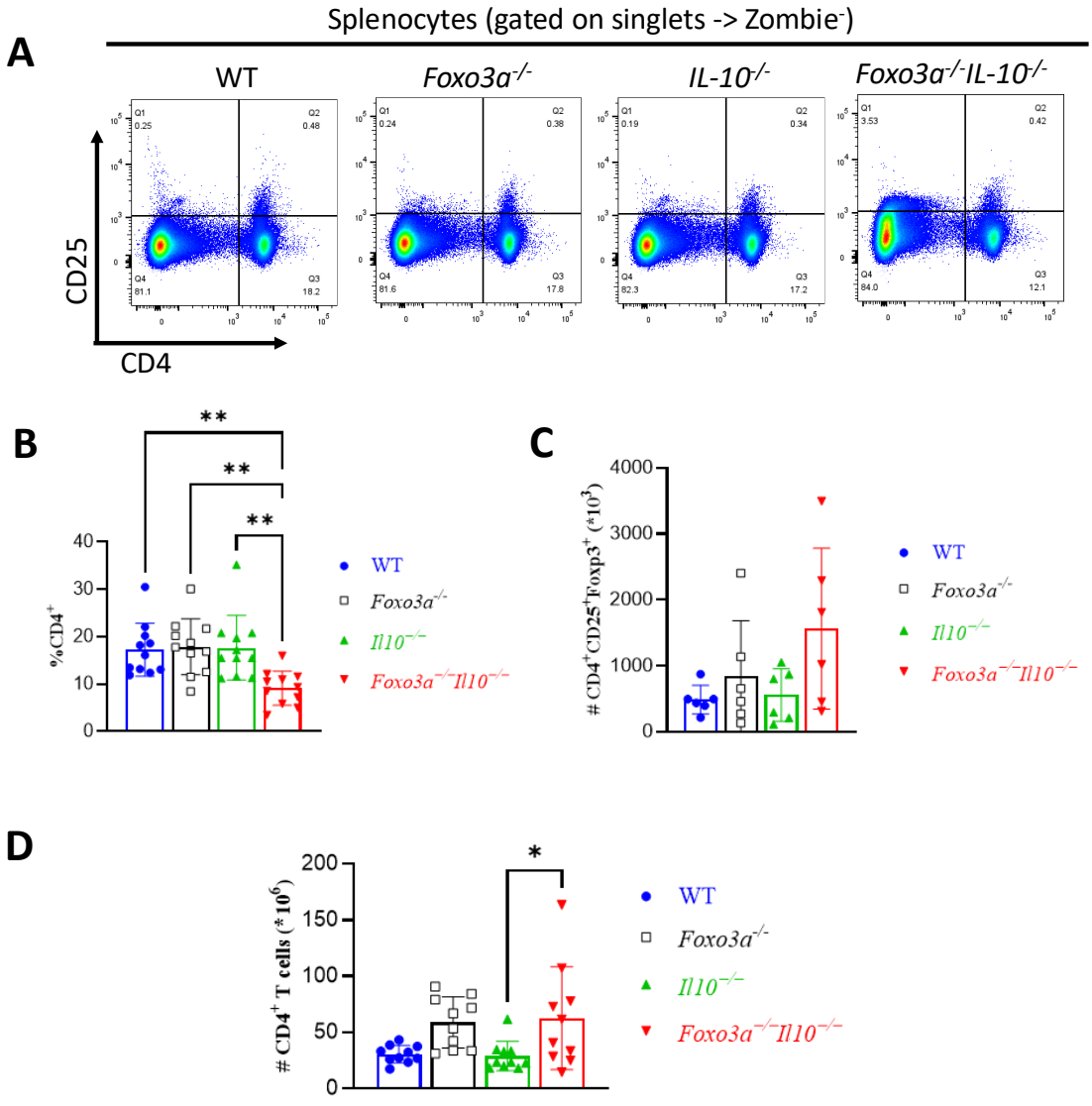

Figure 10. *Foxo3a*$^{-/-}$*IL-10*$^{-/-}$ spleens have a reduced proportion of CD4$^+$ T cells and a similar overall number of Tregs. (A) Representative FACS plots of CD4$^+$CD25$^+$ populations from all four genotypes (*n*=11). **(B)** Bar graph depicting the proportion of CD4$^+$ splenocytes from all four genotypes (*n*=11). **(C)** Bar graph depicting the number of Tregs in the spleens from all four genotypes as determined by combining splenocyte count and proportion of Tregs (*n*=6). **(D)** Bar graph depicting the number of CD4$^+$ T cells in the spleens of all four genotypes determined by combining splenocyte count and proportion of CD4$^+$ T cells (*n*=10). Experiments conducted on 8-week-old to 12-week-old mice. Splenocytes were stained with fluorescent antibodies, acquired on a BD LSRFortessa™, and analyzed using FlowJo™ software. Individual bars depict the respective mean ± SEM. Statistical significance determined using a 1-way ANOVA and reported for each comparison by "*" (*P<0.05, **P<0.01, ***P<0.001, ****P<0.0001).

3.4 Foxo3a maintains Foxp3 expression in the nTregs of *IL-10*-deficient mice.

The nTregs from spleens of healthy *Foxo3a*$^{-/-}$*IL-10*$^{-/-}$ mice have an insignificant decrease in Foxp3 expression (e.g., *Foxo3a*$^{-/-}$ vs *Foxo3a*$^{-/-}$*IL-10*$^{-/-}$, *P* = 0.6585), while the nTregs from sick *Foxo3a*$^{-/-}$*IL-10*$^{-/-}$ mice have significant reduction in Foxp3 expression compared to *IL-10*$^{-/-}$ mice (P = 0.0430; **Figure 11 a, b**). The nTregs from the control genotypes have no difference in Foxp3 expression (e.g., WT vs *Foxo3a*$^{-/--}$, *P* = 0.9378). Because *Foxo3a*$^{-/-}$*IL-10*$^{-/-}$ nTregs have lower expression of Foxp3, tTregs expression of Foxp3 was assessed to see if tTregs contributed to this difference. *Foxo3a*$^{-/-}$*IL-10*$^{-/-}$ tTregs also have slightly reduced Foxp3 expression, while the tTregs from sick *Foxo3a*$^{-/-}$*IL-10*$^{-/-}$ mice have a greater reduction in the expression of Foxp3 (**Figure 12 a**). If there was a change in the number of tTregs in the thymus, it would indicate dysfunctional differentiation. The thymuses of *Foxo3a*$^{-/-}$*IL-10*$^{-/-}$ mice are no different in cell count than the control genotypes (e.g., WT vs *Foxo3a*$^{-/-}$*IL-10*$^{-/-}$, *P* > 0.9999; **Figure 12 b**). In addition, there is no difference in number of tTregs from the thymuses of *Foxo3a*$^{-/-}$*IL-10*$^{-/-}$ mice (e.g., WT vs *Foxo3a*$^{-/-}$*IL-10*$^{-/-}$, *P* = 0.9985; **Figure 12 c**). Problems with inconsistent thymus harvesting and an overall low proportion of Foxp3^{+} T cells in thymuses mean that these data should be interpreted with caution.

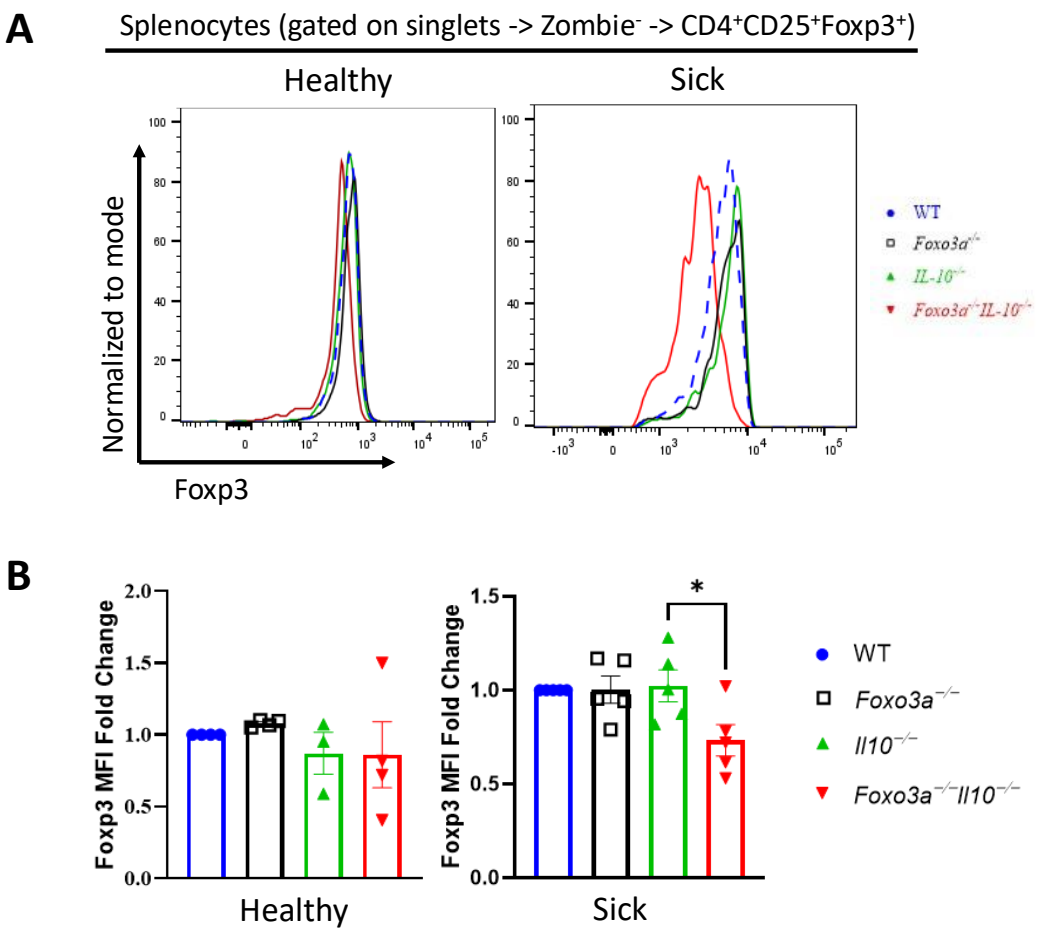

Figure 11. *Foxo3a*$^{-/-}$*IL-10*$^{-/-}$ nTregs have slightly reduced Foxp3 expression, which worsens upon development of a CrD-like phenotype. (A) Representative FACS plots of Foxp3 expression in CD4^{+}CD25^{+}Foxp3^{+} splenocyte populations of healthy (left) or sick (right) *Foxo3a*$^{-/-}$*IL-10*$^{-/-}$ mice and control genotypes. Foxp3 expression is normalized to the mode (*n*=4 and *n*=5, respectively). **(B)** Bar graphs depicting the Foxp3 MFI fold change in CD4^{+}CD25^{+}Foxp3^{+} splenocyte populations from healthy (left) or sick (right) *Foxo3a*$^{-/-}$*IL-10*$^{-/-}$ mice and control genotypes. Foxp3 MFI is normalized to WT MFI (*n*=4 and *n*=5, respectively). Experiments conducted on 8-week-old to 12-week-old mice. Individual bars depict the respective mean ± SEM. Splenocytes were stained with fluorescent antibodies, acquired on a BD LSRFortessa™, and analyzed using FlowJo™ software. Individual bars depict the respective mean ± SEM. Statistical significance determined using a 1-way ANOVA and reported for each comparison by "*" (*P<0.05, **P<0.01, ***P<0.001, ****P<0.0001).

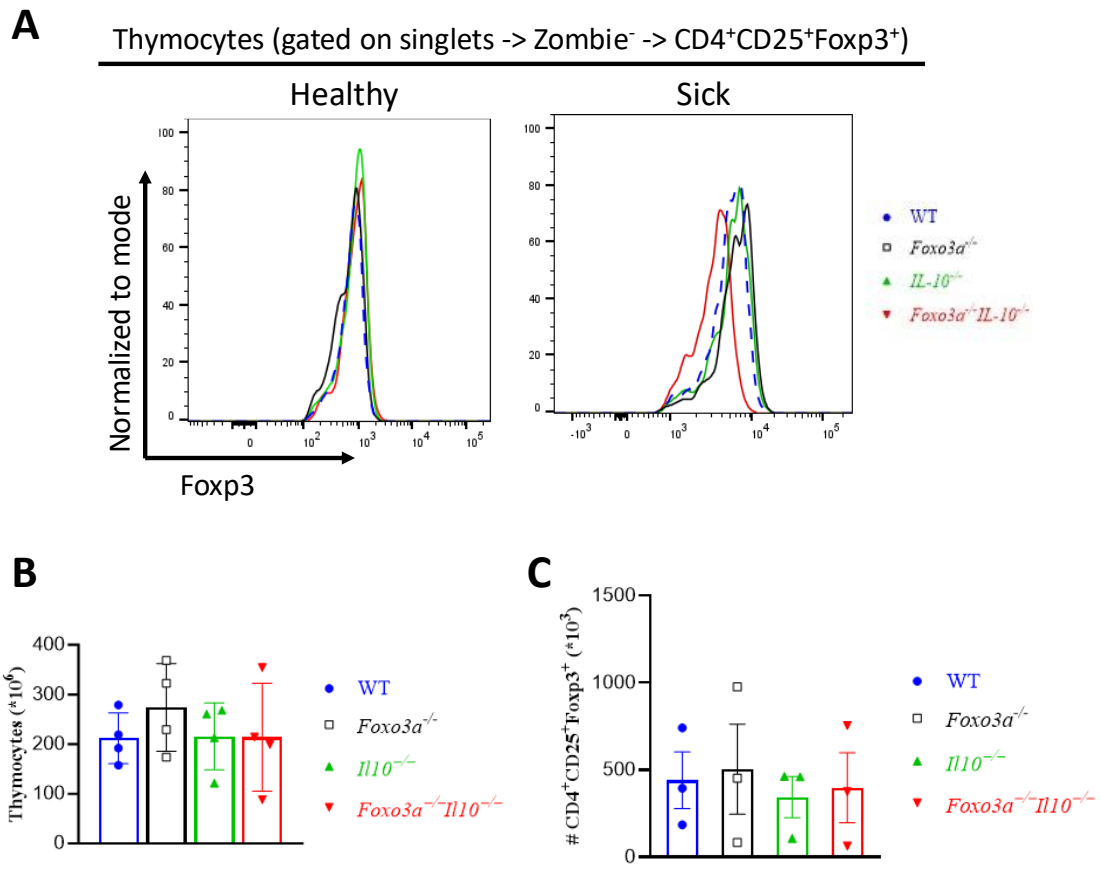

Figure 12. *Foxo3a*$^{-/-}$*IL-10*$^{-/-}$ tTregs have slightly reduced Foxp3 expression which worsens upon development of a CrD-like phenotype. (A) Representative FACS plots of Foxp3 expression in CD4^{+}CD25^{+}Foxp3^{+} thymocyte populations of healthy (left) or sick (right) *Foxo3a*$^{-/-}$*IL-10*$^{-/-}$ mice and control genotypes (*n*=3, *n*=1, respectively). Foxp3 expression is normalized to the mode. **(B)** Bar graph depicting the thymocyte count of all four genotypes. Thymocytes were counted manually using methylene blue and a hemocytometer (*n*=4). **(C)** Bar graph depicting the number of Tregs in the thymuses as determined by combining thymocyte count and proportion of Tregs (*n*=3). Experiments conducted on 8-week-old to 12-week-old mice. Thymocytes were stained with fluorescent antibodies, acquired on a BD LSRFortessa™, and analyzed using FlowJo™ software. Individual bars depict the respective mean ± SEM. Statistical significance determined using a 1-way ANOVA and reported for each comparison by "*" (*P<0.05, **P<0.01, ***P<0.001, ****P<0.0001).

3.5 Foxo3a contributes to proper suppression by nTregs in *IL-10*-deficient mice.

Foxo3a$^{-/-}$*IL-10*$^{-/-}$ nTregs have reduced expression of Foxp3, therefore the function of nTregs from *Foxo3a*$^{-/-}$*IL-10*$^{-/-}$ mice was assessed. *Foxo3a*$^{-/-}$*IL-10*$^{-/-}$ nTregs have a reduced capacity to suppress the proliferation of WT CD45.1^{+}CD4^{+} T cells (**Figure 13 a**). The reduced proliferation of WT CD45.1^{+}CD4^{+} T cells was consistent with significantly higher production of IL-17a and IFN-γ (e.g., WT vs *Foxo3a*$^{-/-}$*IL-10*$^{-/-}$, $P < 0.0001$; **Figure 13 b**). The co-cultures with WT and *Foxo3a*$^{-/-}$ nTregs have higher production of IL-10, while the cultures with *IL-10*$^{-/-}$ and *Foxo3a*$^{-/-}$*IL-10*$^{-/-}$ nTregs produce low amounts of IL-10. The IL-10 from the cultures with *IL-10*$^{-/-}$ and *Foxo3a*$^{-/-}$*IL-10*$^{-/-}$ nTregs likely come from WT CD45.1^{+}CD4^{+} T cells. The ability of *Foxo3a*$^{-/-}$*IL-10*$^{-/-}$ nTregs to suppress the proliferation of isolated WT CD8^{+} T cells was also assessed. *Foxo3a*$^{-/-}$*IL-10*$^{-/-}$ nTregs and *IL-10*$^{-/-}$ iTregs also demonstrate reduced capacity to suppress the proliferation of WT CD45.1^{+}CD8^{+} T cells (**Figure 13 c**). In the preceding experiments, *IL-10*$^{-/-}$ nTregs also have a slightly reduced capacity to suppress the proliferation of WT CD45.1^{+}CD4^{+} T cells.

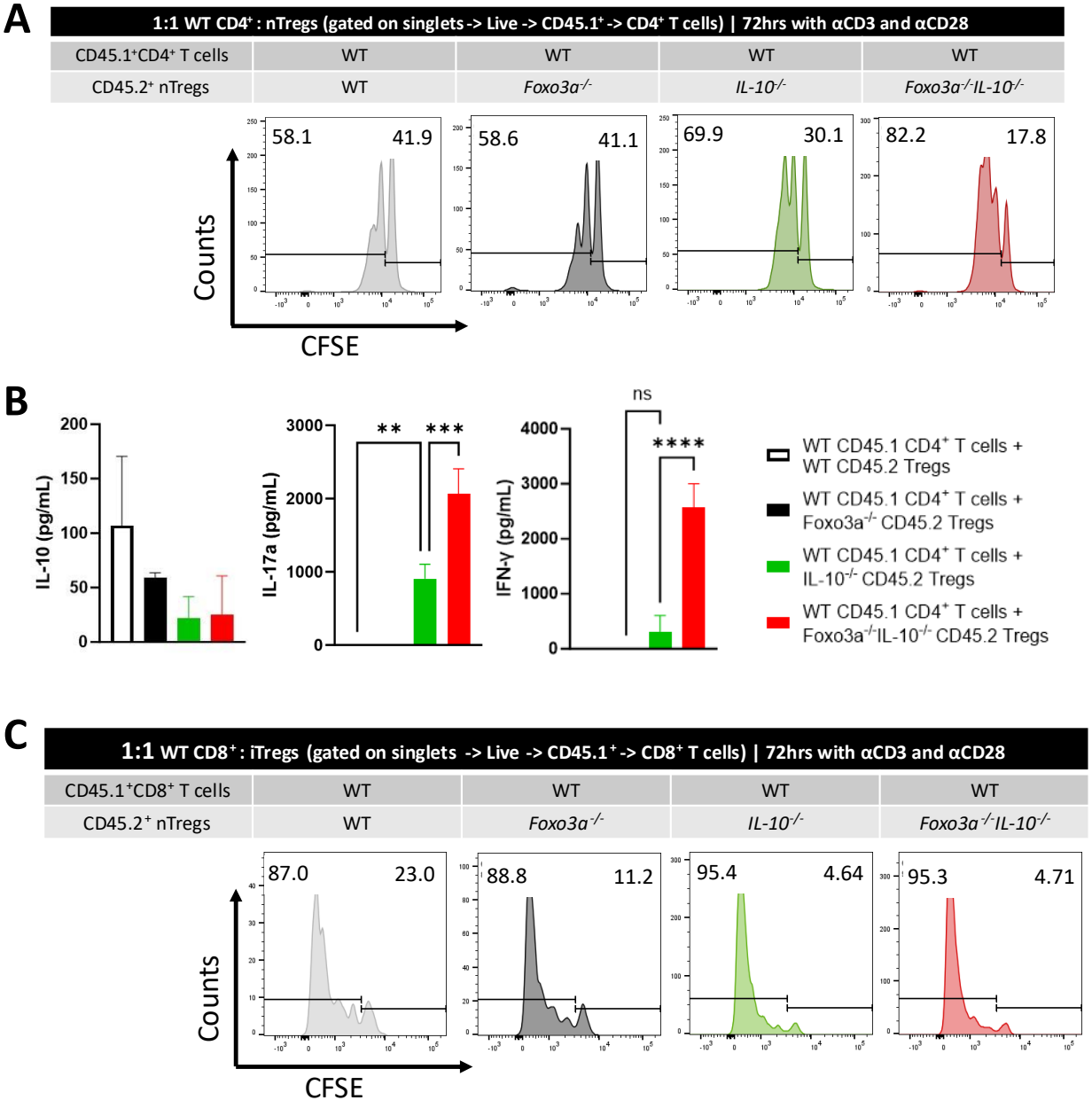

Figure 13. The ability of *Foxo3a*$^{-/-}$*IL-10*$^{-/-}$ nTregs to suppress the proliferation of WT CD4^{+} and CD8^{+} T cells is compromised. (A) Representative FACS plots of CFSE dilution in CD45.1^{+}CD4^{+} WT T cells co-cultured 1:1 with CD45.2^{+} nTregs from all four genotypes (*n*=3). **(B)** Bar graphs depicting IL-10, IL-17a, and IFN-γ levels measured from the supernatants of CD45.1^{+}CD4^{+} WT T cells co-cultured 1:1 with CD45.2^{+} nTregs from all four genotypes. Concentrations of IL-10, IL-17a, and IFN-γ were determined using sandwich ELISA (*n*=3). **(C)** Representative FACS plots of CFSE dilution in CD45.1^{+}CD8^{+} WT T cells co-cultured 1:1 with CD45.2^{+} nTregs from all four genotypes (*n*=2). CD45.1^{+}CD4^{+} WT T cells and CD45.2^{+} nTregs in co-culture were stimulated for 72 hours in plates coated overnight at 4°C with 1 µg/mL αCD3 and αCD28 antibodies. Experiments conducted on 8-week-old to 12-week-old mice. Cells were stained with fluorescent antibodies, acquired on a BD LSRFortessa™, and analyzed using FlowJo™ software. Individual bars depict the respective mean ± SEM. Statistical significance determined using a 1-way ANOVA and reported for each comparison by "*" (*P<0.05, **P<0.01, ***P<0.001, ****P<0.0001).

3.6 Foxo3a contributes to proper suppression by iTregs in *IL-10*-deficient mice.

The Treg suppression assay was repeated using iTregs to determine if they also had diminished suppressive capacity on WT CD4$^+$ T cells. *Foxo3a$^{-/-}$IL-10$^{-/-}$* iTregs also have diminished suppressive capacity on the proliferation of WT CD45.1$^+$CD4$^+$ T cells (**Figure 14 a**). This is consistent with a significant increase in the production of IL-17a and IFN-γ (e.g., WT vs *Foxo3a$^{-/-}$IL-10$^{-/-}$*, IL-17a: $P < 0.0003$, IFN-γ: $P < 0.0001$;**Figure 14 b**). Co-cultures with iTregs from the control genotypes produce only background amounts of IL-17a and IFN-γ. Interestingly, when *Foxo3a$^{-/-}$IL-10$^{-/-}$* iTregs are present at a 2:1 (iTregs: WT CD4$^+$ T cells) ratio rather than the normal 1:1 ratio, the proliferation of WT CD45.1$^+$CD4$^+$ T cells is increased when co-cultured with *Foxo3a$^{-/-}$IL-10$^{-/-}$* iTregs as compared to a 1:1 ratio (**Figure 14 c**). The iTregs from the control genotypes suppress the proliferation of WT CD45.1$^+$CD4$^+$ T cells to similar degrees when co-cultured at a 1:1 and 2:1 ratio. In both co-cultures with *Foxo3a$^{-/-}$IL-10$^{-/-}$* iTregs, the WT CD45.1$^+$CD4$^+$ T cells proliferate more than if there were no iTregs present.

Although Tregs suppress the proliferation of effector T cells primarily through cytokines, other receptors involved with cell-to-cell interaction with DCs were assessed to determine if the reduction in Foxp3 expression was reflected in cell-surface markers. ST2 was assessed because it has been found to stabilize pTregs *in vivo*, as well as CTLA-4, which inhibits B7 molecules on DCs, and TIGIT, which binds to nectin on DCs[148, 263, 264]. *Foxo3a$^{-/-}$, IL-10$^{-/-}$*, and *Foxo3a$^{-/-}$IL-10$^{-/-}$* nTregs have reduced expression of ST2[262]. *Foxo3a$^{-/-}$IL-10$^{-/-}$* iTregs had similar expression of ST2, CTLA-4, and TIGIT (**Figure 14 d**).

Rapamycin, which is a mTORC1 inhibitor, is able to restore Foxp3 and ST2 expression in *Foxo3a$^{-/-}$IL-10$^{-/-}$* nTregs *in vivo*[262]. Therefore, rapamycin was added to an iTreg suppression assay and is able to restore the suppressive capacity of *Foxo3a$^{-/-}$IL-10$^{-/-}$* iTregs (**Figure S31**

a). Rapamycin treatment also improves the survival of CD45.2^{+} iTregs when cultured in the Treg suppression assay (**Figure S31 b**).

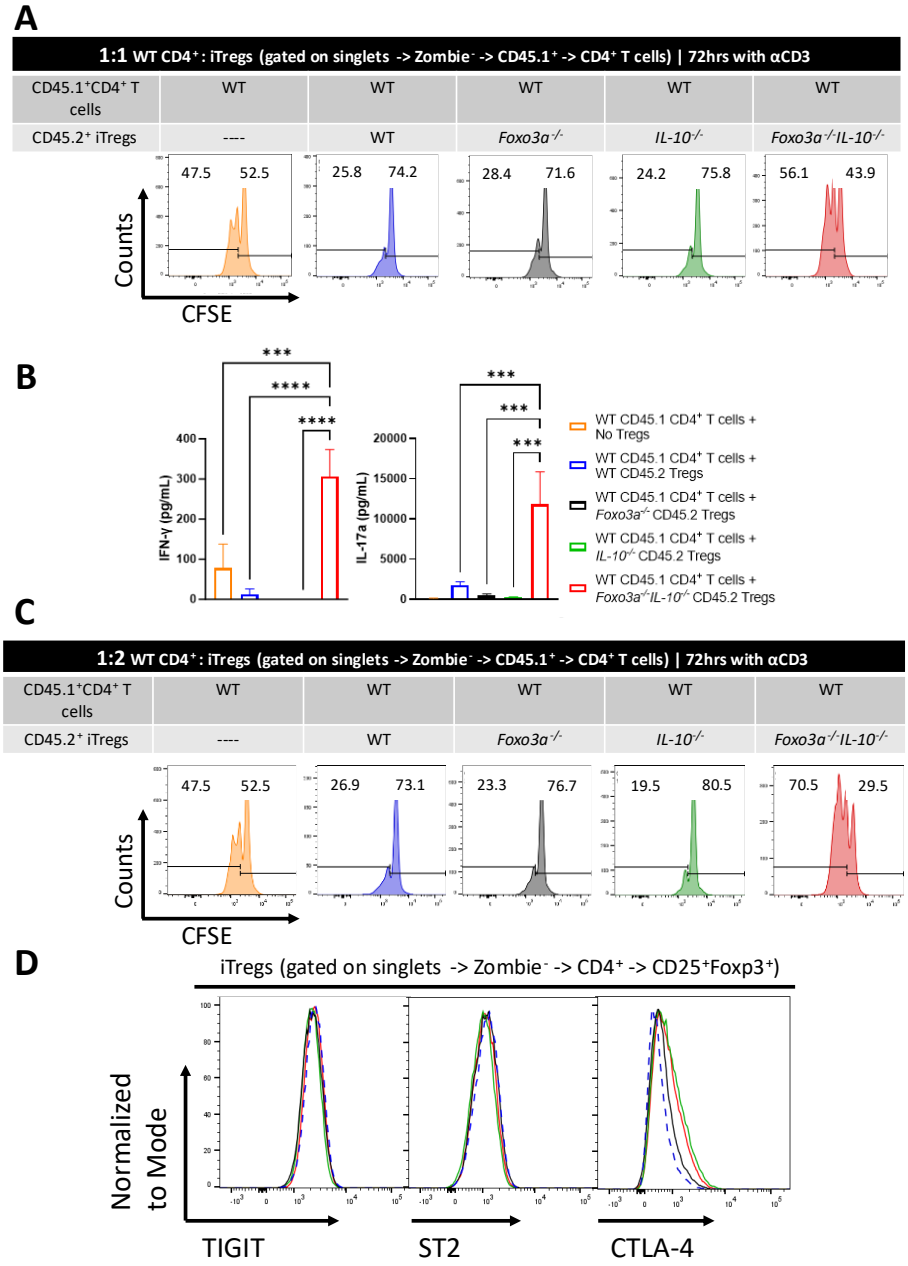

Figure 14. The ability of *Foxo3a*$^{-/-}$*IL-10*$^{-/-}$ iTregs to suppress the proliferation of WT CD4^{+} T cells is compromised. (A) Representative FACS plots of CFSE dilution in CD45.1^{+}CD4^{+} WT T cells co-cultured 1:1 with CD45.2^{+} iTregs from all four genotypes (*n*=3). **(B)** Bar graphs depicting IL-17a and IFN-γ levels measured from the supernatants of CD45.1^{+}CD4^{+} WT T cells co-cultured 1:1 with CD45.2^{+} iTregs from all four genotypes. Supernatants were harvested after 72 hours co-culture. Concentrations of IL-17a and IFN-γ were determined using sandwich ELISA (*n*=3). **(C)** Representative FACS plots of CFSE dilution in CD45.1^{+}CD4^{+} WT T cells co-cultured 1:2 with CD45.2^{+} iTregs from all four genotypes (*n*=2). **A-C** shows CD45.1^{+}CD4^{+} WT T cells co-cultured with CD45.2^{+} iTregs stimulated for 72 hours in plates coated for 3 hours at 37°C with 20 µg/mL αCD3 antibodies. **(D)** Representative FACS plots of TIGIT, ST2, and CTLA-4 expression in *in vitro* differentiated iTregs. Expression of TIGIT, ST2, and CTLA-4 are normalized to the mode (*n*=3). Experiments conducted on 8-week-old to 12-week-old mice. Cells were stained with fluorescent antibodies, acquired on a BD LSRFortessa™, and analyzed using FlowJo™ software. Individual bars depict the respective mean ± SEM. Statistical significance determined using a 1-way ANOVA and reported for each comparison by "*" (*P<0.05, **P<0.01, ***P<0.001, ****P<0.0001).

Aim 3 -> Characterize the differentiation of Foxo3a$^{-/-}$IL-10$^{-/-}$ Tregs.

3.7 Foxo3a plays a non-redundant role in maintaining Treg differentiation *in vitro* in *IL-10*-deficient mice.

Despite the significant increase in the number of splenocytes in *Foxo3a$^{-/-}$IL-10$^{-/-}$* mice, there is no difference in the number of Tregs present in the spleens of *Foxo3a$^{-/-}$IL-10$^{-/-}$* mice. Therefore, an assessment was made to determine if the differentiation of *Foxo3a$^{-/-}$IL-10$^{-/-}$* Tregs was compromised *in vitro*. The differentiation of iTregs from the CD4^{+} T cell of healthy *Foxo3a$^{-/-}$IL-10$^{-/-}$* mice is not significantly compromised (e.g., WT vs *Foxo3a$^{-/-}$IL-10$^{-/-}$*, P = 0.7327; **Figure 15 a, b**). However, the differentiation of iTregs from the CD4^{+} T cells of *Foxo3a$^{-/-}$IL-10$^{-/-}$* mice with a CrD-like phenotype is significantly compromised, only reaching approximately 50% iTregs (e.g., WT vs *Foxo3a$^{-/-}$IL-10$^{-/-}$*, P = 0.0033; **Figure 15 a, b**). The proportion of *Foxo3a$^{-/-}$* and *Foxo3a$^{-/-}$IL-10$^{-/-}$* iTregs from healthy mice is insignificantly reduced compared to WT and *IL-10$^{-/-}$*, the latter pair having the highest proportion of iTregs. To determine an approximate idea of the functional ability of the *Foxo3a$^{-/-}$IL-10$^{-/-}$* iTregs, Foxp3 expression was measured and compared to the control genotypes. *Foxo3a$^{-/-}$IL-10$^{-/-}$* iTregs from healthy mice have a significant decrease in Foxp3 expression compared to *IL-10$^{-/-}$* iTregs (P = 0.0312) and a nonsignificant decrease compared to WT and *Foxo3a$^{-/-}$* iTregs (P = 0.1661, P = 0.9475, respectively; **Figure 16 a, b**). Similarly to iTreg differentiation, *Foxo3a$^{-/-}$IL-10$^{-/-}$* iTregs from mice with a CrD-like phenotype have a significant reduction in Foxp3 expression, and even more so than in healthy mice (e.g., WT vs *Foxo3a$^{-/-}$IL-10$^{-/-}$*, P = 0.0032; **Figure 16 a, b**). Addition of decitabine, a DNA methyltransferase inhibitor, to the differentiation medium, is not able to rescue the compromised differentiation of iTregs from the CD4^{+} T cells of *Foxo3a$^{-/-}$IL-10$^{-/-}$* mice with a CrD-like phenotype but is able to increase the median fluorescence intensity of Foxp3 (**Figure S32 a, b).**

The viability of iTregs during differentiation was assessed to observe any changes in cell death which may contribute to change in numbers. *Foxo3a*$^{-/-}$*IL-10*$^{-/-}$ iTregs from sick and healthy mice have similar viability after *in vitro* differentiation compared to the control genotypes (e.g., WT vs *Foxo3a*$^{-/-}$*IL-10*$^{-/-}$, $P = 0.9926$; **Figure 17 c**). In all four genotypes, none of the dead cells are Foxp3^{+} and a low proportion of them are CD25^{+} (**Figure 17 a, b**). Regardless of differentiation and the initial proportion, *Foxo3a*$^{-/-}$*IL-10*$^{-/-}$ iTregs from sick and healthy mice both have compromised suppression of CD4^{+} T cells (**Figure 18 a-d**). In other words, even if *Foxo3a*$^{-/-}$*IL-10*$^{-/-}$ iTregs come from a healthy mouse and differentiation is uncompromised, *Foxo3a*$^{-/-}$*IL-10*$^{-/-}$ iTregs have compromised suppressive capacity.

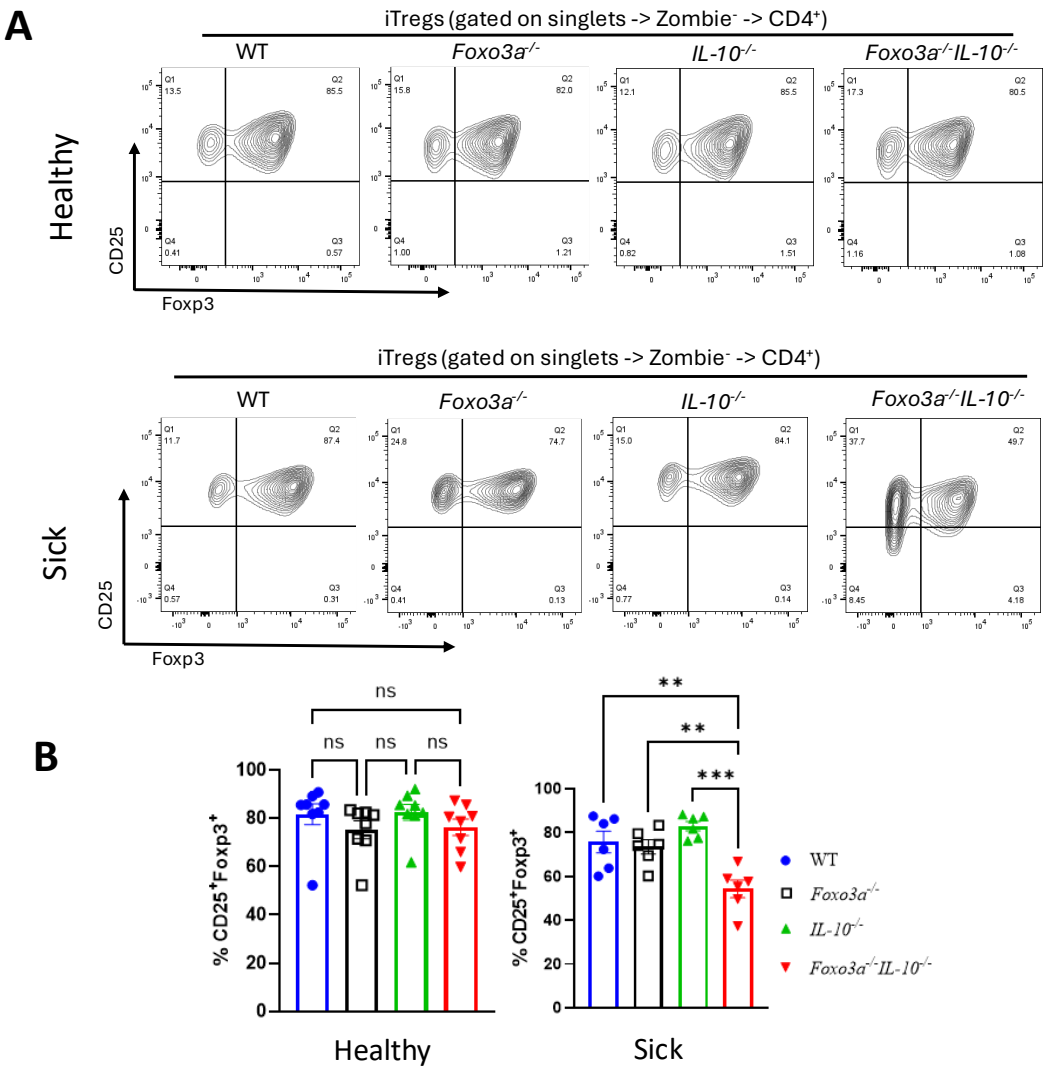

Figure 15. The development of a CrD-like phenotype in *Foxo3a*$^{-/-}$*IL-10*$^{-/-}$ mice compromises the *in vitro* differentiation of *Foxo3a*$^{-/-}$*IL-10*$^{-/-}$ iTregs. (A) Representative FACS plots of proportion of CD25^{+}Foxp3^{+} iTregs from healthy (top) or sick (bottom) *Foxo3a*$^{-/-}$*IL-10*$^{-/-}$ mice and control genotypes (*n*=8 and *n*=6, respectively). **(B)** Bar graphs depicting the proportion of CD25^{+}Foxp3^{+} iTregs from healthy (left) or sick (right) *Foxo3a*$^{-/-}$*IL-10*$^{-/-}$ mice and control genotypes (*n*=8 and *n*=6, respectively). For **A-B**, iTregs were induced using the ***In Vitro* Differentiation of Regulatory T Cells** protocol. Experiments conducted on 8-week-old to 12-week-old mice. iTregs were stained with fluorescent antibodies, acquired on a BD LSRFortessa™, and analyzed using FlowJo™ software. Individual bars depict the respective mean ± SEM. Statistical significance determined using a 1-way ANOVA and reported for each comparison by "*" (*P<0.05, **P<0.01, ***P<0.001, ****P<0.0001).

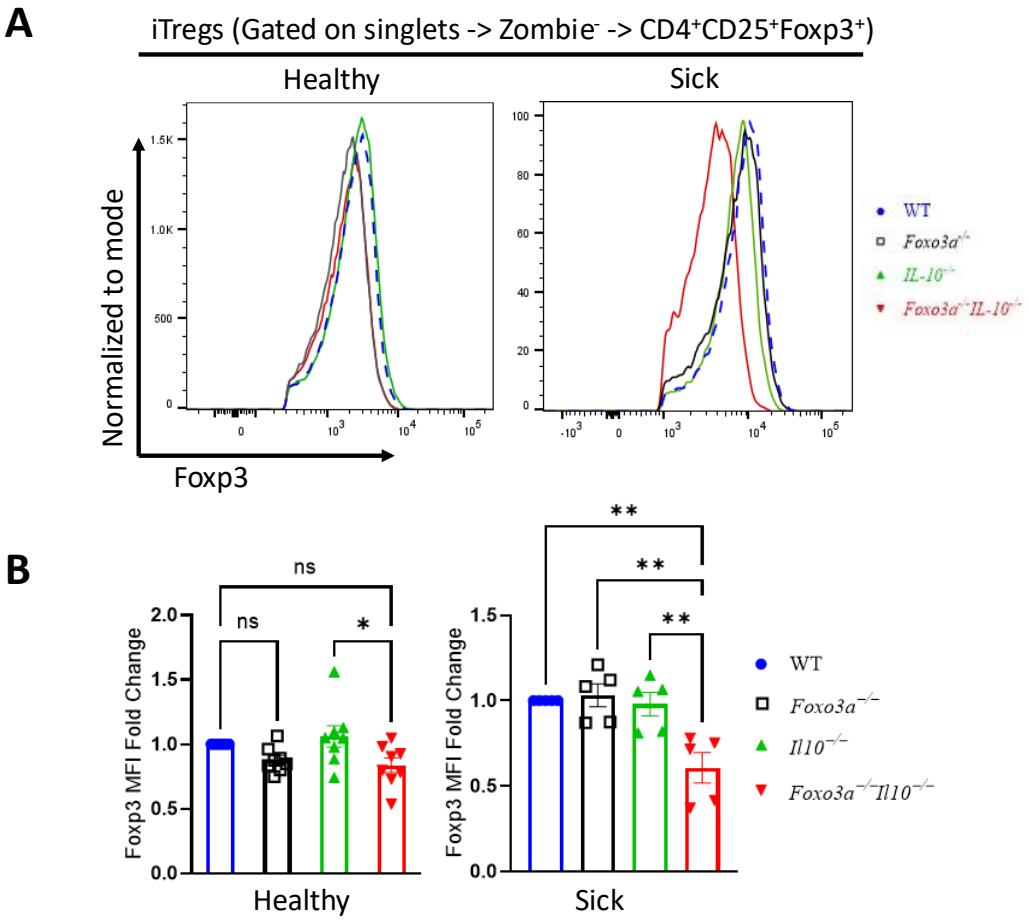

Figure 16. *Foxo3a*$^{-/-}$*IL-10*$^{-/-}$ iTregs differentiated from *Foxo3a*$^{-/-}$*IL-10*$^{-/-}$ mice with a CrD-like phenotype have a lower expression of Foxp3. (A) Representative FACS plots of Foxp3 expression in CD4^{+}CD25^{+}Foxp3^{+} populations of iTregs from healthy (left) or sick (right) *Foxo3a*$^{-/-}$*IL-10*$^{-/-}$ mice and control genotypes (*n*=8 and *n*=5, respectively). Foxp3 expression is normalized to the mode. **(B)** Bar graphs depicting Foxp3 MFI fold change in CD4^{+}CD25^{+}Foxp3^{+} populations of iTregs from healthy (left) or sick (right) *Foxo3a*$^{-/-}$*IL-10*$^{-/-}$ mice and control genotypes (*n*=8 and *n*=5, respectively). Foxp3 MFI is normalized to WT. Experiments conducted on 8-week-old to 12-week-old mice. iTregs were stained with fluorescent antibodies, acquired on a BD LSRFortessa™, and analyzed using FlowJo™ software. Individual bars depict the respective mean ± SEM. Statistical significance determined using a 1-way ANOVA and reported for each comparison by "*" (*P<0.05, **P<0.01, ***P<0.001, ****P<0.0001) (min. *n*=4).

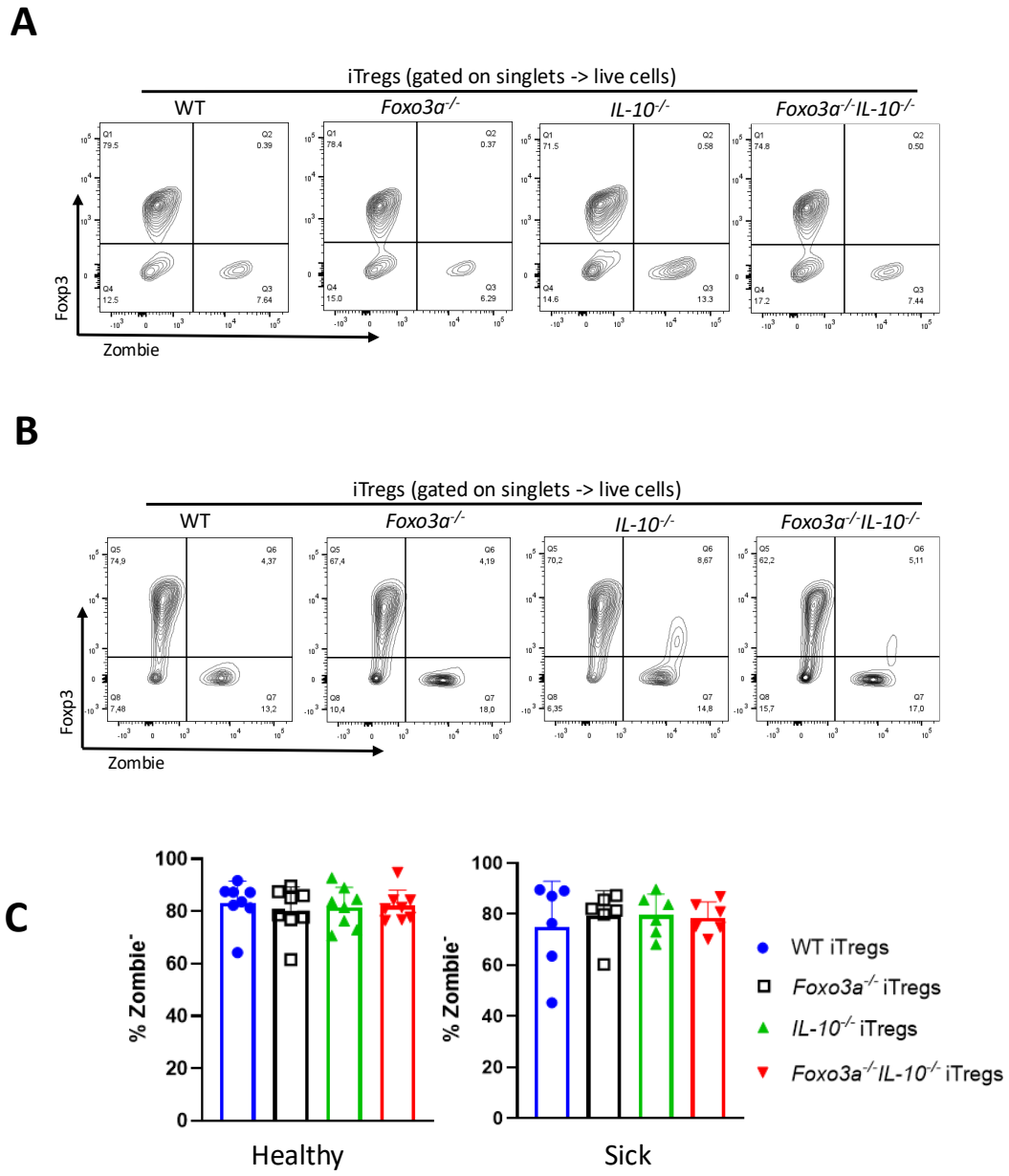

Figure 17. No difference between genotypes in viability of iTregs during *in vitro* differentiation. (A) Representative FACS plots of Zombie Yellow uptake versus Foxp3 in iTregs (*n*=14). **(B)** Representative FACS plots of Zombie Yellow uptake versus CD25 in iTregs (*n*=14). **(C)** Bar graphs depicting the proportion of Zombie$^-$ iTregs from healthy (left) or sick (right) *Foxo3a*$^{-/-}$*IL-10*$^{-/-}$ mice and control genotypes (*n*=8 and *n*=6, respectively). Experiments conducted on 8-week-old to 12-week-old mice. iTregs were stained with fluorescent antibodies, acquired on a BD LSRFortessa™, and analyzed using FlowJo™ software. Individual bars depict the respective mean ± SEM. Statistical significance determined using a 1-way ANOVA and reported for each comparison by "*" (*P<0.05, **P<0.01, ***P<0.001, ****P<0.0001).

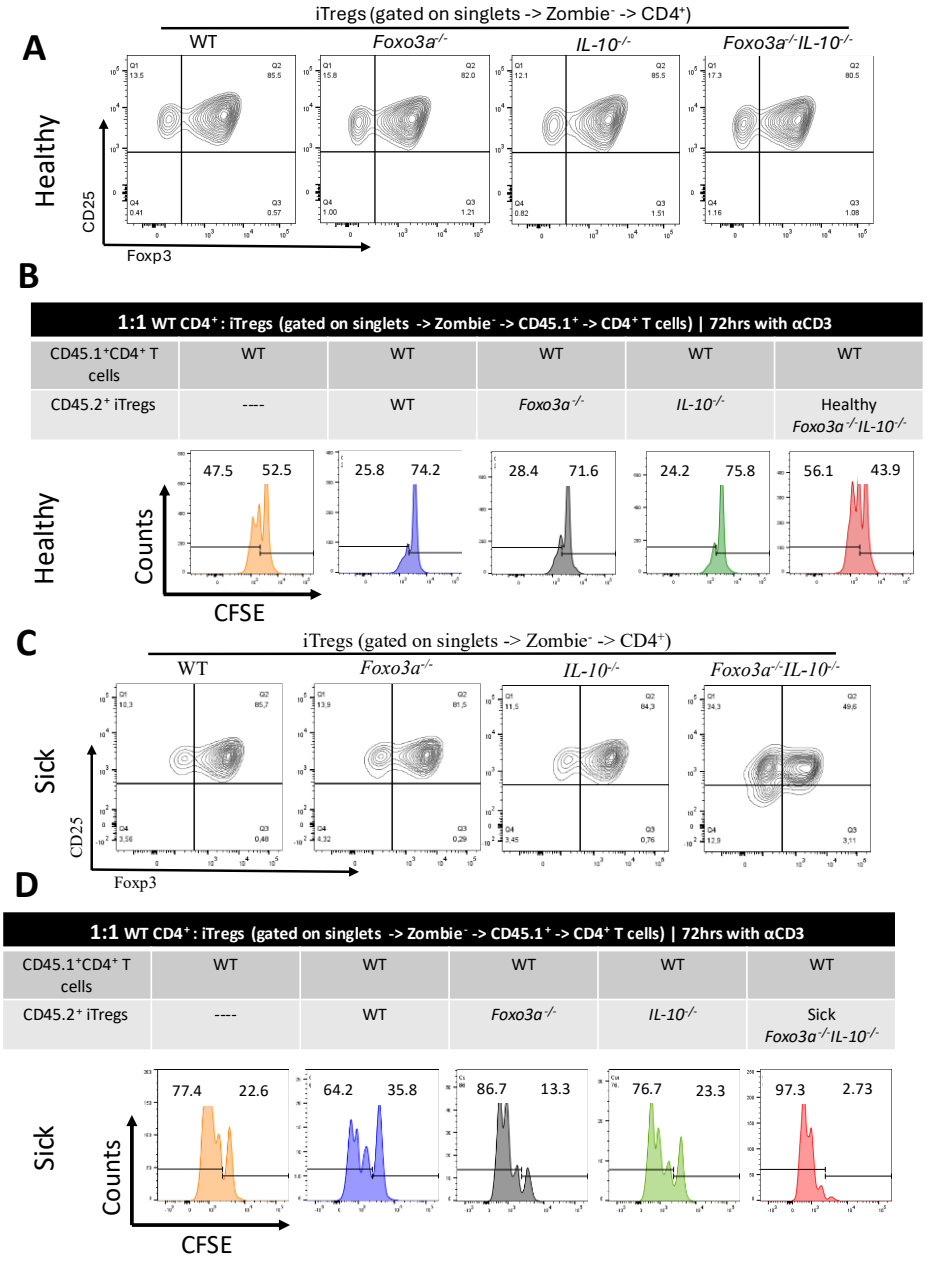

Figure 18. The ability of *Foxo3a*$^{-/-}$*IL-10*$^{-/-}$ iTregs to suppress the proliferation of WT CD4⁺ is compromised irrespective of if differentiation is compromised. (A) Representative FACS plots showing the purity of iTregs used in the Treg suppression assay depicted in (B) before the 72 hour co-culture. **(B)** Representative FACS plots of CFSE dilution in CD45.1⁺CD4⁺ WT T cells co-cultured 1:1 with CD45.2⁺ iTregs from all four genotypes *Foxo3a*$^{-/-}$*IL-10*$^{-/-}$ iTregs came from a healthy mouse where iTreg differentiation was not compromised. **(C)** FACS plots showing the purity of iTregs used in the Treg suppression assay depicted in (D) before the 72 hour co-culture. **(D)** Representative FACS plots of CFSE dilution in CD45.1⁺CD4⁺ WT T cells co-cultured 1:1 with CD45.2⁺ iTregs from all four genotypes. *Foxo3a*$^{-/-}$*IL-10*$^{-/-}$ iTregs came from a sick mouse where iTreg differentiation was compromised (n=3). **B** and **D** shows CD45.1⁺CD4⁺ WT T cells co-cultured with CD45.2⁺ iTregs stimulated for 72 hours in plates coated for 3 hours at 37°C with 20 µg/mL αCD3 antibodies. Experiments conducted on 8-week-old to 12-week-old mice. Cells were stained with fluorescent antibodies, acquired on a BD LSRFortessa™, and analyzed using FlowJo™ software.

3.8 Foxo3a plays a critical role in maintaining proper proliferation of *IL-10*-deficient iTregs.

Foxo3a$^{-/-}$*IL-10*$^{-/-}$ iTregs originating from sick mice have compromised differentiation, and interestingly, they also have increased proliferation. *Foxo3a*$^{-/-}$*IL-10*$^{-/-}$ iTregs differentiated from sick *Foxo3a*$^{-/-}$*IL-10*$^{-/-}$ mice have a significantly greater number of cells in culture after 96 hours of differentiation under saturating conditions *in vitro* (e.g., WT vs *Foxo3a*$^{-/-}$*IL-10*$^{-/-}$, $P < 0.0001$; **Figure 19 a**). *Foxo3a*$^{-/-}$*IL-10*$^{-/-}$ iTregs differentiated from healthy mice do not have a significantly greater number of cells in culture (e.g., WT vs *Foxo3a*$^{-/-}$*IL-10*$^{-/-}$, $P = 0.9924$; **Figure 19 a**). From a starting amount of $1*10^5$ CD4$^+$ T cells, *Foxo3a*$^{-/-}$*IL-10*$^{-/-}$ iTregs finish differentiation with about $3.5*10^5$ T cells. Other than *Foxo3a*$^{-/-}$*IL-10*$^{-/-}$ iTregs from sick mice, all other genotypes only proliferate a small amount during iTreg differentiation, ending with about $1.5*10^5$ T cells. There is no significant difference in the number of iTregs differentiated from any of the genotypes (e.g., WT vs *Foxo3a*$^{-/-}$*IL-10*$^{-/-}$, $P = 0.8321$; **Figure 19 b**). There is a significant increase in the number of non-iTregs differentiated from sick *Foxo3a*$^{-/-}$*IL-10*$^{-/-}$ mice compared to the control genotypes (e.g., WT vs *Foxo3a*$^{-/-}$*IL-10*$^{-/-}$, $P < 0.0001$; **Figure 19 c**). To determine at what stage of differentiation *Foxo3a*$^{-/-}$*IL-10*$^{-/-}$ iTregs begin proliferating faster, iTregs were stained with CFSE and iTregs were harvested after 24, 48, 72, and 96 hours of differentiation. At each of the latter points of time, *Foxo3a*$^{-/-}$*IL-10*$^{-/-}$ iTregs have a CFSE peak with lower brightness, indicating that they have proliferated more than the control genotypes (**Figure 20 a**). The difference in CFSE is greatest at 72 hours, and lowest at 24 hours. *Foxo3a*$^{-/-}$*IL-10*$^{-/-}$ Foxp3$^+$ and Foxp3$^-$ CD4$^+$CD25$^+$ T cells all have a lower CFSE profile than the control genotypes at all points of time examined (**Figure 20 b**). Of particular note is that the difference in CFSE profile is similar in *Foxo3a*$^{-/-}$*IL-10*$^{-/-}$ iTregs from both sick and healthy mice.

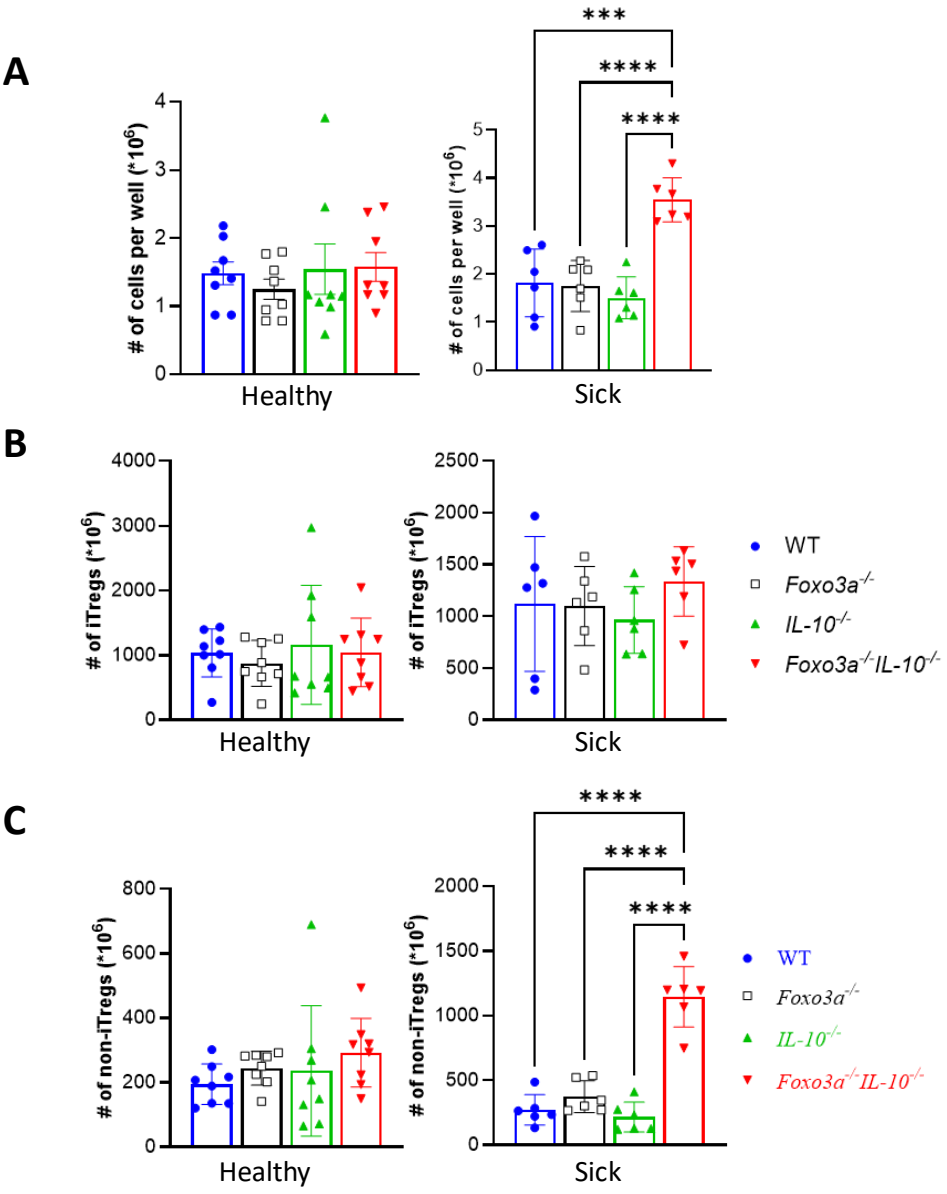

Figure 19. *Foxo3a*$^{-/-}$*IL-10*$^{-/-}$ mice with a CrD-like phenotype demonstrate increased proliferation during iTreg differentiation. (A) Bar graphs depicting the number of cells per well. **(B)** Bar graphs depicting the number of iTregs per well. **(C)** Bar graphs depicting the number of non-iTregs per well. **A-C** shows cells from **In Vitro Differentiation of Regulatory T Cells** from healthy (left) or sick (right) *Foxo3a*$^{-/-}$*IL-10*$^{-/-}$ mice and control genotypes (n=8 and n=6, respectively). iTregs were counted manually using methylene blue and a hemocytometer. Count is normalized to one well so that multiple experiments can be compared. Experiments conducted on 8-week-old to 12-week-old mice. Individual bars depict the respective mean ± SEM. Statistical significance determined using a 1-way ANOVA and reported for each comparison by "*" (*P<0.05, **P<0.01, ***P<0.001, ****P<0.0001).

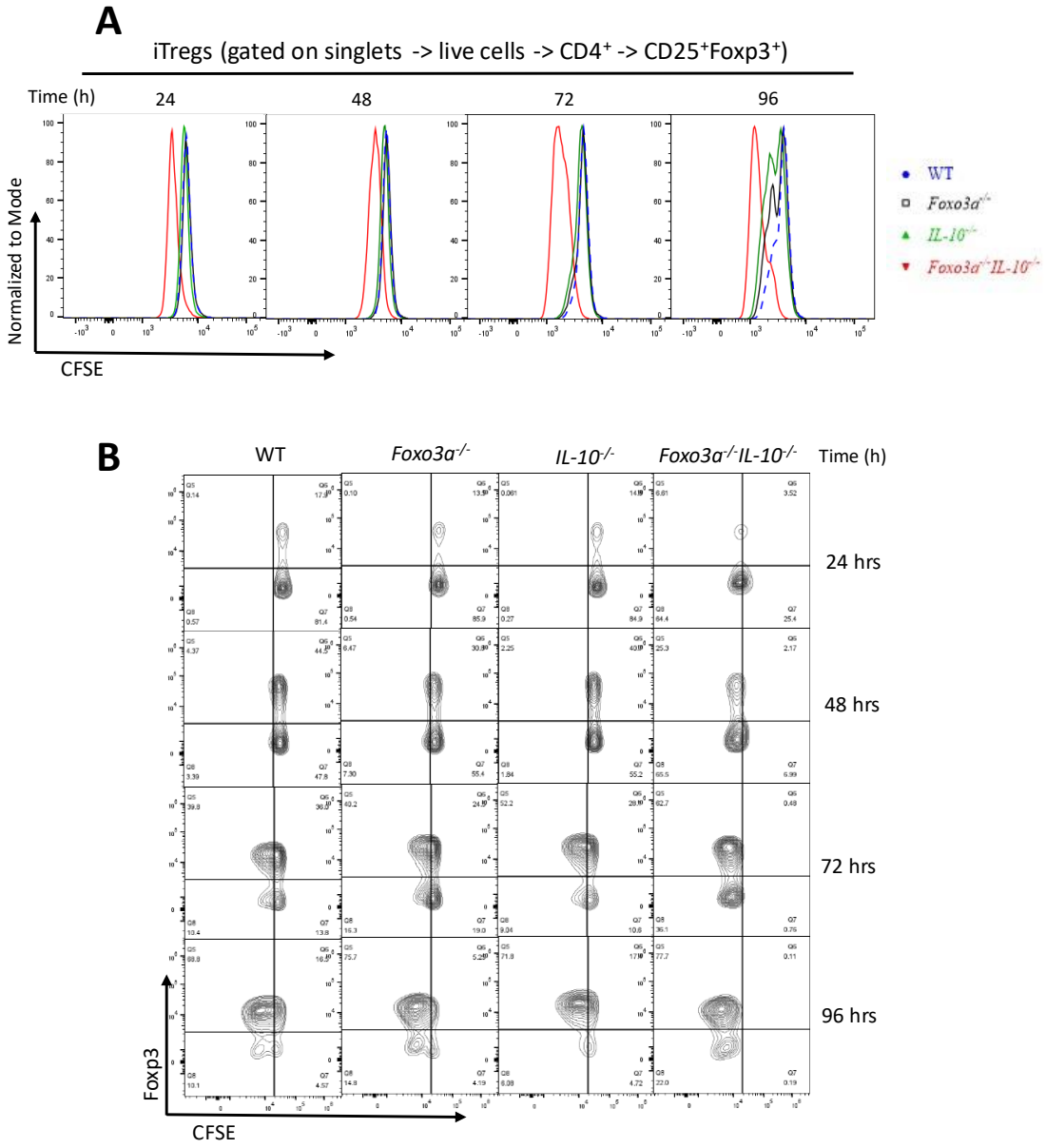

Figure 20. *Foxo3a*$^{-/-}$*IL-10*$^{-/-}$ iTregs and Foxp3^{-}CD4^{+} T cells undergo increased proliferation during iTreg differentiation. (A) Representative FACS plots of CFSE levels in iTregs at 24, 48, 72, and 96 hours through the iTreg differentiation process. CFSE expression is normalized to the mode (*n*=2). **(B)** Representative FACS plots showing CFSE levels in Foxp3^{+} and Foxp3^{-} CD25^{+}CD4^{+} T cells at 24, 48, 72, and 96 hours through the iTreg differentiation process (*n*=2). Experiments conducted on 8-week-old to 12-week-old mice. Cells were stained with fluorescent antibodies, acquired on a BD LSRFortessa™, and analyzed using FlowJo™ software.

3.9 Foxo3a controls TCR signaling sensitivity in *IL-10*-deficient iTregs through development of a CrD-like phenotype.

An increase in proliferation could originate from increased signaling through the TCR. Therefore, the effect of varying levels of αCD3 antibodies on the differentiation of iTregs was assessed. At low levels of αCD3 antibodies (plated coated with 1 μg/mL and 4 μg/mL) *Foxo3a*$^{-/-}$*IL-10*$^{-/-}$ iTreg differentiation is improved, while at normal levels (plates coated with 20 μg/mL), as determined by optimization in WT CD4^{+} T cells, *Foxo3a*$^{-/-}$*IL-10*$^{-/-}$ iTreg differentiation is compromised (**Figure 21 a, b**). This difference is only present when iTregs are differentiated from the CD4^{+} T cells of sick *Foxo3a*$^{-/-}$*IL-10*$^{-/-}$ mice. iTregs differentiated from the CD4^{+} T cells of healthy *Foxo3a*$^{-/-}$*IL-10*$^{-/-}$ mice have similar differentiation at all concentrations of αCD3 antibodies (**Figure 21 b**). At low concentration of αCD3 antibodies, *Foxo3a*$^{-/-}$*IL-10*$^{-/-}$ iTregs have increased survival, which normalizes at 20 μg/mL αCD3 (**Figure 22 a, b**). None of the dead cells are Foxp3^{+}, and only a small proportion of dead *Foxo3a*$^{-/-}$*IL-10*$^{-/-}$ cells are CD25^{+} (**Figure 22 c, d**). An increase in sensitivity to TCR stimulation by αCD3 antibodies allows *Foxo3a*$^{-/-}$*IL-10*$^{-/-}$ iTregs from sick mice to differentiate better at low concentrations, but worse at higher concentrations.

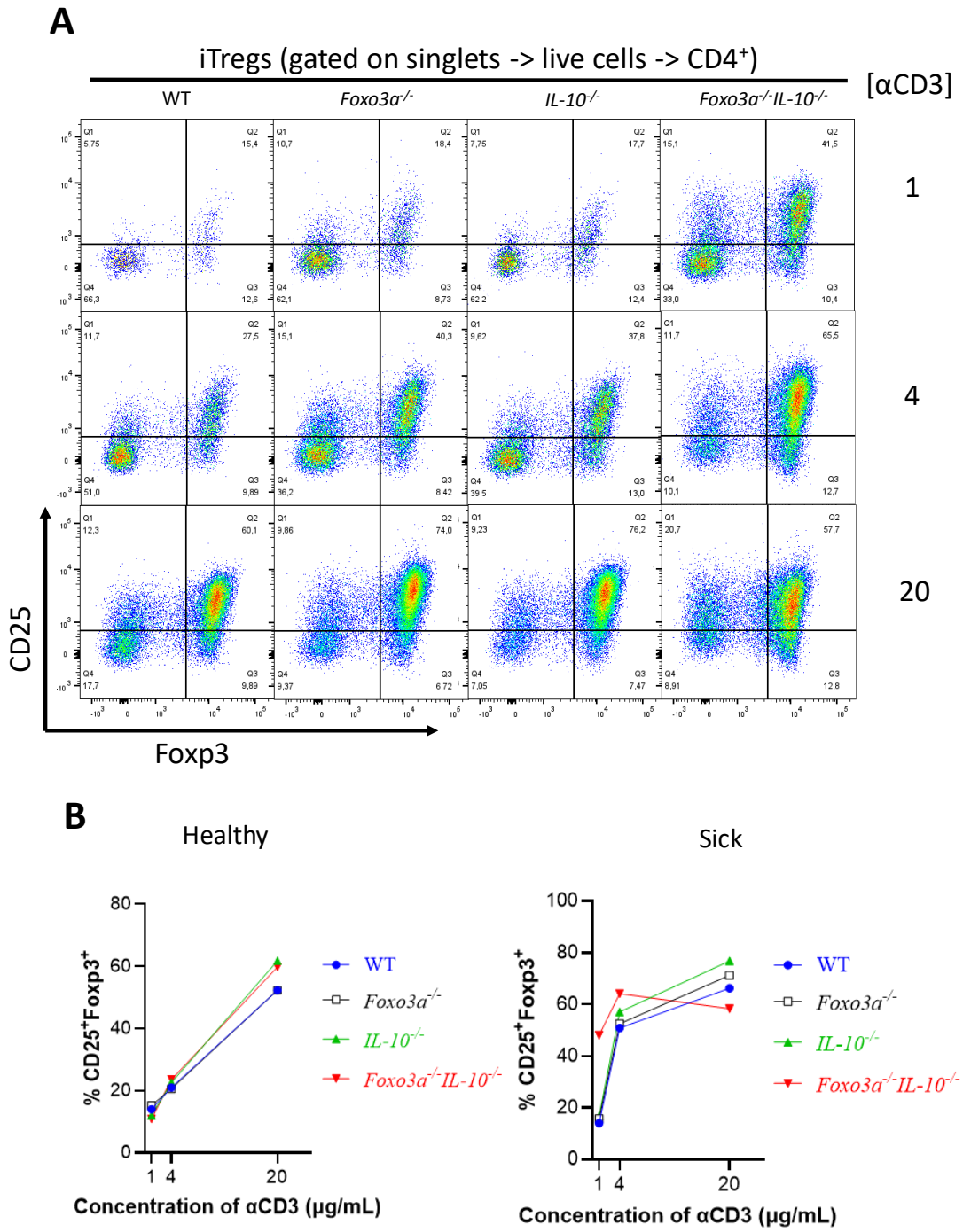

Figure 21. The development of a CrD-like phenotype in *Foxo3a*$^{-/-}$*IL-10*$^{-/-}$ mice causes increased stimulation and proliferation by αCD3 antibodies. (A) Representative FACS plots of proportion of iTregs differentiated from sick *Foxo3a*$^{-/-}$*IL-10*$^{-/-}$ mice and control genotypes (*n*=2). **(B)** Line graphs depicting the proportion of CD25^{+}Foxp3^{+} iTregs differentiated from from healthy (left) or sick (right) *Foxo3a*$^{-/-}$*IL-10*$^{-/-}$ mice and control genotypes (*n*=1 and *n*=2, respectively). In **A-B**, iTregs were differentiated in plates coated for 3 hours at 37°C with 1, 4, and 20 μg/mL αCD3 antibodies. Experiments conducted on 8-week-old to 12-week-old mice. iTregs were stained with fluorescent antibodies, acquired on a BD LSRFortessa™, and analyzed using FlowJo™ software.

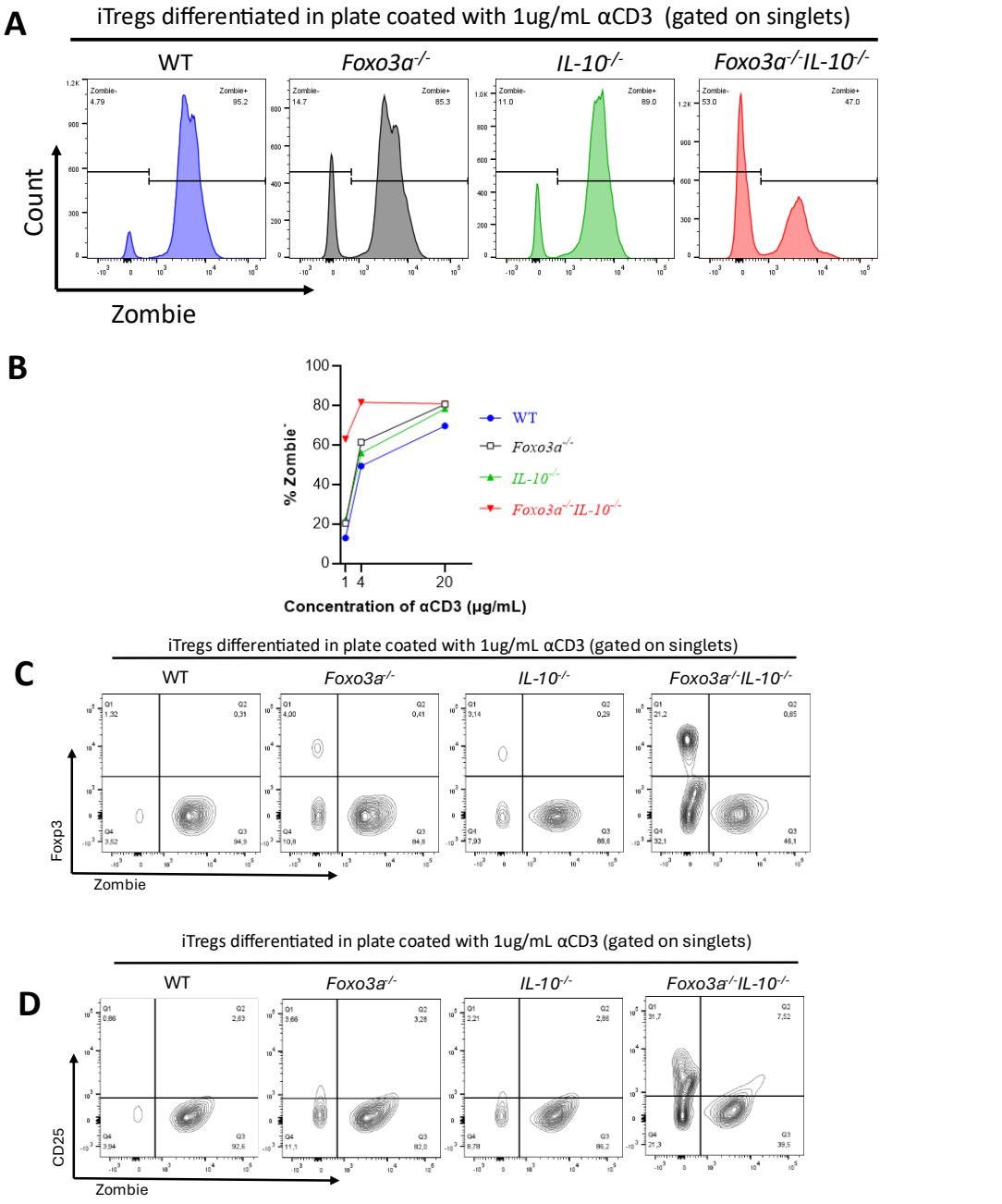

Figure 22. The development of a CrD-like phenotype in *Foxo3a*$^{-/-}$*IL-10*$^{-/-}$ mice causes increased viability when stimulated with low concentrations of αCD3 antibodies. (A) Representative FACS plots of Zombie Yellow uptake from iTregs differentiated from sick *Foxo3a*$^{-/-}$*IL-10*$^{-/-}$ mice and control genotypes (*n*=2). iTregs differentiated from wells coated for 3 hours at 37°C with 1 μg/mL αCD3 antibodies. **(B)** Line graph depicting the proportion of Zombie^{-} iTregs differentiated from sick *Foxo3a*$^{-/-}$*IL-10*$^{-/-}$ mice and control genotypes. iTregs differentiated from wells coated for 3 hours at 37°C with 1, 4, and 20 μg/mL αCD3 antibodies. **(C)** Representative FACS plots of Zombie Yellow uptake versus Foxp3 in iTregs from sick *Foxo3a*$^{-/-}$*IL-10*$^{-/-}$ mice and control genotypes. **(D)** Representative FACS plots of Zombie Yellow uptake versus CD25 from iTregs differentiated from sick *Foxo3a*$^{-/-}$*IL-10*$^{-/-}$ mice and control genotypes. In **C-D**, iTregs were differentiated from wells coated for 3 hours at 37°C with 1 μg/mL αCD3 antibodies. Experiments conducted on 8-week-old to 12-week-old mice. Cells were stained with fluorescent antibodies, acquired on a BD LSRFortessa™, and analyzed using FlowJo™ software.

3.10 Foxo3a modulates metabolic activity in *IL-10*-deficient iTregs.

To determine where the difference in proliferation versus differentiation originates, different metabolic pathways were assessed in *Foxo3a*$^{-/-}$*IL-10*$^{-/-}$ CD4^{+} T cells that were modulated in other cell types. The first target chosen was fatty acid metabolism as *Foxo3a*$^{-/-}$ *IL-10*$^{-/-}$ DCs have increased fatty acid synthesis (**Figure 7**). Bodipy is a fluorescent molecule which dissolves into and stains lipid droplets, and filipin fluorescently stains cholesterol. *Foxo3a*$^{-/-}$*IL-10*$^{-/-}$ CD4^{+} T cells and nTregs from spleens of *Foxo3a*$^{-/-}$*IL-10*$^{-/-}$ mice have an increase in lipids droplets (**Figure 23 a**). In comparison, there is no difference in the amount of cholesterol or lipids in *Foxo3a*$^{-/-}$*IL-10*$^{-/-}$ iTregs as compared to the control genotypes (**Figure 23 b**).

To get a general understanding of the metabolic activity in *Foxo3a*$^{-/-}$*IL-10*$^{-/-}$ T cells during iTreg differentiation, oxygen consumption rate (OCR) was measured in real time. *Foxo3a*$^{-/-}$*IL-10*$^{-/-}$ CD4^{+} T cells undergoing differentiation into iTregs have similar OCR during the first 48 hours of differentiation (**Figure S33 a**). At 72 hours, the oxygen consumption rate of *Foxo3a*$^{-/-}$*IL-10*$^{-/-}$ CD4^{+} T cells increases significantly compared to *IL-10*$^{-/-}$ CD4^{+} T cells (P = 0.0283; **Figure S33 a**). By 96 hours, *Foxo3a*$^{-/-}$*IL-10*$^{-/-}$ CD4^{+} T cells consume significantly more oxygen than the control genotypes (e.g., WT vs *Foxo3a*$^{-/-}$*IL-10*$^{-/-}$, *P* = 0.0342; **Figure S33 a**). This trend remains consistent when the oxygen consumption rate is normalized to the number of cells per well, where *Foxo3a*$^{-/-}$*IL-10*$^{-/-}$ CD4^{+} T cells consume significantly more oxygen than the control genotypes (e.g., WT vs *Foxo3a*$^{-/-}$*IL-10*$^{-/-}$, *P* = 0.0003; **Figure S33 b**).

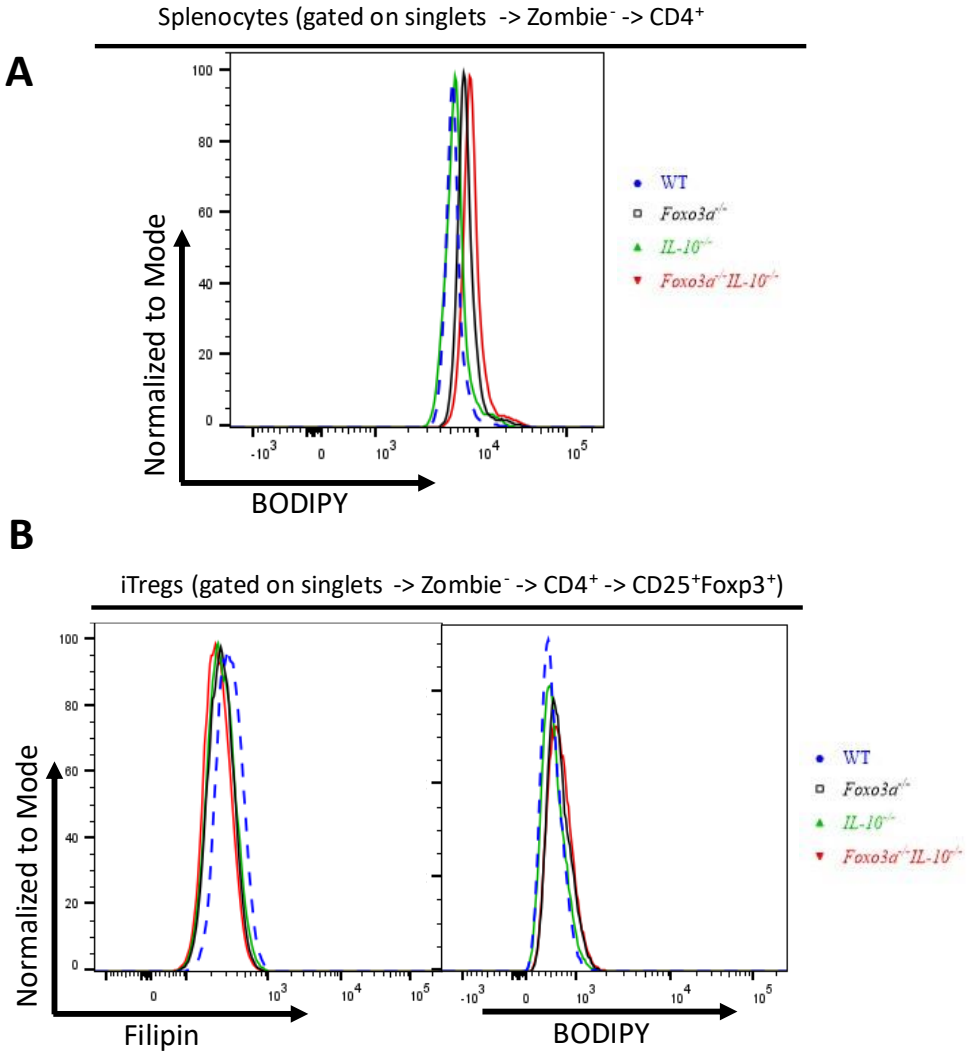

Figure 23. *Foxo3a*$^{-/-}$*IL-10*$^{-/-}$ CD4^{+} T cells have increased lipids while *Foxo3a*$^{-/-}$*IL-10*$^{-/-}$ iTregs have similar levels of lipids and cholesterol to the control genotypes. (A) Representative FACS plots of BODIPY fluorescence in splenic CD4^{+} T cells from all four genotypes. BODIPY is dissolved in lipid droplets and stains lipids (*n*=5). **(B)** Representative FACS plots of filipin (left) and BODIPY (right) fluorescence in iTregs from all four genotypes. Filipin fluorescently stains cholesterol (*n*=2 and *n*=4). Experiments conducted on 8-week-old to 12-week-old mice. Splenocytes and iTregs were stained with fluorescent antibodies, acquired on a BD LSRFortessa™, and analyzed using FlowJo™ software. Expression is normalized to the mode in all panels.

Aim 4: Characterize the stability of Foxo3a$^{-/-}$IL-10$^{-/-}$ iTregs under varying conditions

3.11 Foxo3a is critical in maintaining Foxp3 expression in *IL-10*-deficient iTregs by preventing excessive DNA methylation.

Foxo3a$^{-/-}$IL-10$^{-/-}$ iTregs have compromised suppression of WT CD4$^+$ T cells regardless of whether their differentiation and Foxp3 expression are compromised, therefore there must be another reason that they have decreased suppression. *Foxo3a$^{-/-}$IL-10$^{-/-}$* iTregs also have similar expression of eTreg cell surface markers as the control genotypes. Foxp3$^+$ pTregs in mice have been reported to lose Foxp3 expression and demonstrate plasticity between CD4$^+$ T cell subsets. Therefore, an assessment was completed to determine if *Foxo3a$^{-/-}$IL-10$^{-/-}$* iTregs were able to maintain expression of Foxp3 in the absence of Treg growth factors (TGF-β and IL-2). First, Foxp3 expression in *Foxo3a$^{-/-}$IL-10$^{-/-}$* iTregs from the Treg suppression assay was assessed (**Figure 14 a**). After 72 hours of co-culture with WT CD4$^+$ T cells, *Foxo3a$^{-/-}$IL-10$^{-/-}$* CD45.2$^+$ T cells have the lowest proportion of CD4$^+$CD25$^+$Foxp3$^+$ T cells even when starting with the same proportion of iTregs post-differentiation (**Figure 24 a, b**). *Foxo3a$^{-/-}$* CD45.2$^+$ T cells also have a slightly reduced proportion of CD4$^+$CD25$^+$Foxp3$^+$ T cells as compared to the other control genotypes.

To assess the stability of iTregs outside of the Treg suppression assay, iTregs were stimulated with αCD3 antibodies without IL-2 or TGF-β for 24 hours, then the proportion of CD4$^+$CD25$^+$Foxp3$^+$ T cells was assessed. Regardless of starting proportion of iTregs, *Foxo3a$^{-/-}$IL-10$^{-/-}$* iTregs lose Foxp3 expression quicker than the control genotypes and have a significantly lower proportion of iTregs compared to WT and *IL-10$^{-/-}$* (P = 0.0047, P = 0.0430, respectively; **Figure 25 a, b**). On average, 50% of *Foxo3a$^{-/-}$IL-10$^{-/-}$* iTregs remain after 24 hour stimulation with αCD3 antibodies. *Foxo3a$^{-/-}$* and *IL-10$^{-/-}$* iTregs have a non-significant decrease in proportion of remaining iTregs compared to WT (P = 0.0938, P = 0.5988,

respectively). As expected, *Foxo3a*$^{-/-}$*IL-10*$^{-/-}$ iTregs, also have lower expression of Foxp3 (**Figure 25 c**). Thus, not only are there lower numbers of iTregs, but these cells also have a lower expression of Foxp3. At 20 µg/mL αCD3, *Foxo3a*$^{-/-}$*IL-10*$^{-/-}$ iTregs have an insignificant difference in viability compared to the control genotypes (e.g., WT vs *Foxo3a*$^{-/-}$*IL-10*$^{-/-}$, P = 0.7766; **Figure 26 a, d**). Dead cells were Foxp3^{-}, but there is a higher proportion of dead CD25^{+} cells in the culture of *Foxo3a*$^{-/-}$*IL-10*$^{-/-}$ iTregs (**Figure 26 b, c**). Both *Foxo3a*$^{-/-}$ and *IL-10*$^{-/-}$ iTregs have a higher proportion of dead CD25^{+} cells compared to WT. The lack of IL-2 contributes substantially to the high proportion of dead cells in this assay.

iTregs stability was also assessed in the absence of αCD3 antibodies, but with IL-2 to maintain viability for 24 hours. *Foxo3a*$^{-/-}$*IL-10*$^{-/-}$ iTregs cultured in this way maintain CD25 expression and have restored Foxp3 expression when compared to the control genotypes (**Figure 27 a, b**). *Foxo3a*$^{-/-}$*IL-10*$^{-/-}$ iTregs are the only genotype with a substantial remaining population of CD25^{hi}Foxp3^{+} T cells. Addition of IL-2 to *Foxo3a*$^{-/-}$*IL-10*$^{-/-}$ iTregs stimulated for 24 hours with αCD3 antibodies are not able to restore the stability of iTregs when compared to the control genotypes but IL-2 is able to restore Foxp3 expression to levels similar to the control genotypes (**Figure 27 c, d**). Interestingly, iTregs that differentiated in the presence of decitabine, which is a DNA methyltransferase inhibitor, have partially rescued stability. *Foxo3a*$^{-/-}$*IL-10*$^{-/-}$ iTregs differentiated with 50 nM decitabine have similar stability to the control genotypes (**Figure S34 a, b**). This corresponds to about 70% of *Foxo3a*$^{-/-}$*IL-10*$^{-/-}$ iTregs remaining after stimulation with αCD3 antibodies for 24 hours. The stability of *Foxo3a*$^{-/-}$*IL-10*$^{-/-}$ nTregs was also assessed under different conditions. *Foxo3a*$^{-/-}$*IL-10*$^{-/-}$ nTregs have slightly reduced stability after 72 hours, albeit with a low concentration of αCD3 antibodies and in the presence of TGF-β and IL-2 (**Figure S35 a**).

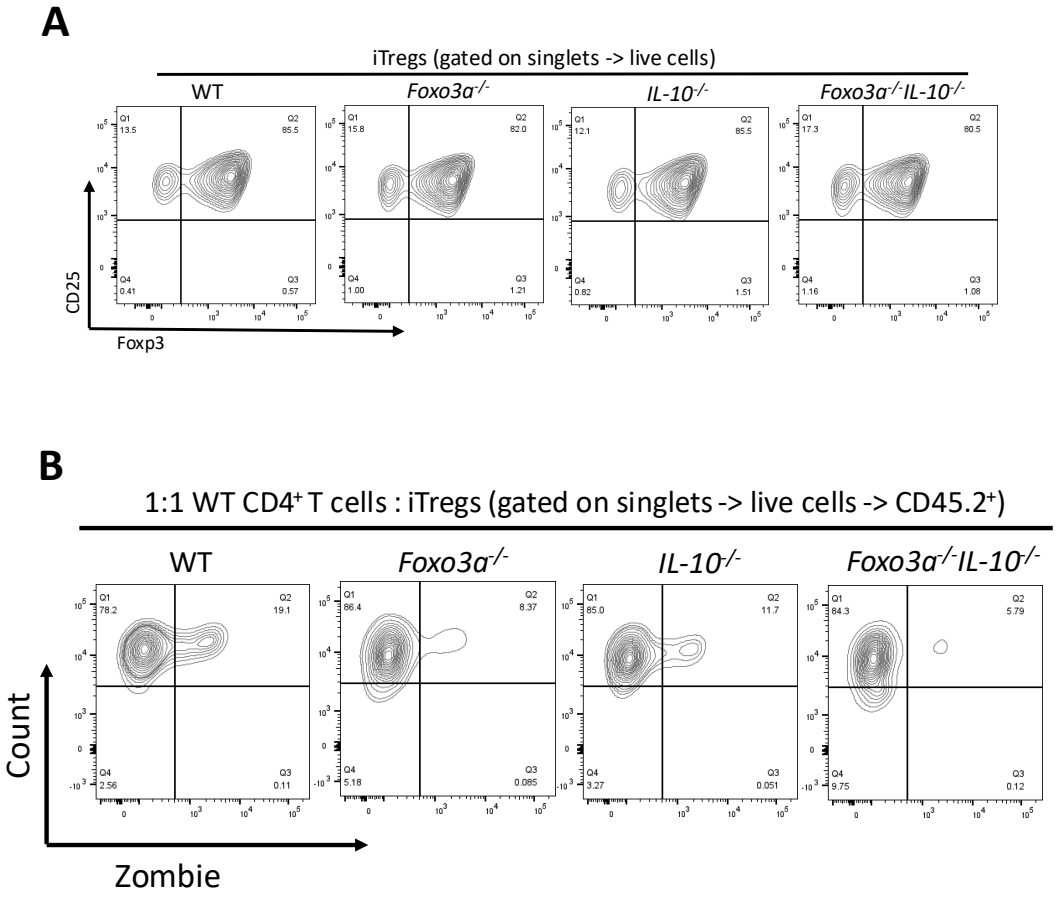

Figure 24. *Foxo3a*$^{-/-}$*IL-10*$^{-/-}$ and *Foxo3a*$^{-/-}$ iTregs have decreased stability in maintaining Foxp3 expression when co-cultured with WT CD4^{+} T cells. (A) Representative FACS plots of proportion of iTregs from all four genotypes used in the Treg suppression assay depicted in (B). **(B)** Representative FACS plots of CD45.2^{+} iTregs from all four genotypes remaining in the co-culture after 72 hours. Experiments conducted on 8-week-old to 12-week-old mice. Cells were stained with fluorescent antibodies, acquired on a BD LSRFortessa™, and analyzed using FlowJo™ software.

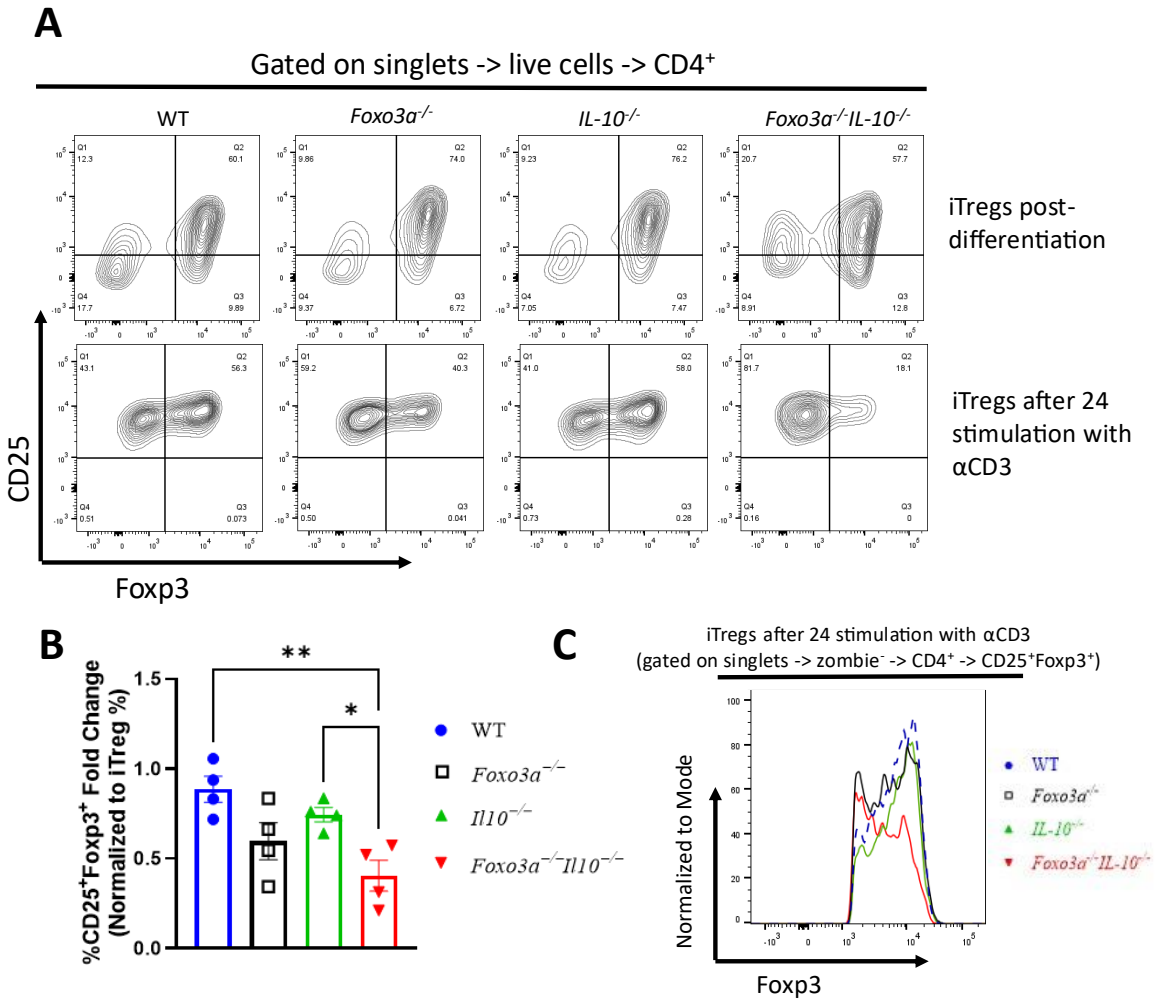

Figure 25. *Foxo3a*$^{-/-}$*IL-10*$^{-/-}$ iTregs have reduced stability in maintaining Foxp3 expression when stimulated with αCD3 antibodies. (A) Representative FACS plots of proportion of iTregs from all four genotypes before (top) and after (bottom) 24 hour stimulation (*n*=4). **(B)** Bar graph depicting the proportion of iTregs from all four genotypes remaining after 24 hour stimulation. iTreg proportion after stimulation normalized to iTreg proportion before stimulation (*n*=4). **(C)** Representative FACS plot of Foxp3 expression in iTregs after 24 hour stimulation (*n*=4). In **A-C**, iTregs were stimulated in plates coated for 3 hours at 37°C with 20 µg/mL αCD3 antibodies. Experiments conducted on 8-week-old to 12-week-old mice. Cells were stained with fluorescent antibodies, acquired on a BD LSRFortessa™, and analyzed using FlowJo™ software. Individual bars depict the respective mean ± SEM. Statistical significance determined using a 1-way ANOVA and reported for each comparison by "*" (*P<0.05, **P<0.01, ***P<0.001, ****P<0.0001).

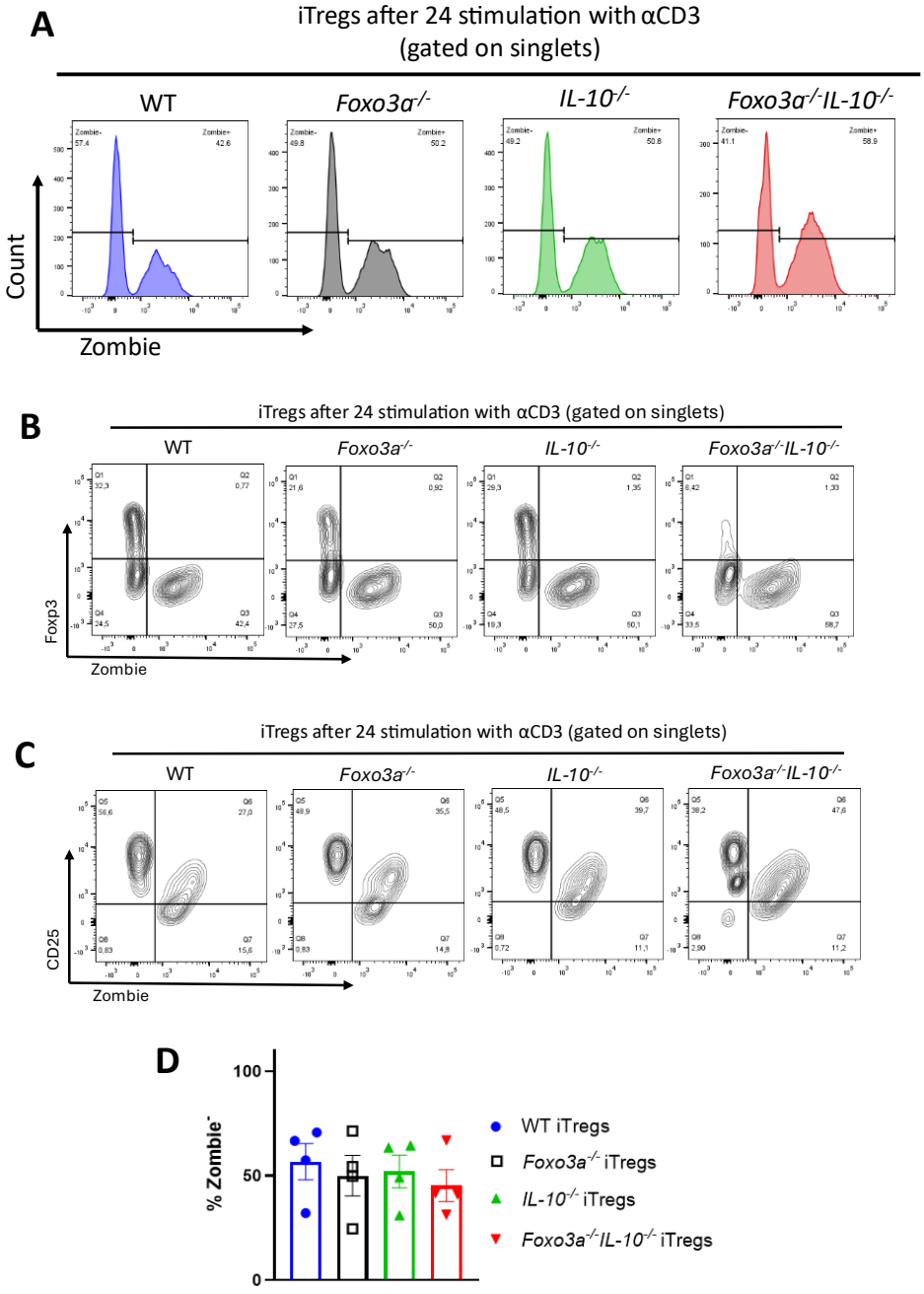

Figure 26. *Foxo3a*$^{-/-}$*IL-10*$^{-/-}$ iTregs have similar viability to the control genotypes when stimulated with αCD3 antibodies. (A) Representative FACS plots of Zombie Yellow uptake in iTregs from all four genotypes after 24 hour stimulation (*n*=4). **(B)** Representative FACS plots of Zombie Yellow uptake versus Foxp3 in iTregs from all four genotypes after 24 hour stimulation (*n*=4). **(C)** Representative FACS plots of Zombie Yellow uptake versus CD25 in iTregs from all four genotypes after 24 hour stimulation (*n*=4). **(D)** Bar graph depicting the proportion of Zombie^{-} iTregs from all four genotypes after 24 hour stimulation (*n*=4). In **A-D**, iTregs were stimulated in plates coated for 3 hours at 37°C with 20 µg/mL αCD3 antibodies. Experiments conducted on 8-week-old to 12-week-old mice. Cells were stained with fluorescent antibodies, acquired on a BD LSRFortessa™, and analyzed using FlowJo™ software. Individual bars depict the respective mean ± SEM. Statistical significance determined using a 1-way ANOVA and reported for each comparison by "*" (*P<0.05, **P<0.01, ***P<0.001, ****P<0.0001) (*n*=3).

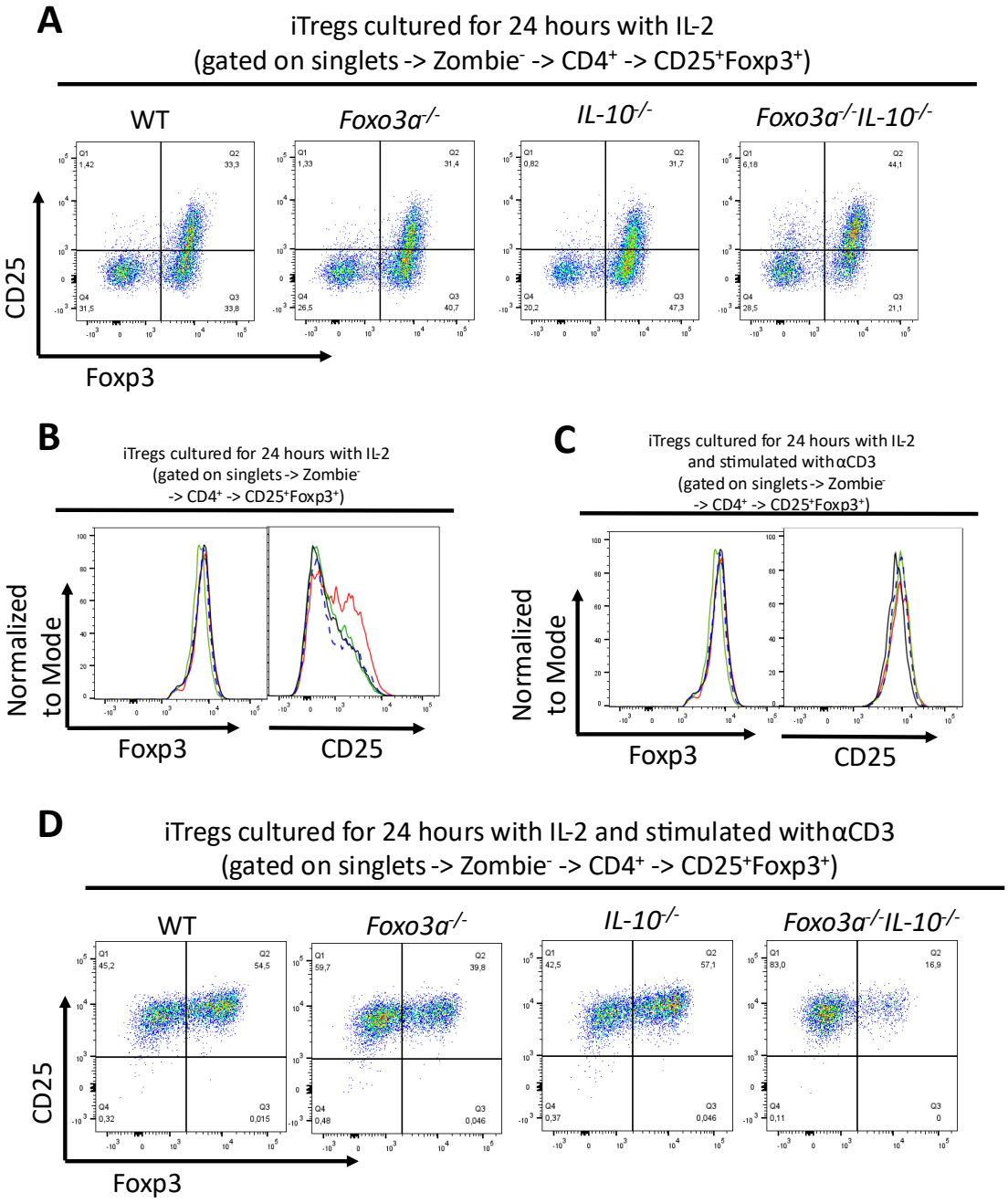

Figure 27. *Foxo3a*$^{-/-}$*IL-10*$^{-/-}$ iTregs maintain CD25 expression for longer in the absence of αCD3 stimulation. **(A)** Representative FACS plots of iTregs from all four genotypes after 24 hour culture with 2.5 ng/mL IL-2 (*n*=2). **(B)** Representative FACS plots of Foxp3 (left) and CD25 (right) expression in iTregs from all four genotypes after 24 hour culture with 2.5 ng/mL IL-2 (*n*=2). **(C)** Representative FACS plots of Foxp3 (left) and CD25 (right) expression in iTregs from all four genotypes after 24 hour culture with 2.5 ng/mL IL-2 in plates coated for 3 hours at 37°C with 20 µg/mL αCD3 antibodies. **(D)** Representative FACS plots of iTregs from all four genotypes after 24 hour culture with 2.5 ng/mL IL-2 in plates coated for 3 hours at 37°C with 20 µg/mL αCD3 antibodies (*n*=3). Experiments conducted on 8-week-old to 12-week-old mice. Cells were stained with fluorescent antibodies, acquired on a BD LSRFortessa™, and analyzed using FlowJo™ software.

3.12 Foxo3a maintains iTregs stability in *IL-10*-deficient mice by preventing over stimulation of the TCR at low thresholds of stimulation.

Because differentiation of *Foxo3a*$^{-/-}$*IL-10*$^{-/-}$ iTregs is dependant on the concentration of αCD3 antibodies in *Foxo3a*$^{-/-}$*IL-10*$^{-/-}$ mice with a CrD-like phenotype, the stability of iTregs for 24 hours with varying concentrations of αCD3 antibodies was also assessed. To evaluate this, iTregs were stimulated in plates coated with 1, 4, or 20 µg/mL of αCD3 antibodies for 24 hours in the absence of IL-2 and TGF-β. *Foxo3a*$^{-/-}$*IL-10*$^{-/-}$ iTregs differentiated from the CD4^{+} T cells of both sick and healthy *Foxo3a*$^{-/-}$*IL-10*$^{-/-}$ mice have compromised stability at 4 µg/mL of αCD3 antibodies, and worsens at 20 µg/mL of αCD3 when compared to the control genotypes (**Figure 28**). *Foxo3a*$^{-/-}$ and *IL-10*$^{-/-}$ iTregs also have reduced stability at all concentrations of αCD3 antibodies in comparison with WT, but not to the same degree as *Foxo3a*$^{-/-}$*IL-10*$^{-/-}$ iTregs. *Foxo3a*$^{-/-}$*IL-10*$^{-/-}$ iTregs stability worsens at higher concentrations of αCD3 antibodies, while *Foxo3a*$^{-/-}$ and *IL-10*$^{-/-}$ iTreg stability remains similar at all concentrations of αCD3 antibodies. Conversely, WT iTregs only have compromised stability at 1 µg/mL of αCD3 antibodies. iTregs from both healthy and sick *Foxo3a*$^{-/-}$*IL-10*$^{-/-}$ mice are similar and were pooled in **Figure 28**.

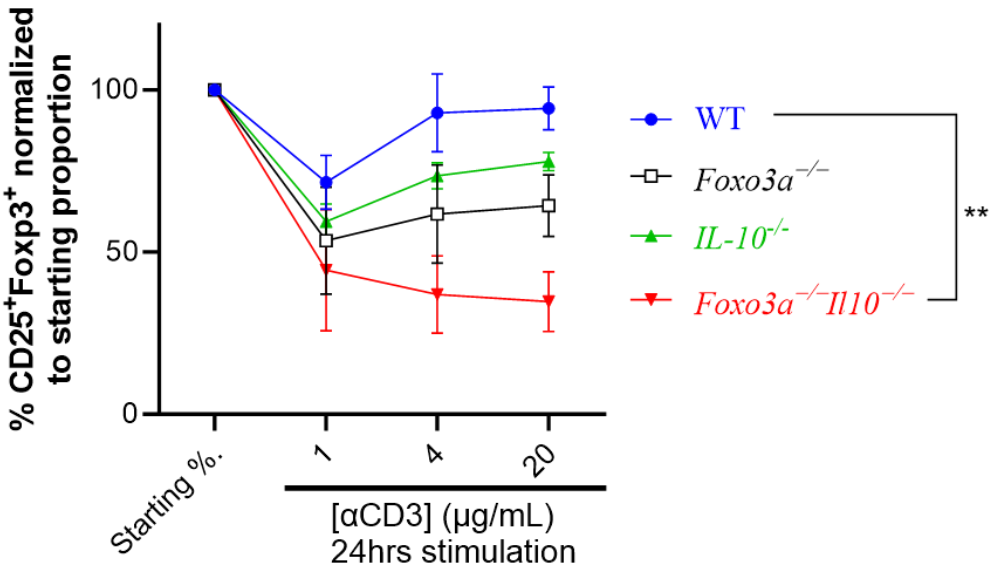

Figure 28. *Foxo3a*$^{-/-}$*IL-10*$^{-/-}$ iTregs have compromised stability which worsens as the concentration of αCD3 antibodies used to stimulate them increases. Line graph depicting the proportion of iTregs from all four genotypes remaining after 24 hour stimulation in plates coated for 3 hours at 37°C with 1, 4, and 20 μg/mL αCD3 antibodies with 20 μg/mL αCD3 antibodies coated for 3 hours at 37°C. iTreg proportion after stimulation normalized to iTreg proportion before stimulation (*n*=3). Experiments conducted on 8-week-old to 12-week-old mice. iTregs were stained with fluorescent antibodies, acquired on a BD LSRFortessa™, and analyzed using FlowJo™ software. Individual bars depict the respective mean ± SEM. Statistical significance determined using a 1-way ANOVA and reported for each comparison by "*" (*P<0.05, **P<0.01, ***P<0.001, ****P<0.0001).

3.13 In maintaining the stability of Foxp3, Foxo3a is critical in maintaining the proper balance of cytokine production in *IL-10*-deficient T cells.

In the Treg suppression assay, the wells with *Foxo3a*$^{-/-}$*IL-10*$^{-/-}$ nTregs and iTregs both produce more IL-17a and IFN-γ than the control genotypes (**Figure 13 b** and **Figure 14 b**). What is not clear is if the cytokines are coming from the WT CD45.1^{+}CD4^{+} T cells or the CD45.2^{+} Tregs. To answer this question, the supernatants of *Foxo3a*$^{-/-}$*IL-10*$^{-/-}$ iTregs alone that were stimulated with 20 μg/mL of αCD3 for 24 hours were analyzed for the production of IL-17a and IFN-γ. *Foxo3a*$^{-/-}$*IL-10*$^{-/-}$ iTregs produce significantly more IL-17a and IFN-γ than the control genotypes when stimulated with 20 μg/mL of αCD3 for 24 hours (e.g., WT vs *Foxo3a*$^{-/-}$*IL-10*$^{-/-}$, IL-17a: $P < 0.0001$, IFN-γ: $P < 0.0001$; **Figure 29 a**). The control genotypes only produce very low levels of IL-17a and IFN-γ. *Foxo3a*$^{-/-}$*IL-10*$^{-/-}$ iTregs have compromised stability, and most of the T cells in culture are not Foxp3^{+}. To determine if the IL-17a and IFN-γ is coming from the Foxp3^{-} or Foxp3^{+} T cells, cytokine production was assessed by flow cytometry through intracellular staining of IL-17a and IFN-γ. The majority of IL-17a and IFN-γ is being produced in the Foxp3^{-} T cells in all genotypes (**Figure 29 b**). There is a greater proportion of *Foxo3a*$^{-/-}$*IL-10*$^{-/-}$ Foxp3^{-} T cells, and levels of IL-17a^{+} and IFN-γ^{+} are also higher in the latter cells.

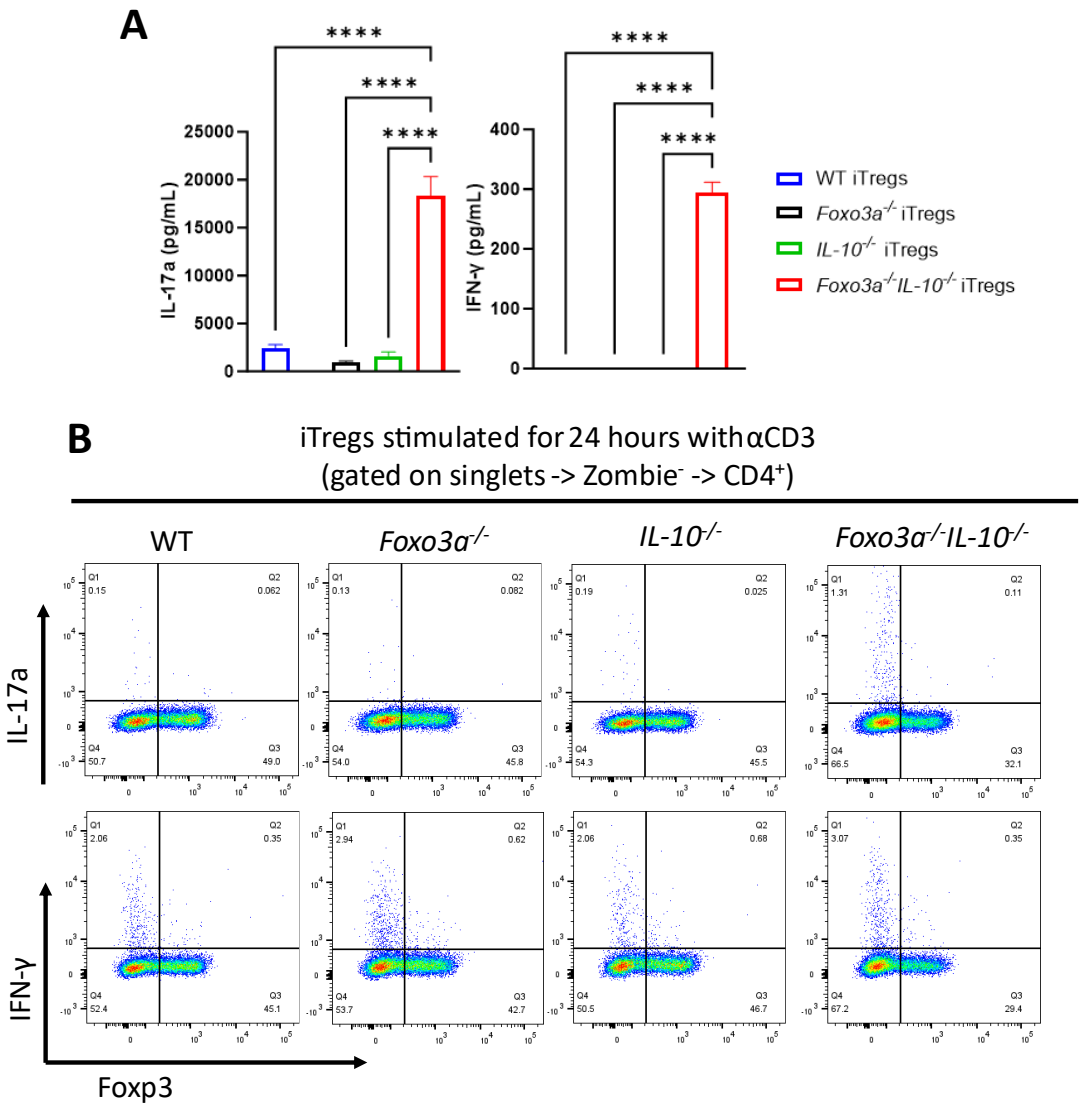

Figure 29. *Foxo3a*$^{-/-}$*IL-10*$^{-/-}$ CD4^{+}Foxp3^{-} T cells produce significantly more IL-17a and IFN-γ upon stimulation with αCD3. (A) Bar graphs depicting IL-17a (left) and IFN-γ (right) levels measured from the supernatants of iTregs from all four genotypes stimulated for 24 hours in plates coated for 3 hours at 37°C with 20 µg/mL αCD3 antibodies. Concentrations of IL-17a and IFN-γ were determined using sandwich ELISA (*n*=3). **(B)** Representative FACS plots of intracellular IL-17a (top) and IFN-γ (bottom) in iTregs from all four genotypes after 24 hour stimulation in plates coated for 3 hours at 37°C with 20 µg/mL αCD3 antibodies. After 12 hours of stimulation, BFA was added, and iTregs were harvested another 12 hours after the addition of BFA. Experiments conducted on 8-week-old to 12-week-old mice. Cells were stained with fluorescent antibodies, acquired on a BD LSRFortessa™, and analyzed using FlowJo™ software. Individual bars depict the respective mean ± SEM. Statistical significance determined using a 1-way ANOVA and reported for each comparison by "*" (*P<0.05, **P<0.01, ***P<0.001, ****P<0.0001).

4.0 Discussion

In this thesis, novel pathways involved in the development of CrD are presented. Foxo3a and IL-10 work cooperatively to maintain proper differentiation and cytokine production in DCs. In addition, Foxo3a and IL-10 work synergistically to maintain proper iTreg differentiation and stability and Foxp3 expression. The data from this study provide insight into the development of intestinal inflammation in *IL-10*-deficient mice. In addition, this study elucidates novel roles for Foxo3a in the development and function of DCs and Tregs. The latter roles may provide new therapeutic pathways for IBD. Furthermore, these novel roles may be used for therapeutics involved in promoting dysfunctional DCs and Tregs when inflammation is beneficial, such as in the treatment of cancer.

Foxo3a is an important member of the FoxO family of transcription factors. Foxo3a is highly expressed in the ovaries, skeletal muscle, heart, and spleen[265]. Foxo3a is regulated by phosphorylation, acetylation, and ubiquitination. Upon phosphorylation, Foxo3a is transported from the nucleus to the cytoplasm, inhibiting its function. The following kinases phosphorylate Foxo3a: AKT, IkB kinase (IKK), JNK, glucocorticoid regulated kinase (SGK), AMPK, mitogen-activated protein kinases (MAPKs), and mammalian sterile 20-like kinase 1 (MST1)[218, 266-268]. Foxo3a degradation through ubiquitination is regulated by murine double minute 2 (MDM2)[269]. Foxo3a is regulated by acetylation and miRNAs, although the exact mechanism is unclear[270, 271].

Much of the interest surrounding Foxo3a is a result of diverse GWASs that link *Foxo3a* to extreme old age[272]. *Foxo3a* is also linked to milder progression of CrD and rheumatoid arthritis, and to increased risk of severe malaria[273]. GWASs demonstrate that *Foxo3a* is associated with a lower risk of tumor development and dysregulation leads to resistance to chemotherapy[274, 275]. Foxo3a is important in regulation of suppression of the cell cycle,

promotion of apoptosis, protection against cellular stress, reparation of DNA damage, and aerobic glycolysis[276-280]. Foxo3a is closely associated with autoimmune diseases, but its exact role in these diseases has yet to be fully elucidated. Foxo3a has been shown to regulate T and B cell cycle arrest, apoptosis, and survival, Treg differentiation, neutrophil survival, and DC cytokine production[281]. The findings of this study, it is likely that the inflammatory milieu in *Foxo3a*$^{-/-}$*IL-10*$^{-/-}$ mice drives the plasticity of Tregs towards a pro-inflammatory phenotype and increases the ability of DCs to activate T cells.

4.1 Foxo3a control the differentiation and cytokine production in DCs of *IL-10*-deficient mice.

DCs sit at a critical junction of immune cell interactions in autoimmune diseases by mediating the adaptive immune response. An increase in the activity of pro-inflammatory immune cells is involved in the pathogenesis of IBD, including production of the pro-inflammatory cytokines IFN-γ and IL-17a by Th1 and Th17 T cells, respectively[282]. DCs are the primary cells responsible for activating T cells through MHC antigen presentation, co-stimulation, and cytokine production. DCs from the intestinal tissues of CrD patients excrete higher levels of IL-12 and IL-6, increasing the activation of $CD4^+$ T cells[283]. Thus, increased activation of T cells by DCs could lead to aggressive progression of CrD.

Treatment with αTNF-α or αIL-6 antibodies is effective at improving outcomes in CrD patients[284, 285]. The mechanism by which inflammatory cytokines are produced in higher amounts in CrD patients is largely uncharacterized. In previous studies, *Foxo3a*$^{-/-}$ DCs produce higher amounts of IL-6 and IL-10 induces a tolerogenic phenotype in DCs[230, 286]. Other work in Dr. Sad's laboratory agrees with this finding, but also indicates that loss of *IL-10* and *Foxo3a* significantly increases the amount of IL-6, TNF-α, and IL-12p70 in LPS-

stimulated DCs[262]. An increase in pro-inflammatory cytokine production by *Foxo3a*$^{-/-}$*IL-10*$^{-/-}$ DCs leads to an increase in the cytokine production of CD4^{+} T cells when co-cultured with *Foxo3a*$^{-/-}$*IL-10*$^{-/-}$ DCs[262]. IL-6 is needed to induce polarization of CD4^{+} T cells into Th17 cells; thus an increase in IL-17a production in co-culture of CD4^{+} T cells and *Foxo3a*$^{-/-}$*IL-10*$^{-/-}$ DCs is consistent with the literature[92]. The increase in IL-17a production likely contributes to the development of intestinal inflammation in *Foxo3a*$^{-/-}$*IL-10*$^{-/-}$ mice.

Although αTNF-α or αIL-6 antibodies are effective at dealing with the outcome of a dysregulated immune system, they do not treat the underlying cause for increased cytokine production. RNAseq was performed and found that many pathways involved in immunity and metabolism are upregulated in *Foxo3a*$^{-/-}$*IL-10*$^{-/-}$ DCs (**Figure 7**). Inhibition of mTOR, STAT3, MK2, fatty acid synthase, and IL-1RAP are all effective at reducing the production of IL-6 and TNF-α in LPS stimulated DCs (**Figure 8 a, b**). Previous studies show that inhibition of mTOR leads to a decrease in the expression of TNF-α and IL-6 in other cell types[287, 288]. Decreased IL-6 production in *Foxo3a*$^{-/-}$*IL-10*$^{-/-}$ DCs treated with rapamycin provides a partial mechanistic explanation for the rescue of the CrD-like phenotype in *Foxo3a*$^{-/-}$*IL-10*$^{-/-}$ mice by rapamycin[261]. In previous studies, *STAT3*$^{-/-}$ DCs produce higher levels of IL-6 and TNF-α[289]. In contrast, this study demonstrates that STAT3 inhibition decreased IL-6 and TNF-α production in *Foxo3a*$^{-/-}$*IL-10*$^{-/-}$ DCs. MK2 is a key regulator of IL-6 and TNF-α production, and this study corroborates the latter by showing that MK2 inhibition leads to a decrease in IL-6 and TNF-α production in in *Foxo3a*$^{-/-}$*IL-10*$^{-/-}$ DCs[290, 291]. Fatty acid synthesis has contrasting roles in DCs depending on DC subset and environment[292]. This study supports the role of fatty acid synthesis in the production of pro-inflammatory cytokines in DCs, as its inhibition leads to decreased production of TNF-α and IL-6[293]. IL-1 signaling induces the production of pro-inflammatory cytokines and is important in T cell activation[294, 295]. This study agrees with the latter findings as IL-1RAP inhibition leads to a decrease in IL-6 and TNF-α production in in *Foxo3a*$^{-/-}$*IL-10*$^{-/-}$

DCs. Overall, this study reveals a multitude of pathways that can be inhibited to prevent the inflammatory cytokine production in *Foxo3a*$^{-/-}$*IL-10*$^{-/-}$ DCs.

Patients with CrD show an increased number of mature moDCs in their colonic tissue[247]. Similarly, *Foxo3a*$^{-/-}$*IL-10*$^{-/-}$ mice have an increased number of moDCs in the lamina propria[262]. In *Foxo3a*$^{-/-}$*IL-10*$^{-/-}$ mice, this is especially problematic as *Foxo3a*$^{-/-}$*IL-10*$^{-/-}$ DCs produce more inflammatory cytokines and activate T cells to a greater degree[262]. Studies demonstrate that increased numbers of moDCs result from increased expression of chemokine receptors[247]. As genetics play an important factor in the development of CrD, it is possible that the reasons for increased numbers of moDCs may differ from patient-to-patient. The role of Foxo3a on moDC differentiation has yet to be characterized. However, *Foxo3a*$^{-/-}$ mice exhibit a myeloproliferative syndrome, indicating its role in immune cell differentiation[296]. Conversely, IL-10 reduces the ability of monocytes to differentiate into DCs *in vitro*[297]. This study shows that only *Foxo3a*$^{-/-}$*IL-10*$^{-/-}$ DCs, and not *Foxo3a*$^{-/-}$ or *IL-10*$^{-/-}$ DCs, differentiate from BM in response to GM-CSF in a greater proportion (**Figure 6**). As *IL-10*-deficiency alone does not cause a difference in moDC differentiation *in vitro*, it is likely that Foxo3a plays a compensatory role in preventing abhorrent moDC differentiation. The increased differentiation of moDCs in *Foxo3a*$^{-/-}$*IL-10*$^{-/-}$ mice likely contributes to the role of Foxo3a in preventing aggressive progression of CrD because *Foxo3a*$^{-/-}$*IL-10*$^{-/-}$ moDCs are pro-inflammatory. Thus, Foxo3a and IL-10 work cooperatively to prevent excessive moDC differentiation.

4.2 The development of a CrD-like phenotype compromises the differentiation of iTregs in *Foxo*3a-*IL-10*-deficient mice.

Tregs play a central role in mediating the immune response. Complete loss of Tregs via Foxp3 deficiency leads to development of IPEX syndrome in mice. The intestine is one of the most severely affected organs in IPEX[254]. This demonstrates the key roles Tregs play in regulating intestinal homeostasis. *IL-10, PPARG*, and *MDR1*-deficient mice are used as models for IBD and are IBD susceptibility loci in humans. The latter genes all play roles in Treg function, development, or both[138, 298, 299]. In mouse models with artificially induced colitis, the absence of Tregs leads to aggressive disease[300]. Tregs are also able to rescue intestinal inflammation, because adoptive transfer of $CD4^+CD25^+$ T cells into a T cell transfer model of CrD was able to cure intestinal inflammation[256]. Studies performed in humans have assessed efficacy of infusion of *ex vivo*-expanded Tregs for treatment of UC and demonstrate promising results[301]. The latter studies highlight the key role that Tregs play in development of IBD and CrD.

Given the role that Tregs play in the regulation of the immune response and in mouse models for IBD, the differentiation of Tregs is characterized in this study. Previous data indicate that although the proportion of nTregs in the lamina propria of *Foxo3a*$^{-/-}$*IL-10*$^{-/-}$ mice is reduced, the overall number of the latter cells is increased[262]. This led to the hypothesis that Foxo3a and IL-10 regulate a compensatory mechanism governing Treg differentiation. Foxo3a and Foxo1 also play largely redundant roles in Treg differentiation. Loss of *Foxo3a* and *Foxo1* causes Tregs to lose their suppressive capacity and results in reduced numbers of $Foxp3^+$ cells in the spleen and thymus[233]. Those Tregs that remain have a marked reduction in Foxp3 expression. This study demonstrates that nTregs from the spleen and thymus of *Foxo3a*$^{-/-}$*IL-10*$^{-/-}$ mice have slightly lower expression of Foxp3; the latter expression worsens upon development of a CrD-like phenotype (**Figure 11** and **Figure 12**). iTreg differentiation

from the CD4$^+$ T cells of *Foxo3a*$^{-/-}$*IL-10*$^{-/-}$ mice with a CrD-like phenotype is also severely compromised (**Figure 15** and **Figure 16**). This indicates that Foxo3a and IL-10 play compensatory roles, where only deficiency of both leads to impairment of Foxp3 expression *in vivo*. It also indicates that *Foxo3a* and *IL-10* deficiency leads only to compromised differentiation when the CD4$^+$ T cells originate from an inflammatory environment. Loss of *Foxo3a* deficiency causes splenomegaly[233], which this study corroborates (**Figure 9**). The larger size of the spleens from *Foxo3a*$^{-/-}$*IL-10*$^{-/-}$ mice likely results from internal inflammation, becoming greater with disease progression.

DNA methylation is an important regulator of transcription, preventing the binding of enhancers and promoters. In the case of Tregs, CNS1, CNS2 (also known as the Treg-specific methylated region), and CNS3 are all non-coding sequences that play important roles in the transduction and maintenance of Foxp3 expression[121, 170, 171]. Foxo3a binds to the promotors, CNS1 and CNS3[233]. A variety of other transcription factors also bind to these regions to promote Foxp3 induction and expression[302-304]. These transcription factors may be able to compensate for the loss of *Foxo3a*, and would explain why *Foxo3a*$^{-/-}$*IL-10*$^{-/-}$ iTregs are able to maintain mostly proper differentiation without the development of a CrD-like phenotype, albeit with slightly compromised Foxp3 expression (**Figure 15** and **Figure 16**). With the development of a CrD-like phenotype, *Foxo3a*$^{-/-}$*IL-10*$^{-/-}$ iTregs have significantly compromised differentiation and Foxp3 expression. Introduction of decitabine, a DNA methyltransferase inhibitor, is not able to rescue the differentiation of *Foxo3a*$^{-/-}$*IL-10*$^{-/-}$ iTregs from mice with a CrD-like phenotype but it is able to partially restore Foxp3 expression (**Figure S32**). DNA regions with H3K27me3 become hypermethylated under inflammatory conditions[305]. Furthermore, nTregs have lower proportions of H3K27me3 regions in comparison to other CD4$^+$ T cell subsets, indicating the importance of unmethylated regions in Tregs[306]. Although inflammation increases DNA methylation, it appears that increased

methylation is not the cause of compromised differentiation of iTregs from *Foxo3a*$^{-/-}$*IL-10*$^{-/-}$ mice with a CrD-like phenotype because decitabine was not successful in rescuing differentiation. However, it seems that compromised Foxp3 expression may be partly caused by increased methylation as decitabine increased Foxp3 expression in *Foxo3a*$^{-/-}$*IL-10*$^{-/-}$ iTregs. Thus, a mechanism other than DNA methylation must be responsible for the compromised differentiation of iTregs from *Foxo3a*$^{-/-}$*IL-10*$^{-/-}$ mice with a CrD-like phenotype.

Findings from this study suggest that iTreg differentiation from *Foxo3a*$^{-/-}$*IL-10*$^{-/-}$ mice with a CrD-like phenotype is dependant on TCR simulation (**Figure 21**). CNS3 sets a threshold for TCR stimulation in Tregs, as tTregs depleted of CNS3 demonstrate increased TCR stimulation genes[169]. In tTregs, the latter depletion improves their differentiation. This study's results demonstrate that, at low concentrations of αCD3 antibodies, the TCR simulation threshold is lower in *Foxo3a*$^{-/-}$*IL-10*$^{-/-}$ iTregs and allows for better differentiation of iTregs. Such a reduced threshold compromises iTreg differentiation at high concentrations of αCD3 antibodies, which is ideal for the control genotypes. The idea of a "Goldilocks Zone" for TCR stimulation and Treg development supports the notion that Tregs need TCR stimulation that is "just right"[307]. Other studies suggest that the ideal conditions for pTreg development are sub-immunogenic[308]. The data from this study suggest that *Foxo3a*$^{-/-}$*IL-10*$^{-/-}$ iTreg development may be increased in low-inflammatory conditions. Once a certain threshold is crossed, Treg development becomes compromised. This likely contributes to the aggressive progression of intestinal inflammation in *Foxo3a*$^{-/-}$*IL-10*$^{-/-}$ mice.

Foxo3a is involved in suppressing the cell cycle. In cancer, Foxo3a regulates several genes needed for progression of the cell cycle[309, 310]. Foxo3a plays roles in the proliferation of T and B cells [281]. In T cells, Foxo3a induces the expression of IL-2 regulatory genes[311]. In B cells, Foxo3a contributes to cell cycle arrest[312, 313]. IL-10 is also an important cytokine that

inhibits T cell proliferation[314]. *Foxo3a*$^{-/-}$*IL-10*$^{-/-}$ iTregs, and not *Foxo3a*$^{-/-}$ or *IL-10*$^{-/-}$ iTregs underwent cellular divisions at a greater rate (**Figure 20**). Interestingly, this only results in a greater number of non-iTregs post-differentiation when the initial CD4^{+} T cells originate from a *Foxo3a*$^{-/-}$*IL-10*$^{-/-}$ mouse that developed a CrD-like phenotype (**Figure 19**). It appears that Foxo3a and IL-10 play an antagonistic role in which they can compensate for each other in arresting the cell cycle in T cells. It also appears that there is some yet-to-be-determined mechanism restraining this defect from resulting in increased proliferation, which is only overcome in the presence of inflammation. This may explain the increase in the overall number of nTregs found in the lamina propria of *Foxo3a*$^{-/-}$*IL-10*$^{-/-}$ mice[262]. The unmethylated CNS3 in *Foxo3a*$^{-/-}$*IL-10*$^{-/-}$ iTregs from healthy mice may be preventing increased proliferation by modulating TCR stimulation, which is primarily responsible for transduction of genes related to T cell proliferation[315]. The *Foxo3a*$^{-/-}$*IL-10*$^{-/-}$ iTregs that undergo increased proliferation also have increased sensitivity to TCR stimulation. Thus, methylation of CNS3 in the inflammatory environment may lead to increased TCR-stimulation, compromised Foxp3 expression, and increased proliferation in *Foxo3a*$^{-/-}$*IL-10*$^{-/-}$ non-iTregs.

Foxo3a promotes apoptosis in CD8^{+} T cells, B cells, and tumors[225, 316, 317]. On the other hand, IL-10 promotes T cell survival in various models[318, 319]. *Foxo3a*$^{-/-}$*IL-10*$^{-/-}$ nTregs have increased survival after 72 hour activation with αCD3 and αCD28 antibodies *in vitro*[262]. Furthermore, *Foxo3a*$^{-/-}$*IL-10*$^{-/-}$ leukocyte progenitors, DCs, and monocytes have increased survival *in vivo*[261, 262]. In this study, *Foxo3a*$^{-/-}$*IL-10*$^{-/-}$ iTregs show increased viability only when differentiated at low concentrations of αCD3 antibodies (**Figure 22**). In all other conditions, *Foxo3a*$^{-/-}$*IL-10*$^{-/-}$ iTregs have similar viability to control genotypes (**Figure 17** and **Figure 26**). This indicates the importance in TCR signaling in controlling viability in *Foxo3a*$^{-/-}$*IL-10*$^{-/-}$ iTregs. The lack of viability differences is likely caused by environments that polarize promotion or obstruction of iTreg stability. Thus, it seems that Foxo3a is essential in promoting apoptosis

under certain conditions. Additionally, the lack of *Foxo3a* in promoting survival overcomes the promotion of apoptosis caused by the lack of *IL-10*.

Foxo3a restrains glycolysis in many cell types, largely through mTOR suppression[280, 320]. In Tregs, the promotion of glycolysis seems to compromise their suppressive capacity[211]. Tregs rely on fatty acid synthesis in the initial stages after TCR stimulation, then switch to fatty acid oxidation to maintain their Foxp3 expression and function[203, 204]. The $CD4^+$ T cells of *Foxo3a*$^{-/-}$*IL-10*$^{-/-}$ mice show an increase in neutral lipids (**Figure 23**). This indicates an increase in fatty acid synthesis. On the other hand, *Foxo3a*$^{-/-}$*IL-10*$^{-/-}$ iTregs have similar levels of neutral lipids as the control genotypes. This indicates that the switch from fatty acid synthesis to fatty acid oxidation is functional in *Foxo3a*$^{-/-}$*IL-10*$^{-/-}$ iTregs because the excess neutral lipids in $CD4^+$ T cells are used up after iTregs have differentiated. Published data suggests that *Foxo3a*$^{-/-}$*IL-10*$^{-/-}$ T cells undergo increased glycolysis[261]. Thus, it is important to determine if *Foxo3a*$^{-/-}$*IL-10*$^{-/-}$ iTregs undergo increased glycolysis, which could decrease their Foxp3 expression and compromise their suppressive activity. *Foxo3a*$^{-/-}$*IL-10*$^{-/-}$ T cells also experience increased glutaminolysis, which contributes to increased inflammatory T cell proliferation, activation, and cytokine production[261]. Glutaminolysis also increases the differentiation of $CD4^+$ T cells into Th1 or Th17 cells, but its role in Treg differentiation and function has not been characterized[321]. During the last 48 hours of differentiation, *Foxo3a*$^{-/-}$*IL-10*$^{-/-}$ iTregs consume higher levels of oxygen than control genotypes (**Figure S33**). This agrees with other data that indicates that *Foxo3a*$^{-/-}$*IL-10*$^{-/-}$ T cells have increased metabolic activity[261]. It is unclear which metabolic pathways are modulated, and which pathways result in the increased metabolic activity of *Foxo3a*$^{-/-}$*IL-10*$^{-/-}$ iTregs during differentiation. Promising candidates for the latter pathways are glycolysis, because of the reduced suppressive capacity of *Foxo3a*$^{-/-}$*IL-10*$^{-/-}$, and glutaminolysis, because of existing evidence in *Foxo3a*$^{-/-}$*IL-10*$^{-/-}$ $CD4^+$ T cells.

4.3 Foxo3a maintains Foxp3 expression in *IL-10*-deficient mice.

In inflammatory autoimmune environments, Tregs can lose expression of Foxp3[322]. This leads to a loss of their suppressive function[166]. Thus, the maintenance of Foxp3 expression is important to their function. Other data suggests that pro-inflammatory cytokines promote the conversion of Tregs to Th17 cells[323]. The stability of *Foxo3a*$^{-/-}$*IL-10*$^{-/-}$ iTregs is compromised in the absence of pro-inflammatory cytokines, indicating that another mechanism, other than pro-inflammatory cytokine induced pathways, is responsible for a decrease in Foxp3 stability (**Figure 25**). The role of Foxo3a in maintaining Treg stability has not been characterized. This study shows that loss of *Foxo3a* leads to a slight reduction in iTreg stability. Our results are consistent with published work, as in the presence of the pro-inflammatory environment of the Treg suppression assay, Foxp3 expression is compromised in all 4 genotypes, but to a greater degree in *Foxo3a*$^{-/-}$*IL-10*$^{-/-}$ iTregs (**Figure 24**). This loss of Foxp3 expression increases production of IL-17a and IFN-γ from Foxp3^{-} T cells (**Figure 29**). This then compounds the pro-inflammatory environment that Tregs are supposed to suppress. It is unlikely that the pro-inflammatory environment alone is the reason for decreased stability in *Foxo3a*$^{-/-}$*IL-10*$^{-/-}$ Tregs because *Foxo3a*$^{-/-}$*IL-10*$^{-/-}$ iTregs from both sick and healthy mice have compromised stability. In another study, loss of IL-10R in Tregs has no effect on the stability of Foxp3 expression[138]. This study provides somewhat contradictory results for *IL-10R*$^{-/-}$ Tregs because *IL-10*$^{-/-}$ iTregs have slightly compromised stability (**Figure 25**). This contradiction is most likely due to the aforementioned study using *in vivo* models, whereas this study uses *in vitro* models. IL-2 stabilizes Foxp3 expression by demethylating the TSDR through STAT5 signaling[95]. Addition of IL-2 is not able to rescue the stability of *Foxo3a*$^{-/-}$*IL-10*$^{-/-}$ iTregs (**Figure 27**). Thus, the decreased stability in *Foxo3a*$^{-/-}$*IL-10*$^{-/-}$ iTregs is independent of IL-2 signaling. Stability of Foxp3 expression is largely governed by CNS2[171]. *Foxo3a*$^{-/-}$*IL-10*$^{-/-}$ iTregs that differentiates in the presence of decitabine, which is a DNA

methyltransferase inhibitor, have levels of stability similar to control genotypes. The latter difference supports the key role that DNA methylation has in the loss of stability in *Foxo3a*$^{-/-}$ *IL-10*$^{-/-}$ iTregs. The results of this study also suggest that *Foxo3a* and *IL-10* support the stability of iTregs by maintaining a demethylated state in CD4^{+} T cells. It seems that *Foxo3a* and *IL-10* play an antagonistic role, where only loss of both *Foxo3a* and *IL-10* leads to a biologically relevant decrease in Treg stability.

As previously discussed, TCR signaling plays an essential role in iTreg differentiation. The TCR threshold in Tregs is governed by CNS3[169]. The compromised stability in *Foxo3a*$^{-/-}$ *IL-10*$^{-/-}$ iTregs seems to be dependant on TCR activation, because only high concentrations of αCD3 antibodies is there a marked reduction in iTreg stability (**Figure 28**). The dependence on TCR stimulation for *Foxo3a*$^{-/-}$*IL-10*$^{-/-}$ iTreg stability and differentiation both indicate that *Foxo3a*$^{-/-}$*IL-10*$^{-/-}$ iTregs have increased sensitivity to stimulation, which causes them to leave the “Goldilocks Zone” of TCR stimulation. Demethylation of CNS2 and CNS3 is dependant on TCR stimulation[175]. Additionally, strong TCR stimulation promotes Treg stability[324]. The results with the control genotypes concur with this finding, although this process seems to be compromised in *Foxo3a*$^{-/-}$*IL-10*$^{-/-}$ iTregs because strong TCR stimulation does not lead to stable Foxp3 expression. Also, in the absence of TCR stimulation, *Foxo3a*$^{-/-}$*IL-10*$^{-/-}$ iTregs maintain CD25 expression better than the control genotypes (**Figure 27 b**). Finally, TCR signaling is also responsible for induction and maintenance of CD25 expression[325]. Thus, all results support dysfunction in TCR signalling in *Foxo3a*$^{-/-}$*IL-10*$^{-/-}$ iTregs.

A decrease or loss of *Foxp3* leads to a decrease in the suppressive capacity of Tregs[166, 233]. Loss of *Foxo3a* and *Foxo1* leads to a decrease in the suppressive capacity of Tregs[233]. As well, IL-10 is necessary for proper suppression of effector T cells[138]. This study suggests that only *Foxo3a*$^{-/-}$*IL-10*$^{-/-}$ iTregs have compromised suppressive capacity (**Figure**

14). On the other hand, *Foxo3a*$^{-/-}$*IL-10*$^{-/-}$ nTregs have the most severely compromised suppressive capacity, and *IL-10*$^{-/-}$ nTregs also have only a slightly diminished suppressive capacity (**Figure 13**). The reason *IL-10*$^{-/-}$ nTregs do not have a change in suppressive capacity is likely because they were differentiated *in vitro*, rather than *in vivo*. The greatly diminished suppressive capacity of *Foxo3a*$^{-/-}$*IL-10*$^{-/-}$ iTregs likely results from their lack of stability as they have diminished suppressive capacity regardless of differentiation (**Figure S31**). As stability is not dependant on the development of a CrD-like phenotype in *Foxo3a*$^{-/-}$*IL-10*$^{-/-}$ mice, the loss of stability in *Foxo3a*$^{-/-}$*IL-10*$^{-/-}$ Tregs is solely caused by the deficiency of the antagonistic Foxo3a and IL-10. Thus, the dysregulation of the inflammatory response in *Foxo3a*$^{-/-}$*IL-10*$^{-/-}$ mice is caused, at least in part, by the decrease in stability of *Foxo3a*$^{-/-}$*IL-10*$^{-/-}$ Tregs.

5.0 Conclusion

This study reveals the underlying mechanisms which compromise the suppressive function of Tregs and direct them toward a pro-inflammatory phenotype in *Foxo3a*$^{-/-}$*IL-10*$^{-/-}$ mice. Foxo3a maintains proper iTreg differentiation *in vitro* by preventing the development of a CrD-like phenotype. In addition, Foxo3a promotes iTreg stability in *IL-10*-deficient mice. Thus, Foxo3a prevent Tregs from developing into pro-inflammatory $CD4^+$ T cell subsets and maintains proper suppression of other immune cells. The differentiation of *Foxo3a*$^{-/-}$*IL-10*$^{-/-}$ DCs in response to GM-CSF is increased leading to a higher number of DCs. In addition, *Foxo3a*$^{-/-}$*IL-10*$^{-/-}$ DCs produce more pro-inflammatory cytokines. Many pathways can be inhibited to prevent the excessive production of pro-inflammatory cytokines by *Foxo3a*$^{-/-}$*IL-10*$^{-/-}$ DCs. Further experiments should be conducted to determine the metabolic pathways being modulated in *Foxo3a*$^{-/-}$*IL-10*$^{-/-}$ Tregs to determine how metabolism affects their differentiation. In addition, the methylation status of the non-coding regions of Foxp3 should be assessed in *Foxo3a*$^{-/-}$*IL-10*$^{-/-}$ Tregs. Understanding these mechanisms will provide novel pathways and approaches which can be used to develop therapeutic interventions for IBD.

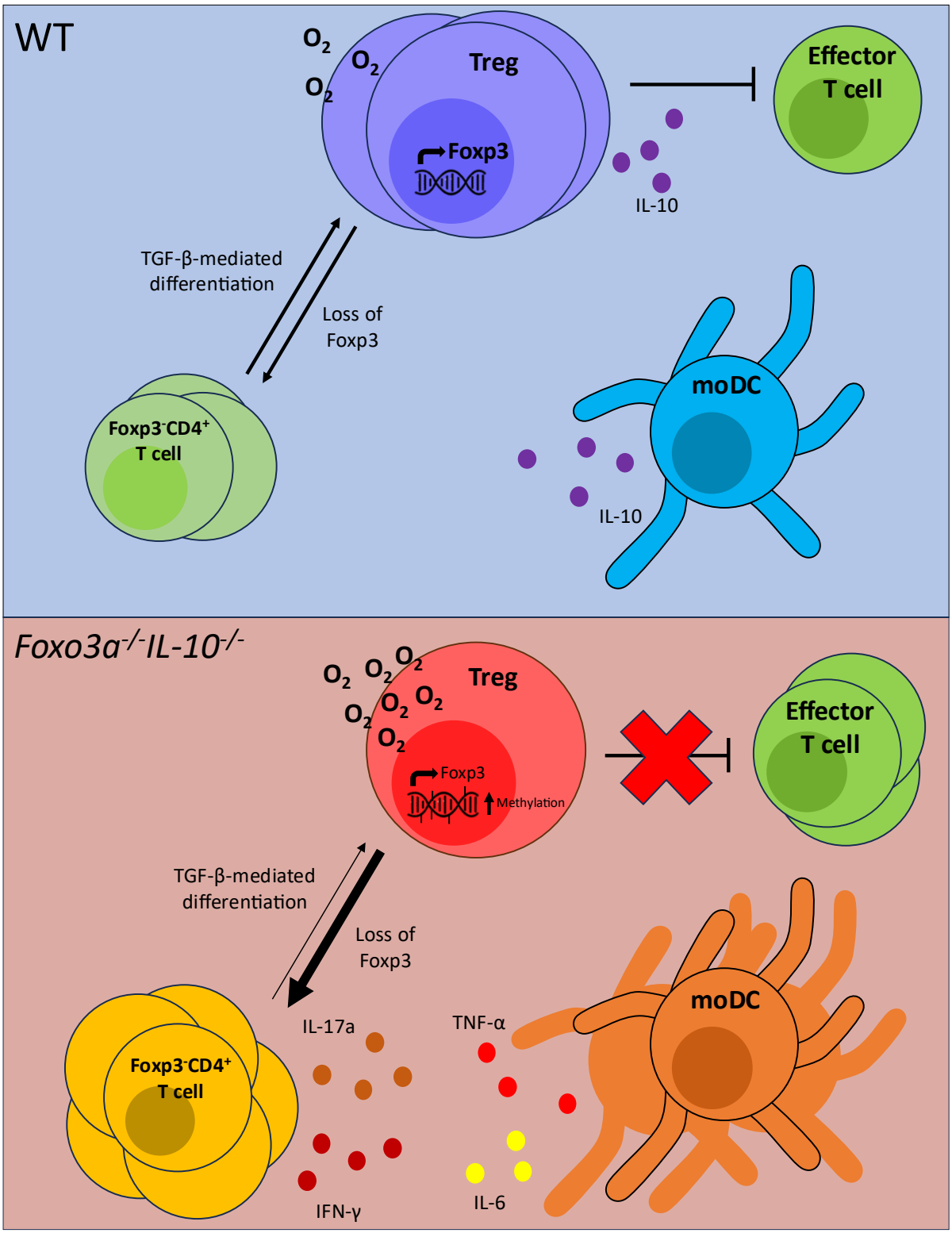

Figure 30. Visual representation of findings from this study. *Foxo3a*$^{-/-}$*IL-10*$^{-/-}$ Tregs are present in lower proportions compared to Foxp3^{-} CD4^{+} T cells and have compromised suppressive capacity. The *Foxo3a*$^{-/-}$*IL-10*$^{-/-}$ Foxp3^{-} CD4^{+} T cells and moDCs produce more inflammatory cytokines. *Foxo3a*$^{-/-}$*IL-10*$^{-/-}$ Tregs consume more oxygen and seem to have increased DNA methylation leading to Foxp3 instability.

6.0 References

1. A. Paillot, Uimmunite acquise chez les insects. *CR Soc* **81cl**, 278-288 (1920).
2. C. A. Janeway, Jr., The immune system evolved to discriminate infectious nonself from noninfectious self. *Immunol Today* **13**, 11-16 (1992).
3. C. A. Janeway, Jr., Approaching the asymptote? Evolution and revolution in immunology. *Cold Spring Harb Symp Quant Biol* **54 Pt 1**, 1-13 (1989).
4. F. Ciacci-Woolwine, P. F. McDermott, S. B. Mizel, Induction of cytokine synthesis by flagella from gram-negative bacteria may be dependent on the activation or differentiation state of human monocytes. *Infect Immun* **67**, 5176-5185 (1999).
5. B. Weidemann *et al.*, Soluble peptidoglycan-induced monokine production can be blocked by anti-CD14 monoclonal antibodies and by lipid A partial structures. *Infect Immun* **62**, 4709-4715 (1994).
6. R. Medzhitov, P. Preston-Hurlburt, C. A. Janeway, Jr., A human homologue of the Drosophila Toll protein signals activation of adaptive immunity. *Nature* **388**, 394-397 (1997).
7. G. Meuret, J. Bammert, G. Hoffmann, Kinetics of human monocytopoiesis. *Blood* **44**, 801-816 (1974).
8. N. V. Serbina, T. P. Salazar-Mather, C. A. Biron, W. A. Kuziel, E. G. Pamer, TNF/iNOS-producing dendritic cells mediate innate immune defense against bacterial infection. *Immunity* **19**, 59-70 (2003).
9. R. van Furth, Z. A. Cohn, The origin and kinetics of mononuclear phagocytes. *J Exp Med* **128**, 415-435 (1968).
10. C. Sunderkötter *et al.*, Subpopulations of mouse blood monocytes differ in maturation stage and inflammatory response. *J Immunol* **172**, 4410-4417 (2004).
11. T. Kurihara, G. Warr, J. Loy, R. Bravo, Defects in macrophage recruitment and host defense in mice lacking the CCR2 chemokine receptor. *J Exp Med* **186**, 1757-1762 (1997).
12. G. J. Randolph, K. Inaba, D. F. Robbiani, R. M. Steinman, W. A. Muller, Differentiation of phagocytic monocytes into lymph node dendritic cells in vivo. *Immunity* **11**, 753-761 (1999).
13. G. Rotta *et al.*, Lipopolysaccharide or whole bacteria block the conversion of inflammatory monocytes into dendritic cells in vivo. *J Exp Med* **198**, 1253-1263 (2003).
14. M. Greter *et al.*, GM-CSF controls nonlymphoid tissue dendritic cell homeostasis but is dispensable for the differentiation of inflammatory dendritic cells. *Immunity* **36**, 1031-1046 (2012).
15. C. Scheicher *et al.*, Recombinant GM-CSF induces in vitro differentiation of dendritic cells from mouse bone marrow. *Adv Exp Med Biol* **329**, 269-273 (1993).
16. M. W. Schreurs, A. A. Eggert, A. J. de Boer, C. G. Figdor, G. J. Adema, Generation and functional characterization of mouse monocyte-derived dendritic cells. *Eur J Immunol* **29**, 2835-2841 (1999).
17. T. M. Hohl *et al.*, Inflammatory monocytes facilitate adaptive CD4 T cell responses during respiratory fungal infection. *Cell Host Microbe* **6**, 470-481 (2009).
18. B. León, M. López-Bravo, C. Ardavín, Monocyte-derived dendritic cells formed at the infection site control the induction of protective T helper 1 responses against Leishmania. *Immunity* **26**, 519-531 (2007).
19. E. R. Stanley *et al.*, Biology and action of colony--stimulating factor-1. *Mol Reprod Dev* **46**, 4-10 (1997).
20. J. Banchereau, R. M. Steinman, Dendritic cells and the control of immunity. *Nature* **392**, 245-252 (1998).
21. C. Théry, S. Amigorena, The cell biology of antigen presentation in dendritic cells. *Curr Opin Immunol* **13**, 45-51 (2001).
22. J. Banchereau *et al.*, Immunobiology of dendritic cells. *Annu Rev Immunol* **18**, 767-811 (2000).
23. O. Tal *et al.*, DC mobilization from the skin requires docking to immobilized CCL21 on lymphatic endothelium and intralymphatic crawling. *J Exp Med* **208**, 2141-2153 (2011).

24. A. T. Satpathy *et al.*, Notch2-dependent classical dendritic cells orchestrate intestinal immunity to attaching-and-effacing bacterial pathogens. *Nat Immunol* **14**, 937-948 (2013).
25. M. Mashayekhi *et al.*, CD8α(+) dendritic cells are the critical source of interleukin-12 that controls acute infection by Toxoplasma gondii tachyzoites. *Immunity* **35**, 249-259 (2011).
26. M. Colonna, G. Trinchieri, Y. J. Liu, Plasmacytoid dendritic cells in immunity. *Nat Immunol* **5**, 1219-1226 (2004).
27. K. V. Chow, A. M. Lew, R. M. Sutherland, Y. Zhan, Monocyte-Derived Dendritic Cells Promote Th Polarization, whereas Conventional Dendritic Cells Promote Th Proliferation. *J Immunol* **196**, 624-636 (2016).
28. M. Merad, F. Ginhoux, M. Collin, Origin, homeostasis and function of Langerhans cells and other langerin-expressing dendritic cells. *Nat Rev Immunol* **8**, 935-947 (2008).
29. A. Schlitzer *et al.*, Identification of cDC1- and cDC2-committed DC progenitors reveals early lineage priming at the common DC progenitor stage in the bone marrow. *Nat Immunol* **16**, 718-728 (2015).
30. D. Traver *et al.*, Development of CD8alpha-positive dendritic cells from a common myeloid progenitor. *Science* **290**, 2152-2154 (2000).
31. S. M. Schlenner *et al.*, Fate mapping reveals separate origins of T cells and myeloid lineages in the thymus. *Immunity* **32**, 426-436 (2010).
32. S. H. Naik *et al.*, Development of plasmacytoid and conventional dendritic cell subtypes from single precursor cells derived in vitro and in vivo. *Nat Immunol* **8**, 1217-1226 (2007).
33. S. Upadhaya *et al.*, Kinetics of adult hematopoietic stem cell differentiation in vivo. *J Exp Med* **215**, 2815-2832 (2018).
34. G. L. Dixon *et al.*, Dendritic cell activation and cytokine production induced by group B Neisseria meningitidis: interleukin-12 production depends on lipopolysaccharide expression in intact bacteria. *Infect Immun* **69**, 4351-4357 (2001).
35. T. Kishimoto, S. Akira, M. Narazaki, T. Taga, Interleukin-6 family of cytokines and gp130. *Blood* **86**, 1243-1254 (1995).
36. L. E. Harrington *et al.*, Interleukin 17-producing CD4+ effector T cells develop via a lineage distinct from the T helper type 1 and 2 lineages. *Nat Immunol* **6**, 1123-1132 (2005).
37. H. Park *et al.*, A distinct lineage of CD4 T cells regulates tissue inflammation by producing interleukin 17. *Nat Immunol* **6**, 1133-1141 (2005).
38. R. Manetti *et al.*, Natural killer cell stimulatory factor (interleukin 12 [IL-12]) induces T helper type 1 (Th1)-specific immune responses and inhibits the development of IL-4-producing Th cells. *J Exp Med* **177**, 1199-1204 (1993).
39. C. S. Hsieh *et al.*, Development of TH1 CD4+ T cells through IL-12 produced by Listeria-induced macrophages. *Science* **260**, 547-549 (1993).
40. P. E. Lipsky *et al.*, Infliximab and methotrexate in the treatment of rheumatoid arthritis. Anti-Tumor Necrosis Factor Trial in Rheumatoid Arthritis with Concomitant Therapy Study Group. *N Engl J Med* **343**, 1594-1602 (2000).
41. A. K. Akobeng, M. Zachos, Tumor necrosis factor-alpha antibody for induction of remission in Crohn's disease. *Cochrane Database Syst Rev* **2003**, Cd003574 (2004).
42. G. Bruce, T. Chang, J. George, The Bursa of Fabricius and Antibody Production. *Poultry Science* **35**, 224-225 (1956).
43. J. F. Miller, G. F. Mitchell, Cell to cell interaction in the immune response. I. Hemolysin-forming cells in neonatally thymectomized mice reconstituted with thymus or thoracic duct lymphocytes. *J Exp Med* **128**, 801-820 (1968).
44. S. Tonegawa, Somatic generation of antibody diversity. *Nature* **302**, 575-581 (1983).
45. Y. Yanagi *et al.*, A human T cell-specific cDNA clone encodes a protein having extensive homology to immunoglobulin chains. *Nature* **308**, 145-149 (1984).
46. G. Siu *et al.*, The human T cell antigen receptor is encoded by variable, diversity, and joining gene segments that rearrange to generate a complete V gene. *Cell* **37**, 393-401 (1984).
47. R. Kiessling, E. Klein, H. Wigzell, "Natural" killer cells in the mouse. I. Cytotoxic cells with specificity for mouse Moloney leukemia cells. Specificity and distribution according to genotype. *Eur J Immunol* **5**, 112-117 (1975).

48. R. Kiessling, E. Klein, H. Pross, H. Wigzell, "Natural" killer cells in the mouse. II. Cytotoxic cells with specificity for mouse Moloney leukemia cells. Characteristics of the killer cell. *Eur J Immunol* **5**, 117-121 (1975).
49. C. A. Biron, K. S. Byron, J. L. Sullivan, Severe herpesvirus infections in an adolescent without natural killer cells. *N Engl J Med* **320**, 1731-1735 (1989).
50. H. Spits, J. P. Di Santo, The expanding family of innate lymphoid cells: regulators and effectors of immunity and tissue remodeling. *Nat Immunol* **12**, 21-27 (2011).
51. D. Cantrell, T cell antigen receptor signal transduction pathways. *Annu Rev Immunol* **14**, 259-274 (1996).
52. G. Altan-Bonnet, R. N. Germain, Modeling T cell antigen discrimination based on feedback control of digital ERK responses. *PLoS Biol* **3**, e356 (2005).
53. C. Dong *et al.*, JNK is required for effector T-cell function but not for T-cell activation. *Nature* **405**, 91-94 (2000).
54. W. Huang *et al.*, NFAT and NF-κB dynamically co-regulate TCR and CAR signaling responses in human T cells. *Cell Rep* **42**, 112663 (2023).
55. O. Acuto, F. Michel, CD28-mediated co-stimulation: a quantitative support for TCR signalling. *Nat Rev Immunol* **3**, 939-951 (2003).
56. E. Kelly, A. Won, Y. Refaeli, L. Van Parijs, IL-2 and related cytokines can promote T cell survival by activating AKT. *J Immunol* **168**, 597-603 (2002).
57. J. M. Green *et al.*, Absence of B7-dependent responses in CD28-deficient mice. *Immunity* **1**, 501-508 (1994).
58. J. M. Curtsinger, M. F. Mescher, Inflammatory cytokines as a third signal for T cell activation. *Curr Opin Immunol* **22**, 333-340 (2010).
59. J. M. Curtsinger, D. C. Lins, M. F. Mescher, Signal 3 determines tolerance versus full activation of naive CD8 T cells: dissociating proliferation and development of effector function. *J Exp Med* **197**, 1141-1151 (2003).
60. A. R. Townsend, F. M. Gotch, J. Davey, Cytotoxic T cells recognize fragments of the influenza nucleoprotein. *Cell* **42**, 457-467 (1985).
61. P. A. Henkart, Lymphocyte-mediated cytotoxicity: two pathways and multiple effector molecules. *Immunity* **1**, 343-346 (1994).
62. E. R. Podack, A. Kupfer, T-cell effector functions: mechanisms for delivery of cytotoxicity and help. *Annu Rev Cell Biol* **7**, 479-504 (1991).
63. R. M. Zinkernagel *et al.*, On the thymus in the differentiation of "H-2 self-recognition" by T cells: evidence for dual recognition? *J Exp Med* **147**, 882-896 (1978).
64. P. J. Fink, M. J. Bevan, H-2 antigens of the thymus determine lymphocyte specificity. *J Exp Med* **148**, 766-775 (1978).
65. J. Sprent, S. R. Webb, Function and specificity of T cell subsets in the mouse. *Adv Immunol* **41**, 39-133 (1987).
66. G. Anderson, E. J. Jenkinson, N. C. Moore, J. J. Owen, MHC class II-positive epithelium and mesenchyme cells are both required for T-cell development in the thymus. *Nature* **362**, 70-73 (1993).
67. N. Zhang, H. Hartig, I. Dzhagalov, D. Draper, Y. W. He, The role of apoptosis in the development and function of T lymphocytes. *Cell Res* **15**, 749-769 (2005).
68. J. E. Castro *et al.*, Fas modulation of apoptosis during negative selection of thymocytes. *Immunity* **5**, 617-627 (1996).
69. G. J. Nossal, Negative selection of lymphocytes. *Cell* **76**, 229-239 (1994).
70. M. Shinzawa *et al.*, Reversal of the T cell immune system reveals the molecular basis for T cell lineage fate determination in the thymus. *Nat Immunol* **23**, 731-742 (2022).
71. I. A. Parish, S. M. Kaech, Diversity in CD8(+) T cell differentiation. *Curr Opin Immunol* **21**, 291-297 (2009).
72. M. G. Vander Heiden, L. C. Cantley, C. B. Thompson, Understanding the Warburg effect: the metabolic requirements of cell proliferation. *Science* **324**, 1029-1033 (2009).
73. N. S. Joshi *et al.*, Inflammation directs memory precursor and short-lived effector CD8(+) T cell fates via the graded expression of T-bet transcription factor. *Immunity* **27**, 281-295 (2007).

74. R. Carrio, O. F. Bathe, T. R. Malek, Initial antigen encounter programs CD8+ T cells competent to develop into memory cells that are activated in an antigen-free, IL-7- and IL-15-rich environment. *J Immunol* **172**, 7315-7323 (2004).
75. P. A. Henkart, P. J. Millard, C. W. Reynolds, M. P. Henkart, Cytolytic activity of purified cytoplasmic granules from cytotoxic rat large granular lymphocyte tumors. *J Exp Med* **160**, 75-93 (1984).
76. E. R. Podack, J. D. Young, Z. A. Cohn, Isolation and biochemical and functional characterization of perforin 1 from cytolytic T-cell granules. *Proc Natl Acad Sci U S A* **82**, 8629-8633 (1985).
77. D. Chowdhury, J. Lieberman, Death by a thousand cuts: granzyme pathways of programmed cell death. *Annu Rev Immunol* **26**, 389-420 (2008).
78. P. C. Doherty, S. Hou, R. A. Tripp, CD8+ T-cell memory to viruses. *Curr Opin Immunol* **6**, 545-552 (1994).
79. S. K. Kim, K. S. Schluns, L. Lefrançois, Induction and visualization of mucosal memory CD8 T cells following systemic virus infection. *J Immunol* **163**, 4125-4132 (1999).
80. W. E. Paul, R. A. Seder, Lymphocyte responses and cytokines. *Cell* **76**, 241-251 (1994).
81. S. J. Szabo *et al.*, A novel transcription factor, T-bet, directs Th1 lineage commitment. *Cell* **100**, 655-669 (2000).
82. S. Romagnani, Th1/Th2 cells. *Inflamm Bowel Dis* **5**, 285-294 (1999).
83. L. M. Bradley, D. K. Dalton, M. Croft, A direct role for IFN-gamma in regulation of Th1 cell development. *J Immunol* **157**, 1350-1358 (1996).
84. G. R. Lee, Transcriptional regulation of T helper type 2 differentiation. *Immunology* **141**, 498-505 (2014).
85. M. Kopf *et al.*, Disruption of the murine IL-4 gene blocks Th2 cytokine responses. *Nature* **362**, 245-248 (1993).
86. J. F. Urban, Jr., I. M. Katona, W. E. Paul, F. D. Finkelman, Interleukin 4 is important in protective immunity to a gastrointestinal nematode infection in mice. *Proc Natl Acad Sci U S A* **88**, 5513-5517 (1991).
87. S. L. Swain, A. D. Weinberg, M. English, G. Huston, IL-4 directs the development of Th2-like helper effectors. *J Immunol* **145**, 3796-3806 (1990).
88. L. E. Harrington, P. R. Mangan, C. T. Weaver, Expanding the effector CD4 T-cell repertoire: the Th17 lineage. *Curr Opin Immunol* **18**, 349-356 (2006).
89. C. Dong, Diversification of T-helper-cell lineages: finding the family root of IL-17-producing cells. *Nat Rev Immunol* **6**, 329-333 (2006).
90. P. Ye *et al.*, Requirement of interleukin 17 receptor signaling for lung CXC chemokine and granulocyte colony-stimulating factor expression, neutrophil recruitment, and host defense. *J Exp Med* **194**, 519-527 (2001).
91. A. Puel *et al.*, Inborn errors of mucocutaneous immunity to Candida albicans in humans: a role for IL-17 cytokines? *Curr Opin Immunol* **22**, 467-474 (2010).
92. M. Veldhoen, R. J. Hocking, C. J. Atkins, R. M. Locksley, B. Stockinger, TGFbeta in the context of an inflammatory cytokine milieu supports de novo differentiation of IL-17-producing T cells. *Immunity* **24**, 179-189 (2006).
93. S. Crotty, T follicular helper cell differentiation, function, and roles in disease. *Immunity* **41**, 529-542 (2014).
94. R. Ahmed, D. Gray, Immunological memory and protective immunity: understanding their relation. *Science* **272**, 54-60 (1996).
95. S. Sakaguchi, N. Sakaguchi, M. Asano, M. Itoh, M. Toda, Immunologic self-tolerance maintained by activated T cells expressing IL-2 receptor alpha-chains (CD25). Breakdown of a single mechanism of self-tolerance causes various autoimmune diseases. *J Immunol* **155**, 1151-1164 (1995).
96. M. E. Brunkow *et al.*, Disruption of a new forkhead/winged-helix protein, scurfin, results in the fatal lymphoproliferative disorder of the scurfy mouse. *Nat Genet* **27**, 68-73 (2001).
97. M. A. Gavin *et al.*, Foxp3-dependent programme of regulatory T-cell differentiation. *Nature* **445**, 771-775 (2007).

98. O. Akbari *et al.*, Antigen-specific regulatory T cells develop via the ICOS-ICOS-ligand pathway and inhibit allergen-induced airway hyperreactivity. *Nat Med* **8**, 1024-1032 (2002).
99. V. R. Aluvihare, M. Kallikourdis, A. G. Betz, Regulatory T cells mediate maternal tolerance to the fetus. *Nat Immunol* **5**, 266-271 (2004).
100. C. Baecher-Allan, V. Viglietta, D. A. Hafler, Inhibition of human CD4(+)CD25(+high) regulatory T cell function. *J Immunol* **169**, 6210-6217 (2002).
101. Z. Dembic, Beginning of the end of (understanding) the immune response. *Scand J Immunol* **68**, 381-382 (2008).
102. A. M. Thornton *et al.*, Expression of Helios, an Ikaros transcription factor family member, differentiates thymic-derived from peripherally induced Foxp3+ T regulatory cells. *J Immunol* **184**, 3433-3441 (2010).
103. J. Andersson *et al.*, CD4+ FoxP3+ regulatory T cells confer infectious tolerance in a TGF-beta-dependent manner. *J Exp Med* **205**, 1975-1981 (2008).
104. D. Zemmour *et al.*, Single-cell gene expression reveals a landscape of regulatory T cell phenotypes shaped by the TCR. *Nat Immunol* **19**, 291-301 (2018).
105. L. W. Collison *et al.*, The inhibitory cytokine IL-35 contributes to regulatory T-cell function. *Nature* **450**, 566-569 (2007).
106. C. Berasain, M. A. Avila, Amphiregulin. *Semin Cell Dev Biol* **28**, 31-41 (2014).
107. M. L. Sprouse *et al.*, Cutting Edge: Low-Affinity TCRs Support Regulatory T Cell Function in Autoimmunity. *J Immunol* **200**, 909-914 (2018).
108. J. Hua *et al.*, Pathological conversion of regulatory T cells is associated with loss of allotolerance. *Sci Rep* **8**, 7059 (2018).
109. D. Shevyrev, V. Tereshchenko, Treg Heterogeneity, Function, and Homeostasis. *Front Immunol* **10**, 3100 (2019).
110. S. Z. Josefowicz, L. F. Lu, A. Y. Rudensky, Regulatory T cells: mechanisms of differentiation and function. *Annu Rev Immunol* **30**, 531-564 (2012).
111. M. Long, S. G. Park, I. Strickland, M. S. Hayden, S. Ghosh, Nuclear factor-kappaB modulates regulatory T cell development by directly regulating expression of Foxp3 transcription factor. *Immunity* **31**, 921-931 (2009).
112. G. M. Delgoffe *et al.*, The mTOR kinase differentially regulates effector and regulatory T cell lineage commitment. *Immunity* **30**, 832-844 (2009).
113. S. Z. Josefowicz, C. B. Wilson, A. Y. Rudensky, Cutting edge: TCR stimulation is sufficient for induction of Foxp3 expression in the absence of DNA methyltransferase 1. *J Immunol* **182**, 6648-6652 (2009).
114. G. Liu *et al.*, The receptor S1P1 overrides regulatory T cell-mediated immune suppression through Akt-mTOR. *Nat Immunol* **10**, 769-777 (2009).
115. P. Y. Mantel *et al.*, Molecular mechanisms underlying FOXP3 induction in human T cells. *J Immunol* **176**, 3593-3602 (2006).
116. N. Ohkura, S. Sakaguchi, Foxo1 and Foxo3 help Foxp3. *Immunity* **33**, 835-837 (2010).
117. J. D. Fontenot, J. P. Rasmussen, M. A. Gavin, A. Y. Rudensky, A function for interleukin 2 in Foxp3-expressing regulatory T cells. *Nat Immunol* **6**, 1142-1151 (2005).
118. K. B. Vang *et al.*, IL-2, -7, and -15, but not thymic stromal lymphopoeitin, redundantly govern CD4+Foxp3+ regulatory T cell development. *J Immunol* **181**, 3285-3290 (2008).
119. S. Malin *et al.*, Role of STAT5 in controlling cell survival and immunoglobulin gene recombination during pro-B cell development. *Nat Immunol* **11**, 171-179 (2010).
120. Y. Liu *et al.*, A critical function for TGF-beta signaling in the development of natural CD4+CD25+Foxp3+ regulatory T cells. *Nat Immunol* **9**, 632-640 (2008).
121. Y. Zheng *et al.*, Role of conserved non-coding DNA elements in the Foxp3 gene in regulatory T-cell fate. *Nature* **463**, 808-812 (2010).
122. C. S. Hsieh, Y. Zheng, Y. Liang, J. D. Fontenot, A. Y. Rudensky, An intersection between the self-reactive regulatory and nonregulatory T cell receptor repertoires. *Nat Immunol* **7**, 401-410 (2006).
123. K. Kretschmer *et al.*, Inducing and expanding regulatory T cell populations by foreign antigen. *Nat Immunol* **6**, 1219-1227 (2005).

124. S. K. Lathrop *et al.*, Peripheral education of the immune system by colonic commensal microbiota. *Nature* **478**, 250-254 (2011).
125. J. M. Kim, A. Rudensky, The role of the transcription factor Foxp3 in the development of regulatory T cells. *Immunol Rev* **212**, 86-98 (2006).
126. W. Chen *et al.*, Conversion of peripheral CD4+CD25- naive T cells to CD4+CD25+ regulatory T cells by TGF-beta induction of transcription factor Foxp3. *J Exp Med* **198**, 1875-1886 (2003).
127. A. Laurence *et al.*, Interleukin-2 signaling via STAT5 constrains T helper 17 cell generation. *Immunity* **26**, 371-381 (2007).
128. A. G. Levine *et al.*, Stability and function of regulatory T cells expressing the transcription factor T-bet. *Nature* **546**, 421-425 (2017).
129. F. Yu, S. Sharma, J. Edwards, L. Feigenbaum, J. Zhu, Dynamic expression of transcription factors T-bet and GATA-3 by regulatory T cells maintains immunotolerance. *Nat Immunol* **16**, 197-206 (2015).
130. Y. Li *et al.*, Bcl6 Preserves the Suppressive Function of Regulatory T Cells During Tumorigenesis. *Front Immunol* **11**, 806 (2020).
131. O. M. Steinmetz *et al.*, The Th17-defining transcription factor RORγt promotes glomerulonephritis. *J Am Soc Nephrol* **22**, 472-483 (2011).
132. K. Nakamura *et al.*, TGF-beta 1 plays an important role in the mechanism of CD4+CD25+ regulatory T cell activity in both humans and mice. *J Immunol* **172**, 834-842 (2004).
133. A. Izcue, J. L. Coombes, F. Powrie, Regulatory lymphocytes and intestinal inflammation. *Annu Rev Immunol* **27**, 313-338 (2009).
134. M. O. Li, Y. Y. Wan, R. A. Flavell, T cell-produced transforming growth factor-beta1 controls T cell tolerance and regulates Th1- and Th17-cell differentiation. *Immunity* **26**, 579-591 (2007).
135. K. W. Moore, R. de Waal Malefyt, R. L. Coffman, A. O'Garra, Interleukin-10 and the interleukin-10 receptor. *Annu Rev Immunol* **19**, 683-765 (2001).
136. C. Asseman, S. Mauze, M. W. Leach, R. L. Coffman, F. Powrie, An essential role for interleukin 10 in the function of regulatory T cells that inhibit intestinal inflammation. *J Exp Med* **190**, 995-1004 (1999).
137. Y. P. Rubtsov *et al.*, Regulatory T cell-derived interleukin-10 limits inflammation at environmental interfaces. *Immunity* **28**, 546-558 (2008).
138. A. Chaudhry *et al.*, Interleukin-10 signaling in regulatory T cells is required for suppression of Th17 cell-mediated inflammation. *Immunity* **34**, 566-578 (2011).
139. D. K. Sojka, Y. H. Huang, D. J. Fowell, Mechanisms of regulatory T-cell suppression - a diverse arsenal for a moving target. *Immunology* **124**, 13-22 (2008).
140. E. Bardel, F. Larousserie, P. Charlot-Rabiega, A. Coulomb-L'Herminé, O. Devergne, Human CD4+ CD25+ Foxp3+ regulatory T cells do not constitutively express IL-35. *J Immunol* **181**, 6898-6905 (2008).
141. Y. Vercoulen *et al.*, Human regulatory T cell suppressive function is independent of apoptosis induction in activated effector T cells. *PLoS One* **4**, e7183 (2009).
142. D. Q. Tran *et al.*, Analysis of adhesion molecules, target cells, and role of IL-2 in human FOXP3+ regulatory T cell suppressor function. *J Immunol* **182**, 2929-2938 (2009).
143. S. Read, V. Malmström, F. Powrie, Cytotoxic T lymphocyte-associated antigen 4 plays an essential role in the function of CD25(+)CD4(+) regulatory cells that control intestinal inflammation. *J Exp Med* **192**, 295-302 (2000).
144. T. Takahashi *et al.*, Immunologic self-tolerance maintained by CD25(+)CD4(+) regulatory T cells constitutively expressing cytotoxic T lymphocyte-associated antigen 4. *J Exp Med* **192**, 303-310 (2000).
145. T. L. Walunas *et al.*, CTLA-4 can function as a negative regulator of T cell activation. *Immunity* **1**, 405-413 (1994).
146. K. Wing *et al.*, CTLA-4 control over Foxp3+ regulatory T cell function. *Science* **322**, 271-275 (2008).
147. C. J. Workman, D. A. Vignali, Negative regulation of T cell homeostasis by lymphocyte activation gene-3 (CD223). *J Immunol* **174**, 688-695 (2005).
148. N. Joller *et al.*, Treg cells expressing the coinhibitory molecule TIGIT selectively inhibit proinflammatory Th1 and Th17 cell responses. *Immunity* **40**, 569-581 (2014).

149. X. Yu *et al.*, The surface protein TIGIT suppresses T cell activation by promoting the generation of mature immunoregulatory dendritic cells. *Nat Immunol* **10**, 48-57 (2009).
150. C. E. Tadokoro *et al.*, Regulatory T cells inhibit stable contacts between CD4+ T cells and dendritic cells in vivo. *J Exp Med* **203**, 505-511 (2006).
151. D. C. Gondek, L. F. Lu, S. A. Quezada, S. Sakaguchi, R. J. Noelle, Cutting edge: contact-mediated suppression by CD4+CD25+ regulatory cells involves a granzyme B-dependent, perforin-independent mechanism. *J Immunol* **174**, 1783-1786 (2005).
152. W. J. Grossman *et al.*, Human T regulatory cells can use the perforin pathway to cause autologous target cell death. *Immunity* **21**, 589-601 (2004).
153. J. J. Kobie *et al.*, T regulatory and primed uncommitted CD4 T cells express CD73, which suppresses effector CD4 T cells by converting 5'-adenosine monophosphate to adenosine. *J Immunol* **177**, 6780-6786 (2006).
154. G. Borsellino *et al.*, Expression of ectonucleotidase CD39 by Foxp3+ Treg cells: hydrolysis of extracellular ATP and immune suppression. *Blood* **110**, 1225-1232 (2007).
155. P. B. Ernst, J. C. Garrison, L. F. Thompson, Much ado about adenosine: adenosine synthesis and function in regulatory T cell biology. *J Immunol* **185**, 1993-1998 (2010).
156. S. Deaglio *et al.*, Adenosine generation catalyzed by CD39 and CD73 expressed on regulatory T cells mediates immune suppression. *J Exp Med* **204**, 1257-1265 (2007).
157. T. Bopp *et al.*, Cyclic adenosine monophosphate is a key component of regulatory T cell-mediated suppression. *J Exp Med* **204**, 1303-1310 (2007).
158. J. Bodor, J. Bodorova, R. E. Gress, Suppression of T cell function: a potential role for transcriptional repressor ICER. *J Leukoc Biol* **67**, 774-779 (2000).
159. L. A. Smyth *et al.*, CD73 expression on extracellular vesicles derived from CD4+ CD25+ Foxp3+ T cells contributes to their regulatory function. *Eur J Immunol* **43**, 2430-2440 (2013).
160. J. A. Sullivan *et al.*, Treg-Cell-Derived IL-35-Coated Extracellular Vesicles Promote Infectious Tolerance. *Cell Rep* **30**, 1039-1051.e1035 (2020).
161. I. S. Okoye *et al.*, MicroRNA-containing T-regulatory-cell-derived exosomes suppress pathogenic T helper 1 cells. *Immunity* **41**, 89-103 (2014).
162. S. L. Tung *et al.*, Regulatory T cell-derived extracellular vesicles modify dendritic cell function. *Sci Rep* **8**, 6065 (2018).
163. S. Aiello *et al.*, Extracellular vesicles derived from T regulatory cells suppress T cell proliferation and prolong allograft survival. *Sci Rep* **7**, 11518 (2017).
164. J. Chen *et al.*, TGF-β-induced CD4+ FoxP3+ regulatory T cell-derived extracellular vesicles modulate Notch1 signaling through miR-449a and prevent collagen-induced arthritis in a murine model. *Cell Mol Immunol* **18**, 2516-2529 (2021).
165. N. Komatsu *et al.*, Heterogeneity of natural Foxp3+ T cells: a committed regulatory T-cell lineage and an uncommitted minor population retaining plasticity. *Proc Natl Acad Sci U S A* **106**, 1903-1908 (2009).
166. X. Zhou *et al.*, Instability of the transcription factor Foxp3 leads to the generation of pathogenic memory T cells in vivo. *Nat Immunol* **10**, 1000-1007 (2009).
167. H. P. Kim, W. J. Leonard, CREB/ATF-dependent T cell receptor-induced FoxP3 gene expression: a role for DNA methylation. *J Exp Med* **204**, 1543-1551 (2007).
168. S. Z. Josefowicz *et al.*, Extrathymically generated regulatory T cells control mucosal TH2 inflammation. *Nature* **482**, 395-399 (2012).
169. Y. Feng *et al.*, A mechanism for expansion of regulatory T-cell repertoire and its role in self-tolerance. *Nature* **528**, 132-136 (2015).
170. N. Ohkura *et al.*, T cell receptor stimulation-induced epigenetic changes and Foxp3 expression are independent and complementary events required for Treg cell development. *Immunity* **37**, 785-799 (2012).
171. Y. Feng *et al.*, Control of the inheritance of regulatory T cell identity by a cis element in the Foxp3 locus. *Cell* **158**, 749-763 (2014).
172. X. Li, Y. Liang, M. LeBlanc, C. Benner, Y. Zheng, Function of a Foxp3 cis-element in protecting regulatory T cell identity. *Cell* **158**, 734-748 (2014).
173. J. K. Polansky *et al.*, DNA methylation controls Foxp3 gene expression. *Eur J Immunol* **38**, 1654-1663 (2008).

174. Q. Chen, Y. C. Kim, A. Laurence, G. A. Punkosdy, E. M. Shevach, IL-2 controls the stability of Foxp3 expression in TGF-beta-induced Foxp3+ T cells in vivo. *J Immunol* **186**, 6329-6337 (2011).
175. A. Toker *et al.*, Active demethylation of the Foxp3 locus leads to the generation of stable regulatory T cells within the thymus. *J Immunol* **190**, 3180-3188 (2013).
176. X. Yue *et al.*, Control of Foxp3 stability through modulation of TET activity. *J Exp Med* **213**, 377-397 (2016).
177. R. Yang *et al.*, Hydrogen Sulfide Promotes Tet1- and Tet2-Mediated Foxp3 Demethylation to Drive Regulatory T Cell Differentiation and Maintain Immune Homeostasis. *Immunity* **43**, 251-263 (2015).
178. J. K. Polansky *et al.*, Methylation matters: binding of Ets-1 to the demethylated Foxp3 gene contributes to the stabilization of Foxp3 expression in regulatory T cells. *J Mol Med (Berl)* **88**, 1029-1040 (2010).
179. P. Newsholme, R. Curi, S. Gordon, E. A. Newsholme, Metabolism of glucose, glutamine, long-chain fatty acids and ketone bodies by murine macrophages. *Biochem J* **239**, 121-125 (1986).
180. D. Alonso, W. J. Nungester, Comparative study of host resistance of guinea pigs and rats. V. The effect of pneumococcal products on glycolysis and oxygen uptake by polymorphonuclear leucocytes. *J Infect Dis* **99**, 174-181 (1956).
181. R. D. Michalek *et al.*, Cutting edge: distinct glycolytic and lipid oxidative metabolic programs are essential for effector and regulatory CD4+ T cell subsets. *J Immunol* **186**, 3299-3303 (2011).
182. F. Magnani, A. Mattevi, Structure and mechanisms of ROS generation by NADPH oxidases. *Curr Opin Struct Biol* **59**, 91-97 (2019).
183. L. Bruno, H. von Boehmer, J. Kirberg, Cell division in the compartment of naive and memory T lymphocytes. *Eur J Immunol* **26**, 3179-3184 (1996).
184. M. I. Malandrino *et al.*, Enhanced fatty acid oxidation in adipocytes and macrophages reduces lipid-induced triglyceride accumulation and inflammation. *Am J Physiol Endocrinol Metab* **308**, E756-769 (2015).
185. E. N. Posokhova, O. M. Khoshchenko, M. I. Chasovskikh, E. N. Pivovarova, M. I. Dushkin, Lipid synthesis in macrophages during inflammation in vivo: effect of agonists of peroxisome proliferator activated receptors alpha and gamma and of retinoid X receptors. *Biochemistry (Mosc)* **73**, 296-304 (2008).
186. C. Murphy, P. Newsholme, Importance of glutamine metabolism in murine macrophages and human monocytes to L-arginine biosynthesis and rates of nitrite or urea production. *Clin Sci (Lond)* **95**, 397-407 (1998).
187. E. L. Carr *et al.*, Glutamine uptake and metabolism are coordinately regulated by ERK/MAPK during T lymphocyte activation. *J Immunol* **185**, 1037-1044 (2010).
188. M. Rath, I. Müller, P. Kropf, E. I. Closs, M. Munder, Metabolism via Arginase or Nitric Oxide Synthase: Two Competing Arginine Pathways in Macrophages. *Front Immunol* **5**, 532 (2014).
189. R. M. Silver *et al.*, Scleroderma, fasciitis, and eosinophilia associated with the ingestion of tryptophan. *N Engl J Med* **322**, 874-881 (1990).
190. F. Le Naour *et al.*, Profiling changes in gene expression during differentiation and maturation of monocyte-derived dendritic cells using both oligonucleotide microarrays and proteomics. *J Biol Chem* **276**, 17920-17931 (2001).
191. P. Zaccagnino *et al.*, An active mitochondrial biogenesis occurs during dendritic cell differentiation. *Int J Biochem Cell Biol* **44**, 1962-1969 (2012).
192. A. Rehman *et al.*, Role of fatty-acid synthesis in dendritic cell generation and function. *J Immunol* **190**, 4640-4649 (2013).
193. M. Laplante, D. M. Sabatini, mTOR signaling in growth control and disease. *Cell* **149**, 274-293 (2012).
194. H. Hackstein *et al.*, Rapamycin inhibits IL-4--induced dendritic cell maturation in vitro and dendritic cell mobilization and function in vivo. *Blood* **101**, 4457-4463 (2003).
195. A. M. Woltman *et al.*, Rapamycin specifically interferes with GM-CSF signaling in human dendritic cells, leading to apoptosis via increased p27KIP1 expression. *Blood* **101**, 1439-1445 (2003).

196. T. Sathaliyawala *et al.*, Mammalian target of rapamycin controls dendritic cell development downstream of Flt3 ligand signaling. *Immunity* **33**, 597-606 (2010).
197. H. Pan *et al.*, Critical role of the tumor suppressor tuberous sclerosis complex 1 in dendritic cell activation of CD4 T cells by promoting MHC class II expression via IRF4 and CIITA. *J Immunol* **191**, 699-707 (2013).
198. C. M. Krawczyk *et al.*, Toll-like receptor-induced changes in glycolytic metabolism regulate dendritic cell activation. *Blood* **115**, 4742-4749 (2010).
199. M. D. Brand, D. G. Nicholls, Assessing mitochondrial dysfunction in cells. *Biochem J* **435**, 297-312 (2011).
200. B. Everts *et al.*, TLR-driven early glycolytic reprogramming via the kinases TBK1-IKKε supports the anabolic demands of dendritic cell activation. *Nat Immunol* **15**, 323-332 (2014).
201. A. Maroof, N. R. English, P. A. Bedford, D. I. Gabrilovich, S. C. Knight, Developing dendritic cells become 'lacy' cells packed with fat and glycogen. *Immunology* **115**, 473-483 (2005).
202. O. Warburg, On the origin of cancer cells. *Science* **123**, 309-314 (1956).
203. C. H. Chang *et al.*, Posttranscriptional control of T cell effector function by aerobic glycolysis. *Cell* **153**, 1239-1251 (2013).
204. A. Angelin *et al.*, Foxp3 Reprograms T Cell Metabolism to Function in Low-Glucose, High-Lactate Environments. *Cell Metab* **25**, 1282-1293.e1287 (2017).
205. U. H. Beier *et al.*, Essential role of mitochondrial energy metabolism in Foxp3^{+} T-regulatory cell function and allograft survival. *Faseb j* **29**, 2315-2326 (2015).
206. V. A. Gerriets *et al.*, Foxp3 and Toll-like receptor signaling balance T(reg) cell anabolic metabolism for suppression. *Nat Immunol* **17**, 1459-1466 (2016).
207. R. D. Michalek *et al.*, Estrogen-related receptor-α is a metabolic regulator of effector T-cell activation and differentiation. *Proc Natl Acad Sci U S A* **108**, 18348-18353 (2011).
208. L. Berod *et al.*, De novo fatty acid synthesis controls the fate between regulatory T and T helper 17 cells. *Nat Med* **20**, 1327-1333 (2014).
209. D. Howie *et al.*, A Novel Role for Triglyceride Metabolism in Foxp3 Expression. *Front Immunol* **10**, 1860 (2019).
210. V. A. Gerriets *et al.*, Metabolic programming and PDHK1 control CD4+ T cell subsets and inflammation. *J Clin Invest* **125**, 194-207 (2015).
211. N. M. Chapman *et al.*, mTOR coordinates transcriptional programs and mitochondrial metabolism of activated T(reg) subsets to protect tissue homeostasis. *Nat Commun* **9**, 2095 (2018).
212. A. E. Webb, A. Brunet, FOXO transcription factors: key regulators of cellular quality control. *Trends Biochem Sci* **39**, 159-169 (2014).
213. M. V. Kim, W. Ouyang, W. Liao, M. Q. Zhang, M. O. Li, The transcription factor Foxo1 controls central-memory CD8+ T cell responses to infection. *Immunity* **39**, 286-297 (2013).
214. Y. M. Kerdiles *et al.*, Foxo transcription factors control regulatory T cell development and function. *Immunity* **33**, 890-904 (2010).
215. A. Delpoux *et al.*, FOXO1 constrains activation and regulates senescence in CD8 T cells. *Cell Rep* **34**, 108674 (2021).
216. A. K. Brown, A. E. Webb, Regulation of FOXO Factors in Mammalian Cells. *Curr Top Dev Biol* **127**, 165-192 (2018).
217. A. Brunet *et al.*, Protein kinase SGK mediates survival signals by phosphorylating the forkhead transcription factor FKHRL1 (FOXO3a). *Mol Cell Biol* **21**, 952-965 (2001).
218. M. C. Hu *et al.*, IkappaB kinase promotes tumorigenesis through inhibition of forkhead FOXO3a. *Cell* **117**, 225-237 (2004).
219. Y. Liu *et al.*, Critical role of FOXO3a in carcinogenesis. *Mol Cancer* **17**, 104 (2018).
220. Y. Zhao, Y. S. Liu, Longevity Factor FOXO3: A Key Regulator in Aging-Related Vascular Diseases. *Front Cardiovasc Med* **8**, 778674 (2021).
221. S. Davinelli, D. C. Willcox, G. Scapagnini, Extending healthy ageing: nutrient sensitive pathway and centenarian population. *Immun Ageing* **9**, 9 (2012).
222. L. Lin, J. D. Hron, S. L. Peng, Regulation of NF-kappaB, Th activation, and autoinflammation by the forkhead transcription factor Foxo3a. *Immunity* **21**, 203-213 (2004).

223. M. G. Thompson *et al.*, FOXO3-NF-κB RelA Protein Complexes Reduce Proinflammatory Cell Signaling and Function. *J Immunol* **195**, 5637-5647 (2015).
224. J. A. Sullivan, E. H. Kim, E. H. Plisch, S. L. Peng, M. Suresh, FOXO3 regulates CD8 T cell memory by T cell-intrinsic mechanisms. *PLoS Pathog* **8**, e1002533 (2012).
225. F. Tzelepis *et al.*, Intrinsic role of FoxO3a in the development of CD8+ T cell memory. *J Immunol* **190**, 1066-1075 (2013).
226. S. Xu *et al.*, FOXO3a Alleviates the Inflammation and Oxidative Stress via Regulating TGF-β and HO-1 in Ankylosing Spondylitis. *Front Immunol* **13**, 935534 (2022).
227. K. Makrutzki-Zlotek *et al.*, FOXO3A acts as immune response modulator in human virus-negative inflammatory cardiomyopathy. *Heart*, (2023).
228. Z. Li, H. Zhang, Y. Chen, L. Fan, J. Fang, Forkhead transcription factor FOXO3a protein activates nuclear factor κB through B-cell lymphoma/leukemia 10 (BCL10) protein and promotes tumor cell survival in serum deprivation. *J Biol Chem* **287**, 17737-17745 (2012).
229. X. Zhang, Q. Liu, K. Guo, Z. Zhou, FOXO3a regulates lipid accumulation and adipocyte inflammation in adipocytes through autophagy : Role of FOXO3a in obesity. *Inflamm Res* **70**, 591-603 (2021).
230. A. S. Dejean *et al.*, Transcription factor Foxo3 controls the magnitude of T cell immune responses by modulating the function of dendritic cells. *Nat Immunol* **10**, 504-513 (2009).
231. L. Luron, D. Saliba, K. Blazek, A. Lanfrancotti, I. A. Udalova, FOXO3 as a new IKK-ε-controlled check-point of regulation of IFN-β expression. *Eur J Immunol* **42**, 1030-1037 (2012).
232. R. Bouzeyen, M. Haoues, M. R. Barbouche, R. Singh, M. Essafi, FOXO3 Transcription Factor Regulates IL-10 Expression in Mycobacteria-Infected Macrophages, Tuning Their Polarization and the Subsequent Adaptive Immune Response. *Front Immunol* **10**, 2922 (2019).
233. W. Ouyang *et al.*, Foxo proteins cooperatively control the differentiation of Foxp3+ regulatory T cells. *Nat Immunol* **11**, 618-627 (2010).
234. Y. Harada *et al.*, Transcription factors Foxo3a and Foxo1 couple the E3 ligase Cbl-b to the induction of Foxp3 expression in induced regulatory T cells. *J Exp Med* **207**, 1381-1391 (2010).
235. V. Lazar *et al.*, Aspects of Gut Microbiota and Immune System Interactions in Infectious Diseases, Immunopathology, and Cancer. *Front Immunol* **9**, 1830 (2018).
236. P. Vineis *et al.*, What is new in the exposome? *Environ Int* **143**, 105887 (2020).
237. J. Libertucci, V. B. Young, The role of the microbiota in infectious diseases. *Nat Microbiol* **4**, 35-45 (2019).
238. S. Iacob, D. G. Iacob, L. M. Luminos, Intestinal Microbiota as a Host Defense Mechanism to Infectious Threats. *Front Microbiol* **9**, 3328 (2018).
239. A. Nusrat *et al.*, Clostridium difficile toxins disrupt epithelial barrier function by altering membrane microdomain localization of tight junction proteins. *Infect Immun* **69**, 1329-1336 (2001).
240. B. O. Schroeder, Fight them or feed them: how the intestinal mucus layer manages the gut microbiota. *Gastroenterol Rep (Oxf)* **7**, 3-12 (2019).
241. K. L. Mason, G. B. Huffnagle, M. C. Noverr, J. Y. Kao, Overview of gut immunology. *Adv Exp Med Biol* **635**, 1-14 (2008).
242. A. J. Macpherson, T. Uhr, Induction of protective IgA by intestinal dendritic cells carrying commensal bacteria. *Science* **303**, 1662-1665 (2004).
243. C. N. Bernstein *et al.*, The epidemiology of inflammatory bowel disease in Canada: a population-based study. *Am J Gastroenterol* **101**, 1559-1568 (2006).
244. S. K. Murthy *et al.*, The 2023 Impact of Inflammatory Bowel Disease in Canada: Cancer and IBD. *J Can Assoc Gastroenterol* **6**, S83-s96 (2023).
245. J. Z. Liu *et al.*, Association analyses identify 38 susceptibility loci for inflammatory bowel disease and highlight shared genetic risk across populations. *Nat Genet* **47**, 979-986 (2015).
246. J. C. Lee *et al.*, Genome-wide association study identifies distinct genetic contributions to prognosis and susceptibility in Crohn's disease. *Nat Genet* **49**, 262-268 (2017).
247. P. Middel, D. Raddatz, B. Gunawan, F. Haller, H. J. Radzun, Increased number of mature dendritic cells in Crohn's disease: evidence for a chemokine mediated retention mechanism. *Gut* **55**, 220-227 (2006).

248. J. Bates, L. Diehl, Dendritic cells in IBD pathogenesis: an area of therapeutic opportunity? *J Pathol* **232**, 112-120 (2014).
249. S. J. Bell *et al.*, Migration and maturation of human colonic dendritic cells. *J Immunol* **166**, 4958-4967 (2001).
250. M. A. Silva, Intestinal dendritic cells and epithelial barrier dysfunction in Crohn's disease. *Inflamm Bowel Dis* **15**, 436-453 (2009).
251. H. H. Uhlig *et al.*, Characterization of Foxp3+CD4+CD25+ and IL-10-secreting CD4+CD25+ T cells during cure of colitis. *J Immunol* **177**, 5852-5860 (2006).
252. A. Mizoguchi, E. Mizoguchi, A. K. Bhan, Immune networks in animal models of inflammatory bowel disease. *Inflamm Bowel Dis* **9**, 246-259 (2003).
253. C. Niederau, F. Backmerhoff, B. Schumacher, Inflammatory mediators and acute phase proteins in patients with Crohn's disease and ulcerative colitis. *Hepatogastroenterology* **44**, 90-107 (1997).
254. C. G. Mayne, C. B. Williams, Induced and natural regulatory T cells in the development of inflammatory bowel disease. *Inflamm Bowel Dis* **19**, 1772-1788 (2013).
255. Z. Hovhannisyan, J. Treatman, D. R. Littman, L. Mayer, Characterization of interleukin-17-producing regulatory T cells in inflamed intestinal mucosa from patients with inflammatory bowel diseases. *Gastroenterology* **140**, 957-965 (2011).
256. C. Mottet, H. H. Uhlig, F. Powrie, Cutting edge: cure of colitis by CD4+CD25+ regulatory T cells. *J Immunol* **170**, 3939-3943 (2003).
257. E. Elinav, T. Waks, Z. Eshhar, Redirection of regulatory T cells with predetermined specificity for the treatment of experimental colitis in mice. *Gastroenterology* **134**, 2014-2024 (2008).
258. E. Elinav, N. Adam, T. Waks, Z. Eshhar, Amelioration of colitis by genetically engineered murine regulatory T cells redirected by antigen-specific chimeric receptor. *Gastroenterology* **136**, 1721-1731 (2009).
259. Y. Cui *et al.*, IL23R-Specific CAR Tregs for the Treatment of Crohn's Disease. *J Crohns Colitis* **19**, (2025).
260. T. T. Pizarro *et al.*, SAMP1/YitFc mouse strain: a spontaneous model of Crohn's disease-like ileitis. *Inflamm Bowel Dis* **17**, 2566-2584 (2011).
261. S. Hajjar *et al.*, Foxo3a tempers excessive glutaminolysis in activated T cells to prevent fatal gut inflammation in the murine IL-10(-/-) model of colitis. *Cell Death Differ* **29**, 585-599 (2022).
262. S. Hajjar, University of Ottawa, Ottawa, ON Canada (2022).
263. C. Schiering *et al.*, The alarmin IL-33 promotes regulatory T-cell function in the intestine. *Nature* **513**, 564-568 (2014).
264. L. S. Walker, Treg and CTLA-4: two intertwining pathways to immune tolerance. *J Autoimmun* **45**, 49-57 (2013).
265. G. Cao *et al.*, The rules and regulatory mechanisms of FOXO3 on inflammation, metabolism, cell death and aging in hosts. *Life Sci* **328**, 121877 (2023).
266. D. R. Plas, C. B. Thompson, Akt activation promotes degradation of tuberin and FOXO3a via the proteasome. *J Biol Chem* **278**, 12361-12366 (2003).
267. A. Sunters *et al.*, Paclitaxel-induced nuclear translocation of FOXO3a in breast cancer cells is mediated by c-Jun NH2-terminal kinase and Akt. *Cancer Res* **66**, 212-220 (2006).
268. H. Huang, D. J. Tindall, Regulation of FOXO protein stability via ubiquitination and proteasome degradation. *Biochim Biophys Acta* **1813**, 1961-1964 (2011).
269. M. Milkiewicz *et al.*, Identification of a mechanism underlying regulation of the anti-angiogenic forkhead transcription factor FoxO1 in cultured endothelial cells and ischemic muscle. *Am J Pathol* **178**, 935-944 (2011).
270. I. A. Babar *et al.*, Inhibition of hypoxia-induced miR-155 radiosensitizes hypoxic lung cancer cells. *Cancer Biol Ther* **12**, 908-914 (2011).
271. A. Brunet *et al.*, Stress-dependent regulation of FOXO transcription factors by the SIRT1 deacetylase. *Science* **303**, 2011-2015 (2004).
272. J. M. Bao *et al.*, Association between FOXO3A gene polymorphisms and human longevity: a meta-analysis. *Asian J Androl* **16**, 446-452 (2014).
273. J. C. Lee *et al.*, Human SNP links differential outcomes in inflammatory and infectious disease to a FOXO3-regulated pathway. *Cell* **155**, 57-69 (2013).

274. B. J. Willcox *et al.*, FOXO3A genotype is strongly associated with human longevity. *Proc Natl Acad Sci U S A* **105**, 13987-13992 (2008).
275. Y. Song *et al.*, FOXO3a-driven miRNA signatures suppresses VEGF-A/NRP1 signaling and breast cancer metastasis. *Oncogene* **40**, 777-790 (2021).
276. C. R. Rathbone, F. W. Booth, S. J. Lees, FoxO3a preferentially induces p27Kip1 expression while impairing muscle precursor cell-cycle progression. *Muscle Nerve* **37**, 84-89 (2008).
277. J. Gilley, P. J. Coffer, J. Ham, FOXO transcription factors directly activate bim gene expression and promote apoptosis in sympathetic neurons. *J Cell Biol* **162**, 613-622 (2003).
278. Z. S. Chang *et al.*, Forkhead box O3 protects the heart against paraquat-induced aging-associated phenotypes by upregulating the expression of antioxidant enzymes. *Aging Cell* **18**, e12990 (2019).
279. H. Tran *et al.*, DNA repair pathway stimulated by the forkhead transcription factor FOXO3a through the Gadd45 protein. *Science* **296**, 530-534 (2002).
280. K. Zhou, Y. Wei, X. Li, X. Yang, MiR-223-3p targets FOXO3a to inhibit radiosensitivity in prostate cancer by activating glycolysis. *Life Sci* **282**, 119798 (2021).
281. S. Xu, Y. Ma, Y. Chen, F. Pan, Role of Forkhead box O3a transcription factor in autoimmune diseases. *Int Immunopharmacol* **92**, 107338 (2021).
282. G. Rogler, L. Biedermann, M. Scharl, New insights into the pathophysiology of inflammatory bowel disease: microbiota, epigenetics and common signalling pathways. *Swiss Med Wkly* **148**, w14599 (2018).
283. A. L. Hart *et al.*, Characteristics of intestinal dendritic cells in inflammatory bowel diseases. *Gastroenterology* **129**, 50-65 (2005).
284. S. Danese *et al.*, Randomised trial and open-label extension study of an anti-interleukin-6 antibody in Crohn's disease (ANDANTE I and II). *Gut* **68**, 40-48 (2019).
285. S. O. Adegbola, K. Sahnan, J. Warusavitarne, A. Hart, P. Tozer, Anti-TNF Therapy in Crohn's Disease. *Int J Mol Sci* **19**, (2018).
286. T. De Smedt *et al.*, Effect of interleukin-10 on dendritic cell maturation and function. *Eur J Immunol* **27**, 1229-1235 (1997).
287. J. W. Park *et al.*, Destabilization of TNF-α mRNA by Rapamycin. *Biomol Ther (Seoul)* **20**, 43-49 (2012).
288. J. H. Ko, S. O. Yoon, H. J. Lee, J. Y. Oh, Rapamycin regulates macrophage activation by inhibiting NLRP3 inflammasome-p38 MAPK-NFκB pathways in autophagy- and p62-dependent manners. *Oncotarget* **8**, 40817-40831 (2017).
289. J. A. Melillo *et al.*, Dendritic cell (DC)-specific targeting reveals Stat3 as a negative regulator of DC function. *J Immunol* **184**, 2638-2645 (2010).
290. A. Kotlyarov *et al.*, MAPKAP kinase 2 is essential for LPS-induced TNF-alpha biosynthesis. *Nat Cell Biol* **1**, 94-97 (1999).
291. A. B. Tietz *et al.*, Gene deletion of MK2 inhibits TNF-alpha and IL-6 and protects against cerulein-induced pancreatitis. *Am J Physiol Gastrointest Liver Physiol* **290**, G1298-1306 (2006).
292. J. Ibrahim *et al.*, Dendritic cell populations with different concentrations of lipid regulate tolerance and immunity in mouse and human liver. *Gastroenterology* **143**, 1061-1072 (2012).
293. D. L. Herber *et al.*, Lipid accumulation and dendritic cell dysfunction in cancer. *Nat Med* **16**, 880-886 (2010).
294. D. Boraschi, What Is IL-1 for? The Functions of Interleukin-1 Across Evolution. *Front Immunol* **13**, 872155 (2022).
295. B. Van Den Eeckhout, J. Tavernier, S. Gerlo, Interleukin-1 as Innate Mediator of T Cell Immunity. *Front Immunol* **11**, 621931 (2020).
296. S. Yalcin *et al.*, ROS-mediated amplification of AKT/mTOR signalling pathway leads to myeloproliferative syndrome in Foxo3(-/-) mice. *Embo j* **29**, 4118-4131 (2010).
297. P. Allavena *et al.*, IL-10 prevents the differentiation of monocytes to dendritic cells but promotes their maturation to macrophages. *Eur J Immunol* **28**, 359-369 (1998).
298. R. Hontecillas, J. Bassaganya-Riera, Peroxisome proliferator-activated receptor gamma is required for regulatory CD4+ T cell-mediated protection against colitis. *J Immunol* **178**, 2940-2949 (2007).

299. S. M. Tanner, E. M. Staley, R. G. Lorenz, Altered generation of induced regulatory T cells in the FVB.mdr1a-/- mouse model of colitis. *Mucosal Immunol* **6**, 309-323 (2013).
300. F. Boehm *et al.*, Deletion of Foxp3+ regulatory T cells in genetically targeted mice supports development of intestinal inflammation. *BMC Gastroenterol* **12**, 97 (2012).
301. C. Voskens *et al.*, Autologous regulatory T-cell transfer in refractory ulcerative colitis with concomitant primary sclerosing cholangitis. *Gut* **72**, 49-53 (2023).
302. M. Luu, E. Jenike, N. Vachharajani, A. Visekruna, Transcription factor c-Rel is indispensable for generation of thymic but not of peripheral Foxp3(+) regulatory T cells. *Oncotarget* **8**, 52678-52689 (2017).
303. M. A. Burchill, J. Yang, C. Vogtenhuber, B. R. Blazar, M. A. Farrar, IL-2 receptor beta-dependent STAT5 activation is required for the development of Foxp3+ regulatory T cells. *J Immunol* **178**, 280-290 (2007).
304. Q. Ruan *et al.*, Development of Foxp3(+) regulatory t cells is driven by the c-Rel enhanceosome. *Immunity* **31**, 932-940 (2009).
305. S. Yamashita *et al.*, Distinct DNA methylation targets by aging and chronic inflammation: a pilot study using gastric mucosa infected with Helicobacter pylori. *Clin Epigenetics* **11**, 191 (2019).
306. G. Wei *et al.*, Global mapping of H3K4me3 and H3K27me3 reveals specificity and plasticity in lineage fate determination of differentiating CD4+ T cells. *Immunity* **30**, 155-167 (2009).
307. T. J. Yun, M. J. Bevan, The Goldilocks conditions applied to T cell development. *Nat Immunol* **2**, 13-14 (2001).
308. R. A. Gottschalk, E. Corse, J. P. Allison, TCR ligand density and affinity determine peripheral induction of Foxp3 in vivo. *J Exp Med* **207**, 1701-1711 (2010).
309. M. Schmidt *et al.*, Cell cycle inhibition by FoxO forkhead transcription factors involves downregulation of cyclin D. *Mol Cell Biol* **22**, 7842-7852 (2002).
310. Z. Lu *et al.*, S-equol, a Secondary Metabolite of Natural Anticancer Isoflavone Daidzein, Inhibits Prostate Cancer Growth In Vitro and In Vivo, Though Activating the Akt/FOXO3a Pathway. *Curr Cancer Drug Targets* **16**, 455-465 (2016).
311. M. Stahl *et al.*, The forkhead transcription factor FoxO regulates transcription of p27Kip1 and Bim in response to IL-2. *J Immunol* **168**, 5024-5031 (2002).
312. J. Chen, I. Yusuf, H. M. Andersen, D. A. Fruman, FOXO transcription factors cooperate with delta EF1 to activate growth suppressive genes in B lymphocytes. *J Immunol* **176**, 2711-2721 (2006).
313. I. Yusuf *et al.*, KLF4 is a FOXO target gene that suppresses B cell proliferation. *Int Immunol* **20**, 671-681 (2008).
314. C. A. Akdis, K. Blaser, Mechanisms of interleukin-10-mediated immune suppression. *Immunology* **103**, 131-136 (2001).
315. K. Shah, A. Al-Haidari, J. Sun, J. U. Kazi, T cell receptor (TCR) signaling in health and disease. *Signal Transduct Target Ther* **6**, 412 (2021).
316. A. R. Wolfe *et al.*, Simvastatin prevents triple-negative breast cancer metastasis in pre-clinical models through regulation of FOXO3a. *Breast Cancer Res Treat* **154**, 495-508 (2015).
317. K. Ottens *et al.*, Foxo3 Promotes Apoptosis of B Cell Receptor-Stimulated Immature B Cells, Thus Limiting the Window for Receptor Editing. *J Immunol* **201**, 940-949 (2018).
318. N. Yogev *et al.*, CD4(+) T-cell-derived IL-10 promotes CNS inflammation in mice by sustaining effector T cell survival. *Cell Rep* **38**, 110565 (2022).
319. B. S. Hanna *et al.*, Interleukin-10 receptor signaling promotes the maintenance of a PD-1(int) TCF-1(+) CD8(+) T cell population that sustains anti-tumor immunity. *Immunity* **54**, 2825-2841.e2810 (2021).
320. S. Khatri, H. Yepiskoposyan, C. A. Gallo, P. Tandon, D. R. Plas, FOXO3a regulates glycolysis via transcriptional control of tumor suppressor TSC1. *J Biol Chem* **285**, 15960-15965 (2010).
321. M. O. Johnson *et al.*, Distinct Regulation of Th17 and Th1 Cell Differentiation by Glutaminase-Dependent Metabolism. *Cell* **175**, 1780-1795.e1719 (2018).
322. Y. Gao *et al.*, Inflammation negatively regulates FOXP3 and regulatory T-cell function via DBC1. *Proc Natl Acad Sci U S A* **112**, E3246-3254 (2015).
323. X. O. Yang *et al.*, Molecular antagonism and plasticity of regulatory and inflammatory T cell programs. *Immunity* **29**, 44-56 (2008).

324. E. Wakamatsu, H. Omori, A. Kawano, S. Ogawa, R. Abe, Strong TCR stimulation promotes the stabilization of Foxp3 expression in regulatory T cells induced in vitro through increasing the demethylation of Foxp3 CNS2. *Biochem Biophys Res Commun* **503**, 2597-2602 (2018).
325. A. N. Shatrova *et al.*, Time-Dependent Regulation of IL-2R α-Chain (CD25) Expression by TCR Signal Strength and IL-2-Induced STAT5 Signaling in Activated Human Blood T Lymphocytes. *PLoS One* **11**, e0167215 (2016).

7.0 Curriculum Vitae

Willem Brandt

EDUCATION

2023–2025	**M.Sc.**, Microbiology and Immunology Supervisor: Dr. Subash Sad University of Ottawa
2019–2023	**B.Sc.**, Honours in Biochemistry Summa Cum Laude University of Ottawa

HONOURS AND AWARDS

2025	2nd Place Poster M.Sc. Award, Canadian Society of Immunology ($300)
2024	Ontario Graduate Scholarship ($15,000)
2024	JCZP University of Toronto Immunology Travel Award ($500)
2023–2024	Special Merit Scholarship, M.Sc. ($6000)
2023	CIHR Canada Graduate Scholarship (CGS-M) ($17,500)
2023	M.Sc. Admission Scholarship ($4000)
2023	Faculty Plaque in Biochemistry – Highest GPA in B.Sc. Biochemistry
2022	Academic Player of the Year, Eastern Ontario Junior Hockey League
2022	Dwaine Barkley Educational Bursary, Hockey Eastern Ontario ($2000)
2020–2023	Merit Scholarship, B.Sc. ($6000)
2019–2023	Dean's List, B.Sc.
2019	B.Sc. Admission Scholarship ($4000)

RESEARCH EXPERIENCE

2023–2025 **Graduate Student,** University of Ottawa
- Supervisor: Dr. Subash Sad
- Research focus: investigating the protective role of Foxo3a in the regulatory T cells and dendritic cells of IL-10-deficient mice

2022–2023 **Honours Student**, University of Ottawa
- Supervisor: Dr. Subash Sad
- Research focus: investigating the regulation of chronic inflammatory disease by Foxo3a in the bone marrow compartment

2020–2023 **Research Assistant,** Ottawa Hospital Research Institute
- Supervisors: Dr. Marc Carrier and Dr. Deborah Siegal
- Research Focus: Catheter related-thrombosis and stroke in cancer patients

PUBLICATIONS

Brown C, **Brandt W**, Wang TF, Delluc A, Carrier M. Incidence of recurrent venous thromboembolism and bleeding complications in patients with cancer and isolated distal deep vein thrombosis. Thromb Res. 2023 Aug;228:81-84. DOI: 10.1016/j.thromres.2023.05.027.

Brandt W, Brown C, Wang TF, Tagalakis V, Shivakumar S, Ciuffini LA, Mallick R, Wells PS, Carrier M. Efficacy and safety of apixaban for primary prevention of thromboembolism in patients with cancer and a central venous catheter: A subgroup analysis of the AVERT Trial. Thromb Res. 2022 Aug;216:8-10. DOI: 10.1016/j.thromres.2022.05.014.

Li A, **Brandt W**, Brown C, Wang TF, Ikesaka R, Delluc A, Wells P, Carrier M. Efficacy and safety of primary thromboprophylaxis for the prevention of venous thromboembolism in patients with cancer and a central venous catheter: A systematic review and meta-analysis. Thromb Res. 2021 Dec;208:58-65. DOI: 10.1016/j.thromres.2021.10.012.

CONFERENCE PRESENTATIONS

Brandt W, Bhan A, Hajjar S, El Hamra R, Yadav S, Hurley K, Ariana A, Kaul R, Sad S. Foxo3a maintains the suppressive capacity, differentiation, and stability of regulatory T cells in IL-10-deficient mice. *Poster presentation at Canadian Society for Immunology 2025.*

Brandt W, Hajjar S, Bhan A, El Hamra R, Yadav S, Hurley K, Ariana A, Sad S. Foxo3a maintains the suppressive capacity of regulatory T cells and proper activation by dendritic cells in IL-10-deficient mice. *Poster presentation at Canadian Society for Immunology 2024.*

Brandt W, Brown C, Zahrai A, Mallick R, Wells PS, Carrier M. Efficacy and Safety of Apixaban for Primary Prevention of Thromboembolism in Cancer Patients with a Newly Inserted Central Venous Catheter: A Post-Hoc Analysis of the Avert Trial. Blood. 2021 Nov;138: 2133. *Poster presentation at American Society of Hematology Annual Meeting and Exposition 2021.*

LEADERSHIP AND VOLUNTEER EXPERIENCES

2024–present **VP Internal**, BMI Graduate Student Association, uOttawa
- Advocated on behalf of BMI students to department heads
- Maintained strong communication between student body & BMI faculty
- Organized social events (i.e., BBQs, pub nights, trivia, etc.)

2024–present **Friendly Visitor and Info Guide**, the Ottawa Hospital
- Guided patients around the hospital
- Ensured patients reach the ED & get medical attention
- Supported patients with limited support networks

2023–present **Tutor and Mentor**, Go2Grad
- Supported high school students in reaching their max. potential
- Encouraged critical thinking
- Mentored maintenance of a strong school-life balance

2022–present **Volunteer Cook**, the Ottawa Mission
- Prepared healthy meals for homeless people
- Provided supportive & respectful conversation while being mindful of diverse cultural backgrounds

2022–present **Activity Leader,** Let's Talk Science
- Planned & presented science activities to young students from different backgrounds
- Encouraged questions to foster curiosity in science

2021–2022 **Summer Student Seminar Program**, Ottawa Hospital Research Institute
- Provided critical feedback to presenters
- Disseminated research
- Elucidated complexity of medical problems to peers

2018–2022 **Assistant Captain**, Richmond Royals Junior B Hockey Team (EOJHL)
- Developed team cohesion
- Mentored younger players as a trusted confidant
- Facilitated team development

2017–2019 **Skills Coach,** Nepean Girls Hockey Association
- Demonstrated drills in a skilful manner
- Provided constructive feedback to improve players performance & awareness
- Encouraged questions

8.0 Supplemental Figures

A

1:1 WT CD4⁺ : iTregs (gated on singlets -> Zombie⁻ -> CD45.1⁺ -> CD4⁺ T cells) | 72hrs with αCD3		
CD45.1⁺CD4⁺ T cells	WT	WT
CD45.2⁺ iTregs	*Foxo3a*$^{-/-}$*IL-10*$^{-/-}$	*Foxo3a*$^{-/-}$*IL-10*$^{-/-}$
Rapamycin	---	1 µM

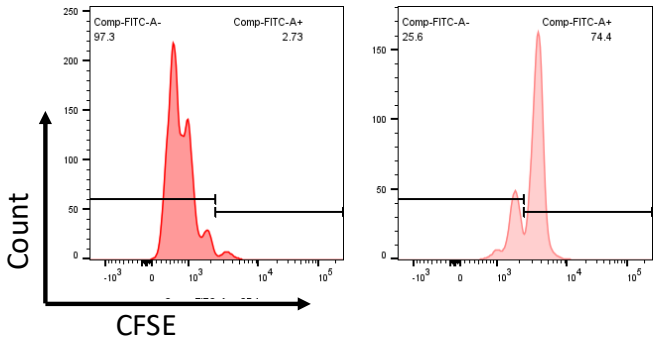

B

1:1 WT CD4⁺ : iTregs (gated on singlets -> CD45.2⁺) | 72hrs with αCD3		
CD45.1⁺CD4⁺ T cells	WT	WT
CD45.2⁺ iTregs	*Foxo3a*$^{-/-}$*IL-10*$^{-/-}$	*Foxo3a*$^{-/-}$*IL-10*$^{-/-}$
Rapamycin	---	1µM

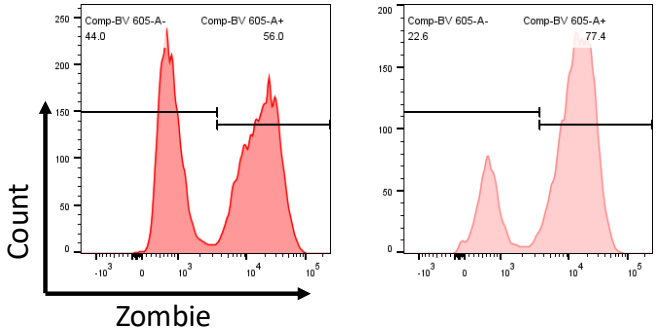

Figure S31. The ability of *Foxo3a*$^{-/-}$*IL-10*$^{-/-}$ iTregs to suppress the proliferation of WT CD4⁺ T cells is restored with rapamycin treatment during co-culture. (A) Representative FACS plots of CFSE dilution in CD45.1⁺CD4⁺ WT T cells co-cultured 1:1 with CD45.2⁺ *Foxo3a*$^{-/-}$*IL-10*$^{-/-}$ iTregs (*n*=1). **(B)** Representative FACS plots of the viability of CD45.2⁺ *Foxo3a*$^{-/-}$*IL-10*$^{-/-}$ iTregs co-cultured 1:1 with CD45.1⁺CD4⁺ WT T cells (*n*=1). **A-B** shows CD45.1⁺CD4⁺ WT T cells co-cultured with CD45.2⁺ *Foxo3a*$^{-/-}$*IL-10*$^{-/-}$ iTregs stimulated in plates coated for 3 hours at 37°C with 20 µg/mL αCD3 antibodies. Cells were harvested after 72 hours co-culture with and without 1 µM rapamycin. Experiments conducted on 8-week-old to 12-week-old mice. Cells were stained with fluorescent antibodies, acquired on a BD LSRFortessa™, and analyzed using FlowJo™ software.

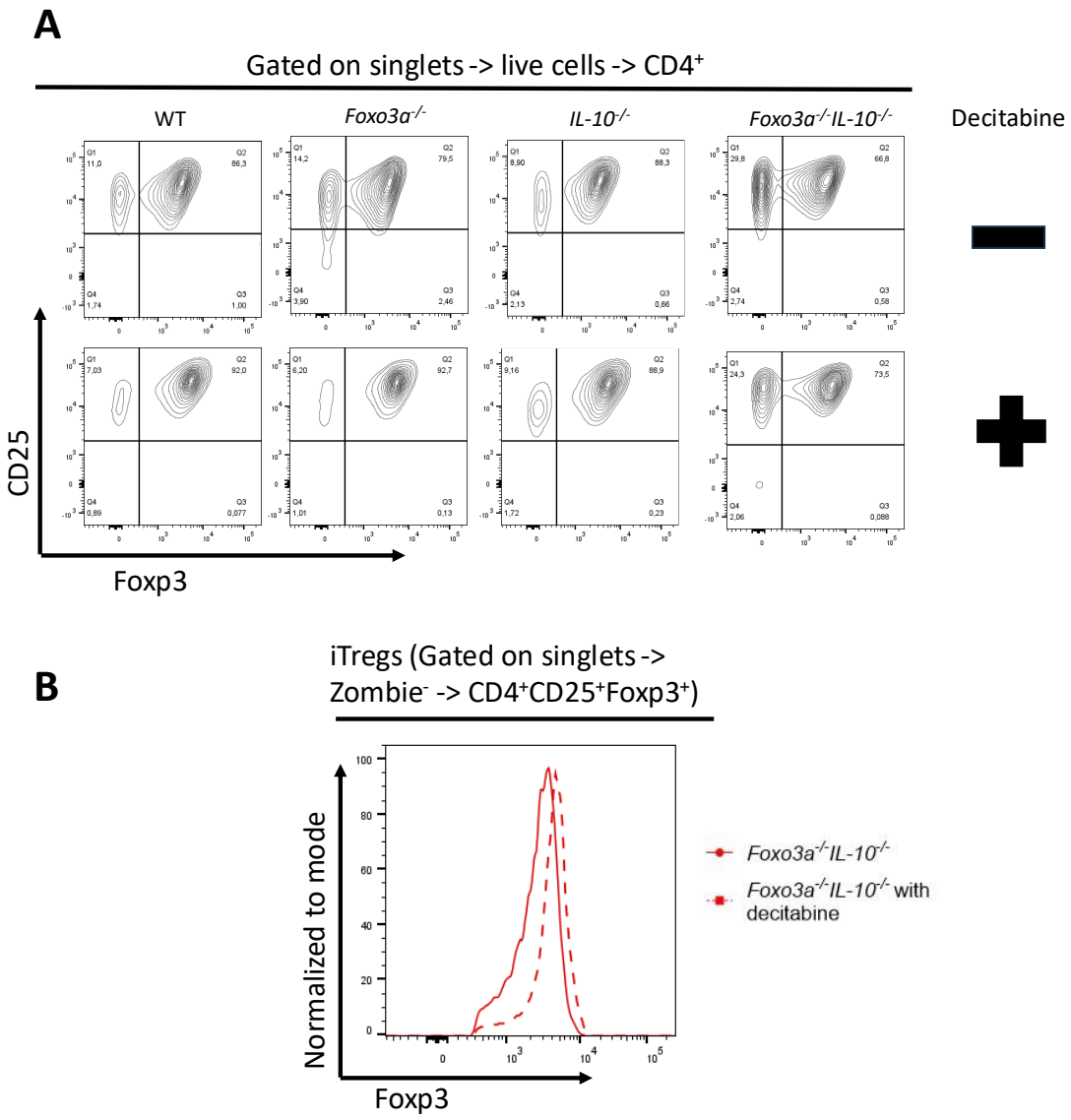

Figure S32. A DNA methyltransferase inhibitor does not rescue the compromised differentiation of *Foxo3a*$^{-/-}$*IL-10*$^{-/-}$ iTregs from mice with a CrD-like phenotype. (A) Representative FACS plots of proportion of CD25^{+}Foxp3^{+} iTregs from all 4 genotypes, differentiated with and without 50 nM decitabine (n=1). **(B)** Representative FACS plot of Foxp3 expression in CD4^{+}CD25^{+}Foxp3^{+} populations comparing *Foxo3a*$^{-/-}$*IL-10*$^{-/-}$ iTregs differentiated with and without 50 nM decitabine. Foxp3 expression is normalized to the mode (n=1). Experiments conducted on 8-week-old to 12-week-old mice. *Foxo3a*$^{-/-}$*IL-10*$^{-/-}$ mice used had developed a CrD-like phenotype. iTregs were stained with fluorescent antibodies, acquired on a BD LSRFortessa™, and analyzed using FlowJo™ software.

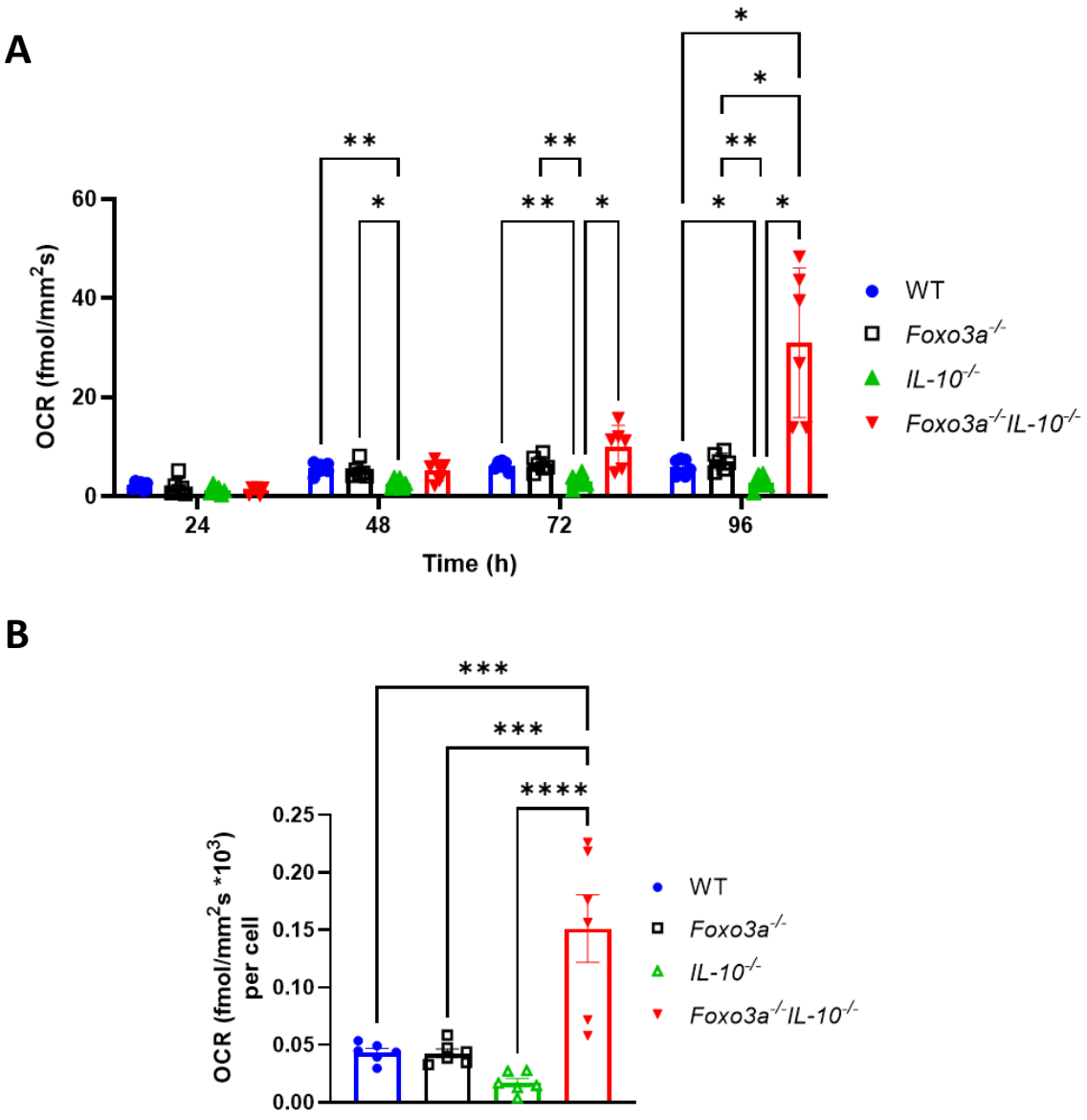

Figure S33. *Foxo3a*$^{-/-}$*IL-10*$^{-/-}$ iTregs differentiated from mice with a CrD-like phenotype consume high levels of oxygen during differentiation. (A) OCR of T cells from **In Vitro Differentiation of Regulatory T Cells** from sick *Foxo3a*$^{-/-}$*IL-10*$^{-/-}$ mice and control genotypes. **(B)** OCR of T cells from **In Vitro Differentiation of Regulatory T Cells** from sick *Foxo3a*$^{-/-}$*IL-10*$^{-/-}$ mice and control genotypes normalized to the number of cells per well at 96 hours. In **A-B**, OCR was measured using the Lucid Scientific Resipher and data were analyzed using Lucid Scientific Lucid Lab software (n=1). Experiments conducted on 8-week-old to 12-week-old mice. Individual bars depict the respective mean ± SEM. Statistical significance determined using a 1-way or 2-way ANOVA and reported for each comparison by "*" (*P<0.05, **P<0.01, ***P<0.001, ****P<0.0001).

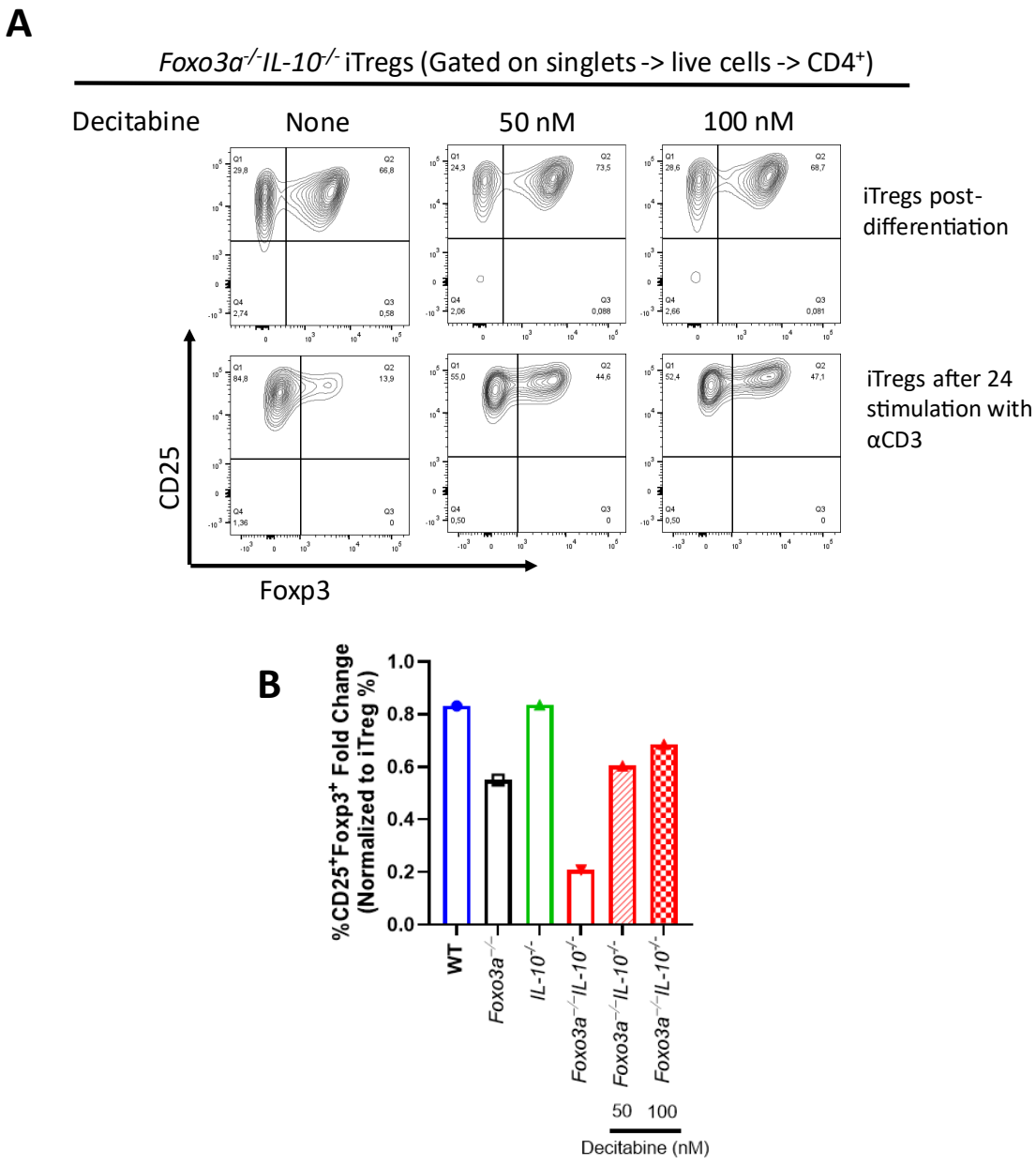

Figure S34. *Foxo3a*$^{-/-}$*IL-10*$^{-/-}$ iTregs stability is partially rescued with a DNA methyltransferase inhibitor. (A) Representative FACS plots of proportion of iTregs from all four genotypes before (top) and after (bottom) 24 hour stimulation. iTregs were differentiated with or without 50 nM or 100 nM decitabine (*n*=1). **(B)** Bar graph depicting the proportion of iTregs remaining after 24 hour stimulation. iTreg proportion after stimulation normalized to iTreg proportion before stimulation. iTregs were differentiated with or without 50 nM or 100 nM decitabine (n=1). In **A-B,** iTregs were stimulated in plates coated for 3 hours at 37°C with 20 µg/mL αCD3 antibodies. Experiments conducted on 8-week-old to 12-week-old mice. Cells were stained with fluorescent antibodies, acquired on a BD LSRFortessa™, and analyzed using FlowJo™ software.

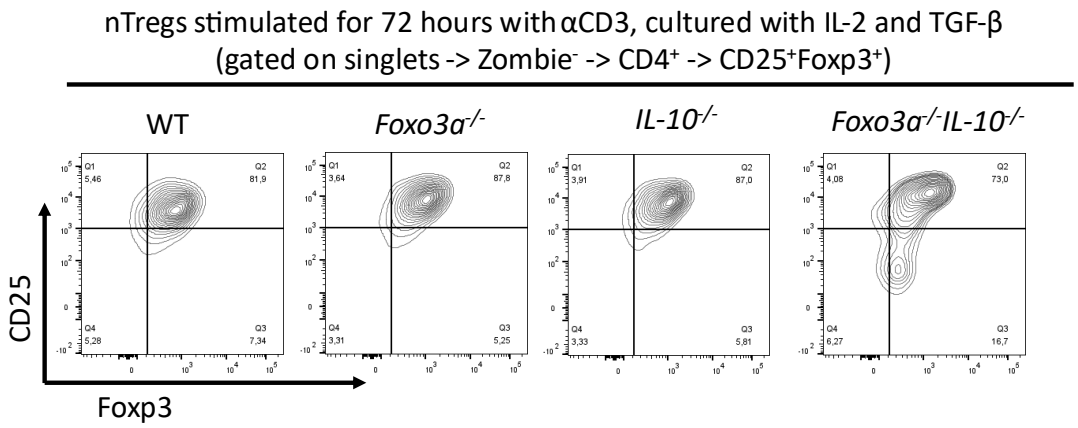

Figure S35. *Foxo3a*$^{-/-}$*IL-10*$^{-/-}$ nTregs have compromised stability when stimulated with αCD3 antibodies in the presence of growth factors. Representative FACS plots of nTregs from all four genotypes after 72 hour stimulation in plates coated overnight at 4°C with 1 µg/mL αCD3 antibodies in the presence of 2.5 ng/mL IL-2 and TGF-β (*n*=1). Experiments conducted on 8-week-old to 12-week-old mice. nTregs were stained with fluorescent antibodies, acquired on a BD LSRFortessa™, and analyzed using FlowJo™ software.